

***Thermal Behavior of Amino Acids
in Inorganic Matrices:
Relevance for Chemical Evolution***

**Dissertation zur Erlangung des Doktorgrades
der Naturwissenschaften (Dr. rer. nat.)**

**Fakultät Naturwissenschaften
Universität Hohenheim**

Institut für Chemie

vorgelegt von
Punam Dalai
aus Allahabad
(India)

2013

Dekan: Prof. Dr. Heinz Breer

1. berichtende Person: Prof. Dr. Henry Strasdeit

2. berichtende Person: Prof. Dr. Hans Brückner

Eingereicht am: 30.08.2013

Mündliche Prüfung am: 17.12.2013

To
My Parents

Acknowledgements

With my profound sense of gratitude, I would like to express thanks to my supervisor Prof. Dr. Henry Strasdeit for providing me the opportunity to pursue my PhD at the Institute of Chemistry, University of Hohenheim. He helped me by excellent supervision, support, and encouragement along the way to understand and explore certain interdisciplinary dimensions. He has been a constant source of ideas and suggestions from the initial planning stage until completion of research.

I wish to express my special thanks to Dr. Stefan Fox for his advice during the experiments and writing of the thesis. I am grateful to Prof. Dr. Hans Brückner and Prof. Dr. Uwe Beifuss for agreeing to be reviewer/examiner for my PhD thesis.

I gratefully thank Sonja Ringer, Melanie Wagner, Claudia Görden, and the late Petra Guni for their help during my research. I would like to express my thanks to Dr. J.-P. deVera from the DLR Institute of Planetary Research, Berlin for providing Martian soil simulants. I would like to thank all my colleagues at the Department of Bioinorganic Chemistry for their advice and support. I would like to extend my special thanks to Mrs. Malmström and Ms. Franziska Wolz for their help in administrative works.

My appreciation also goes to all my friends in Germany and other parts of the world for their warm company and numerous favors during my studies.

Finally, my special thanks and appreciation go to my parents, Vikas and my sister for their love, patience, support, and understanding throughout my studies.

Preliminary Remarks

The work presented in this thesis was carried out under the supervision of Prof. Dr. Henry Strasdeit at the Institute of Chemistry, University of Hohenheim, from April 2008 to December 2012. Part of the results have been presented at international conferences:

Dalai, P. and Strasdeit, H. (2009) Dramatic alteration of the thermal behavior of glycine by Ca-montmorillonite. *Orig Life Evol Biosph* **39**: 230.

(presented at the 15th International Conference on the Origin of Life, Florence, Italy, 2008).

Dalai, P. and Strasdeit, H. (2009) The influence of a clay mineral on the behavior of glycine at 200 degrees celsius. *Orig Life Evol Biosph* **39**: 47.

(presented at the 8th European Workshop on Astrobiology, Neuchatel, Switzerland, 2008).

Dalai, P. and Strasdeit, H. (2010) The influence of various clay matrices on the thermal behavior of glycine. *Orig Life Evol Biosph* **40**: 520.

(presented at the 9th European Workshop on Astrobiology, Brussels, Belgium, 2009).

Dalai, P. and Strasdeit, H. (2010) Peptide formation and glycine protection by clays.

(presented at International Workshop on Chemical Evolution and Origin of Life, Indian Institute of Technology, Roorkee, India, 2010).

Dalai, P. and Strasdeit, H. (2011) Thermal behavior of non-racemic alanine intercalated in calcium-montmorillonite.

(presented at the 11th European Workshop on Astrobiology, Köln, Germany, 2011).

Strasdeit, H., Dalai, P., and Fox, S. (2011) A complex thermal polymer derived from the simplest amino acid.

(presented at the 11th European Workshop on Astrobiology, Köln, Germany, 2011).

1 Introduction	1
1.1 Prebiotic chemical evolution.....	1
1.1.1 Peptides and proteins.....	1
1.1.2 RNA world hypothesis.....	2
1.1.3 Protometabolism and catalytic networks.....	3
1.2 Early climate and geological history of Earth and Mars.....	4
1.2.1 Water and atmosphere on the early Earth.....	5
1.2.2 Geological history of Mars.....	6
1.2.3 Volcanism on Earth and Mars.....	7
1.3 Minerals of possible relevance to prebiotic chemistry.....	8
1.3.1 Clay minerals.....	8
1.3.2 Chlorides.....	11
1.3.3 Carbonates.....	11
1.3.4 Sulfates.....	12
1.3.5 Other minerals.....	13
1.4 Prebiotic amino acids.....	14
1.4.1 Amino acid sources.....	14
1.4.2 Possible origins of biomolecular homochirality of amino acids.....	16
1.4.3 Thermal properties of amino acids.....	20
1.5 Aims and objectives.....	21
2 Results and Discussion	23
2.1 Thermal treatment of neat glycine and glycine homopeptides	23
2.1.1 Thermal treatment of neat glycine.....	23
2.1.2 Thermal treatment of DKP and linear homopeptides of glycine.....	28
2.2 Analysis and properties of the glycine thermo-melanoid.....	32
2.2.1 Thermogravimetric analysis of glycine and homopeptides of glycine.....	32
2.2.2 Solubility and hydrolysis of the thermo-melanoid.....	34
2.2.3 Biodegradability of the thermo-melanoid in soil.....	35
2.3 Protection of glycine by different matrices.....	36
2.3.1 The influence of salts and salt mixtures.....	36
2.3.2 Thermal treatment of glycine embedded in clay minerals.....	47

2.3.3 Terrestrial volcanic rock and Martian soil simulants.....	58
2.4 Racemization of amino acids intercalated in Ca-montmorillonite.....	61
2.4.1 Thermal treatment at 200 °C of Ca-montmorillonite loaded with alanine having different starting L-ee.....	62
2.4.2 Thermal treatment at various temperatures of Ca-montmorillonite loaded with L-alanine.....	66
2.4.3 Thermal treatment of Ca-montmorillonite loaded with other amino acids.....	66
2.4.4 Racemization kinetics of alanine in Ca-montmorillonite.....	70
2.5 Sublimation of neat alanine and valine.....	75
3 Summary / Zusammenfassung.....	78
4 Materials and Methods.....	87
4.1 Analytical methods.....	87
4.1.1 High performance liquid chromatography (HPLC).....	87
4.1.2 Infrared spectroscopy.....	87
4.1.3 Gas chromatography with mass spectrometric and flame ionization detection (GC-MS and GC-FID).....	87
4.1.4 Matrix-assisted laser desorption ionization–time of flight/time of flight mass spectrometry (MALDI–TOF/TOF mass spectrometry).....	89
4.1.5 Thermogravimetric analysis (TGA).....	90
4.1.6 Powder X-ray diffractometry (Powder XRD).....	90
4.1.7 Elemental analysis.....	90
4.2 List of Chemicals.....	90
4.3 Heating apparatus.....	93
4.4 Analysis of the thermo-melanoid.....	94
4.4.1 Hydrolysis of the thermo-melanoid.....	94
4.4.2 Biodegradability of the thermo-melanoid in soil.....	94
4.5 Preparative methods.....	95
4.5.1 Salts and salt mixtures with embedded glycine: Syntheses and thermal treatment	95
4.5.2 Clay minerals with embedded amino acids: Loading procedure and thermal treatment.....	96

4.5.3 Preparation and thermal treatment of glycine-loaded terrestrial volcanic rock and Martian soil simulants.....	100
4.5.4 Extraction of amino acids and peptides from clay minerals.....	101
5 Literature.....	103
6 Appendix.....	126
7 Curriculum Vitae.....	137

1 Introduction

1.1 Prebiotic chemical evolution

Prebiotic chemical evolution describes the series of events that led from simple molecules to complex compounds before the presence of life. Charles Darwin suggested 150 years ago that life may have begun in a “warm little pond” in the presence of inorganic salts and energy sources (Peretó et al., 2009). Later, Oparin and Haldane independently developed the “primordial soup” hypothesis. According to this hypothesis, simple organic molecules (e.g. amino acids) were formed from the Earth’s primitive atmosphere and could have accumulated to form the primordial soup. Based on this hypothesis, Stanley Miller conducted experiments where it was found that amino acids could be synthesized from a simulated early Earth’s atmosphere (CH_4 , H_2 , H_2O , NH_3) in the presence of an energy source (Miller, 1953). It is generally accepted that amino acids were present on the young Earth through endogenous and exogenous sources (see 1.4.1). Thus, at the first instance, it seems obvious that these amino acids could have been the building blocks of the first peptides.

It has been hypothesized that the primitive life may have used simple molecules such as peptide nucleic acids (PNA) as their genetic material (Nielsen, 1993; Nelson et al., 2000). The backbone of a PNA molecule consists of repeating units of diamino monocarboxylic acid linked through a peptide bond (Strasdeit, 2010). The backbone is also attached to purine and pyrimidine bases (Fig. 1). PNA is devoid of sugar and phosphate groups which makes it different from RNA and DNA. A PNA molecule is generally achiral (Nielsen and Egholm, 1999; Pooga et al., 2001). Therefore, the problem of homochirality associated with nucleic acids (RNA and DNA) could also be discarded in PNA. However, RNA and DNA should be exclusively homochiral to be functional in modern organisms.

1.1.1 Peptides and proteins

Peptides are an important class of biomolecules. However, their formation by condensation of amino acids is thermodynamically unfavorable under aqueous conditions (Lambert, 2008). Peptides are susceptible to hydrolysis in aqueous medium. Therefore, the formation of peptides with at least 20 amino acids (for catalytic activity) could have been difficult under the early Earth’s “chaotic” conditions (Bada, 2004). The formation of di- and tripeptides has been shown in Salt-Induced Peptide Formation (SIPF) experiments. These experiments were performed in the presence of high concentrations of NaCl and CuCl_2 . NaCl acts as a

dehydrating agent, and Cu(II) forms the complex with the amino acid (see 1.3.2) (Schwendinger and Rode, 1989, 1991; Rode and Schwendinger, 1990). However, longer peptides were not observed in the SIPF reaction within the experimental time. Rode (1999) assumed that macromolecules could be formed by increasing the reaction time of SIPF reactions. Questions have been raised concerning the availability of soluble Cu(II) on the young Earth. It has been assumed that dissolved Cu(II) was formed in the “green zones” of precambrian rocks in the presence of trace amounts of oxygen (Ochiai, 1978; Rode, 1999). The formation of homochiral peptides from a racemic mixture of amino acids is another unsolved problem. Homochirality is a prerequisite condition for the activity of an enzyme. Nowadays, proteins are required for the formation of nucleic acids and, in turn, nucleic acids are needed for protein synthesis. The apparent paradox of which came first, the protein or the nucleic acid, is referred to as the “chicken and egg problem”.

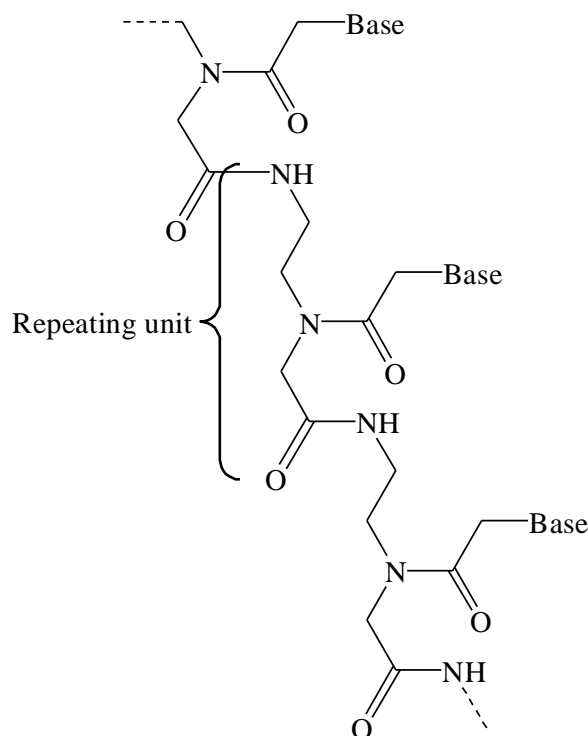


Fig. 1: Structure of a peptide nucleic acid (PNA). Base refers to purines (adenine, guanine) or pyrimidines (thymine, cytosine)

1.1.2 RNA world hypothesis

The “RNA world” hypothesis considers RNA as the first genetic material that could replicate before the evolution of DNA. In this approach, the existence of prebiotic RNA molecules is proposed that had both the properties of catalysis and information storage, similar to present-day ribozymes. According to this hypothesis, proteins were not required for the

synthesis of primitive RNA molecules because ribozymes could have functioned as catalysts. Thus, the “RNA world” hypothesis discards the necessity of protein catalysts for the origin of life (Gilbert, 1986; Joyce, 2002).

The nucleobases (purines and pyrimidines) required for the RNA nucleotide could have been abiotically synthesized (Orò, 1960; Orò and Kimball, 1961, 1962; Saladino et al., 2005). However, RNA as a first genetic material on the early Earth is a topic of debate. The formation of an RNA nucleotide requires a highly organized sequence of events. The nucleotides are unstable and can be hydrolyzed under aqueous conditions (Shapiro, 2000, 2007). Moreover, nucleobases were not synthesized in the Miller spark experiment. The backbone of RNA is made up of a ribose sugar and a phosphate group that are linked by phosphodiester bonds. Synthesis of sugars from formaldehyde by self-condensation is known as the formose reaction. However, the formation of ribose seems unlikely through formose reaction. For instance, the formose reaction requires strongly alkaline conditions and gives a mixture of sugars such as trioses, tetroses, and pentoses (Breslow, 1959). In subsequent steps, the ribose sugar has to react with the phosphate group and a nucleobase to form a nucleotide. The availability of phosphorus as phosphate in the early Earth’s anoxic atmosphere may also be questioned. In an experiment, Powner et al. (2009) have shown the synthesis of activated pyrimidine nucleotides from a reactant mixture.

A possibility to shift reaction equilibrium towards the synthesis of oligomeric biomolecules is to couple it with minerals and salts (Kitadai et al., 2011). In this manner the thermodynamic difficulty may be overcome. The thermodynamic barrier of synthesis and the instability of the biomolecules make their presence on the young Earth less probable (Shapiro, 2006). Therefore, both the PNA and RNA world hypothesis seems implausible as the first step in the origin of life.

1.1.3 Protometabolism and catalytic networks

A possible solution to the “chicken and egg” problem could be a protometabolism. It might be a more realistic approach to assume that a protometabolism had evolved prior to proteins and RNA molecules (Shapiro, 2007). For a protometabolism, a primitive compartment with semipermeability is required. This compartment can be a vesicle made of an amphiphilic molecular bilayer (Deamer et al., 2002) or colloidal FeS (Russell and Hall, 1997). In the presence of an energy source, e.g. an oxidation-reduction system, autocatalytic networks could develop. In an autocatalytic set, molecules involved in a reaction catalyze other reactions of this set. Under a steady supply of reactant molecules A and B, the initial products

AB and BA are constantly formed (Fig. 2). Once the first AB and BA molecules are synthesized they can catalyze the synthesis of other molecules e.g. AB₃B from AB and BB with BA as a catalyst (Fig. 2). Thus, the reactions of the set become collectively autocatalytic (Segré et al., 2000; Shapiro 2006; Kauffman, 2007). Thus, it may be assumed that the first protocells may have formed from simple metabolizing compartments that later evolved into organisms.

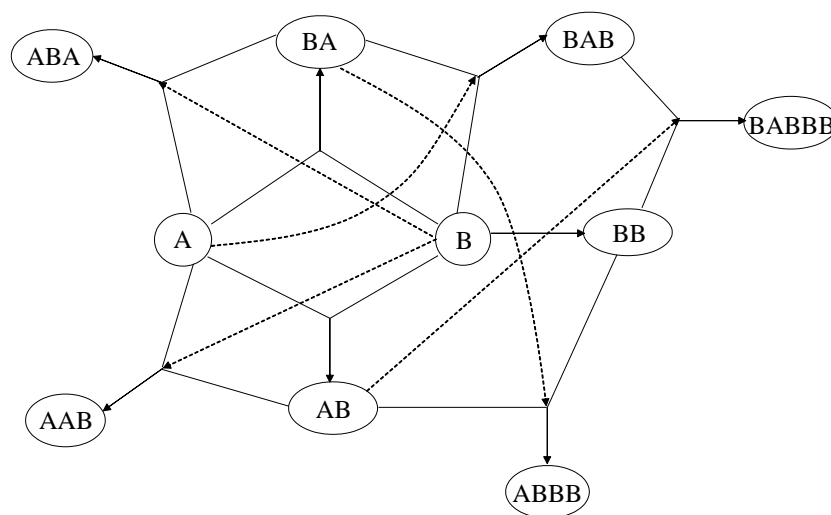


Fig. 2: An autocatalytic set of reactions with A and B as starting reactants. Solid arrows show the reaction paths and dotted arrows represent catalysis. Adapted from Kauffman (2007).

Considering an autotrophic origin, the first organisms survived on simple inorganic molecules, whereas the first heterotrophs may have used abiotically formed organic compounds (Peretó, 2005). Wächtershäuser (1990) proposed a chemoautotrophic origin of life that explains the use of energy from pyrite (FeS_2) formation for an autotrophic metabolism.

Prebiotic chemical evolution is not necessarily limited to Earth. It is also conceivable on other Earth-like planets such as Mars. Both planets had similarities regarding their climate and geology in early history (e.g. liquid water, active volcanoes, anoxic atmosphere, and meteoritic impacts).

1.2 Early climate and geological history of Earth and Mars

After the formation of the Solar System around 4.57 billion years (Ga) ago, both Earth and Mars were hot planets (Patterson, 1956). During the late heavy bombardment (LHB), water and organic molecules were brought to the surface of the Earth by meteorites and comets (Pizzarello and Shock, 2010).

1.2.1 Water and atmosphere on the early Earth

According to various studies, an early atmosphere of the Earth was mainly composed of N₂, CO₂, and H₂O vapor (Kasting, 1993; Kasting and Catling, 2003; Kasting and Howard, 2006; Shaw, 2008). It is assumed that the atmosphere of the primitive Earth had almost no O₂; hence, the ozone layer was absent (Kasting, 1993). Therefore, short-wavelength UV radiation may have reached the Earth's surface as on the present-day Mars. High energy UV radiation is well known to destroy organic molecules. However, in the ocean, organic molecules could have been protected from UV radiation (Cleaves and Miller, 1998). Various organic molecules (polymers) and inorganic salts present in the primitive ocean could have acted as UV absorbers.

It is often assumed that the first organic molecules have formed in the ocean or near coasts (Stetter, 1998; Nisbet and Sleep, 2001; Holm and Andersson, 2005; Bywater and Conde-Frieboes, 2005). For surface liquid water to be present, a planet must lie within the habitable zone, as for example Earth. Liquid water is considered essential for the origin of life. It may be also assumed that the molecules important for the origin of life had accumulated in the "primordial soup". Liquid water is sometimes referred to as the "universal solvent" because it can dissolve a large variety of substances. It is also required for the formation of clay minerals through weathering processes (Brack, 2002).

The terrestrial surface water probably comes from different sources. Comets that came from the outer regions of the solar system could have delivered large amounts of water (Owen and Bar-Nun et al, 1995; Davies et al., 1997). This is referred to as the "late veneer scenario". However, D/H isotope ratios indicate that only about 10 % of the present water was delivered by comets. Therefore, asteroids were assumed as the major source of water on the young Earth (Morbidelli et al., 2000). Recently, Raymond et al. (2009) and Alexander et al. (2012) have proposed that chondritic meteorites from the main asteroid belt between the orbits of Mars and Jupiter may have brought large quantities of water to the early Earth. Moreover, the D/H isotope ratio in micro-meteorites from Antarctica is in agreement with the D/H value of the present ocean (Lécuyer et al., 1998; Engrand et al., 1999). Therefore, it can be concluded that comets, asteroids, and micro-meteorites were the main contributors of water on the young Earth. Additionally, water could also be released from hydrated minerals and volcanic outgassing (Rubey, 1951).

The oldest known terrestrial minerals, the 4.3–4.4 Ga old Jack Hills zircons (ZrSiO₄) from Australia and the 4.2 Ga old zircons from northwestern Canada, possibly indicate the

presence of liquid water and a continental crust (Wilde et al., 2001; Mojzsis et al., 2001; Watson and Harrison, 2005; Harrison et al., 2005; Lizuka et al., 2006). However, the age of these zircons is still debatable (Hoskin, 2005; Nemchin et al., 2006). The general view is that 4.3–4.4 Ga ago the Earth was too hot to sustain liquid water. According to Valley (2006), the first ocean may have appeared around 4.2 Ga. The Isua sedimentary rocks in Greenland (Moorbath, 2005) and banded iron formations (BIFs) provide direct evidence for the presence of water around 3.8 Ga. Therefore, it is generally accepted that a permanent ocean was present around that time. The salt content of the ocean was nearly twice as large as the present value (Knauth, 1998). The pH value of the water possibly changed from weakly acidic in the early Hadean to nearly neutral in the late Hadean eon (Morse and Mackenzie, 1998). Hydrothermal systems could have been the main source of soluble salts on the primitive Earth (Derry and Jacobsen, 1988; Martin et al., 2006). The salinity of the sea water is mainly due to the chlorides of sodium, potassium, magnesium, and calcium (Pinti, 2005).

1.2.2 Geological history of Mars

Prebiotic chemical evolution on Mars could have taken place in the Noachian and Hesperian eons (Tanaka, 1986). The corresponding eons on Earth are the Hadean (4.5–3.8 Ga) and the early Archean (Fig. 3). The pre-Noachian period on Mars (4.6–4.1 Ga) had numerous large basin-forming impacts. The Noachian lasted from 4.1 to 3.7 Ga and was dominated by high rates of volcanism, valley formation, erosion, and weathering. These events led to the formation of phyllosilicates (Carr and Head III, 2010). In the early Hesperian, volcanism was still increasing at a high rate, whereas processes such as basin-forming impacts, valley formation, and erosion decreased considerably. Then, at the beginning of the Amazonian eon (3.0 Ga), the rate of volcanism had also slowed down. According to Bibring et al. (2006), the Martian geological time scale can also be divided in a different way to account for the surface alteration activities. These mineralogical eras are: the “Phyllosian” (4.5–4.1 Ga), the “Theiikian” (3.8–3.5 Ga) and the “Siderikian” (3.5 Ga to present) (Fig. 3). As the name suggests, the Phyllosian era was dominated by phyllosilicates which were formed by non-acidic aqueous alteration. Sulfates were formed in the Theiikian era by acidic aqueous alteration. The change from a non-acidic environment in the Phyllosian era to an acidic environment in the Theiikian era may be an indication of intense volcanic outgassing of H₂S and SO₂. Anhydrous ferric oxides were formed in the Siderikian era (Bibring et al., 2006).

Mars is smaller and lighter in comparison to Earth. Furthermore, several consecutive and large impacts may have contributed to an effective surface heating. Therefore, Mars had

lost its early atmosphere (Chassefière and Leblanc, 2004; Lammer et al., 2008). Additionally, it was proposed that non-thermal escape processes such as photochemical and ion escape account for the loss of an early Martian atmosphere (Chassefière and Leblanc, 2004). Moreover, large impacts on Mars may have been responsible for the heating of its core and mantle. This could have resulted in the loss of its internal dynamo due to the loss of convection currents. Consequently, Mars lost its magnetic field (Acuña et al., 1998). Due to the absence of an atmosphere, high amounts of cosmic and UV radiation would have been able to reach the Martian surface, as it is still the case today (Dartnell et al., 2007). The hostile conditions on Mars could have made it difficult for life to survive. Currently, there are no indications for the former or present-day existence of life on Mars.

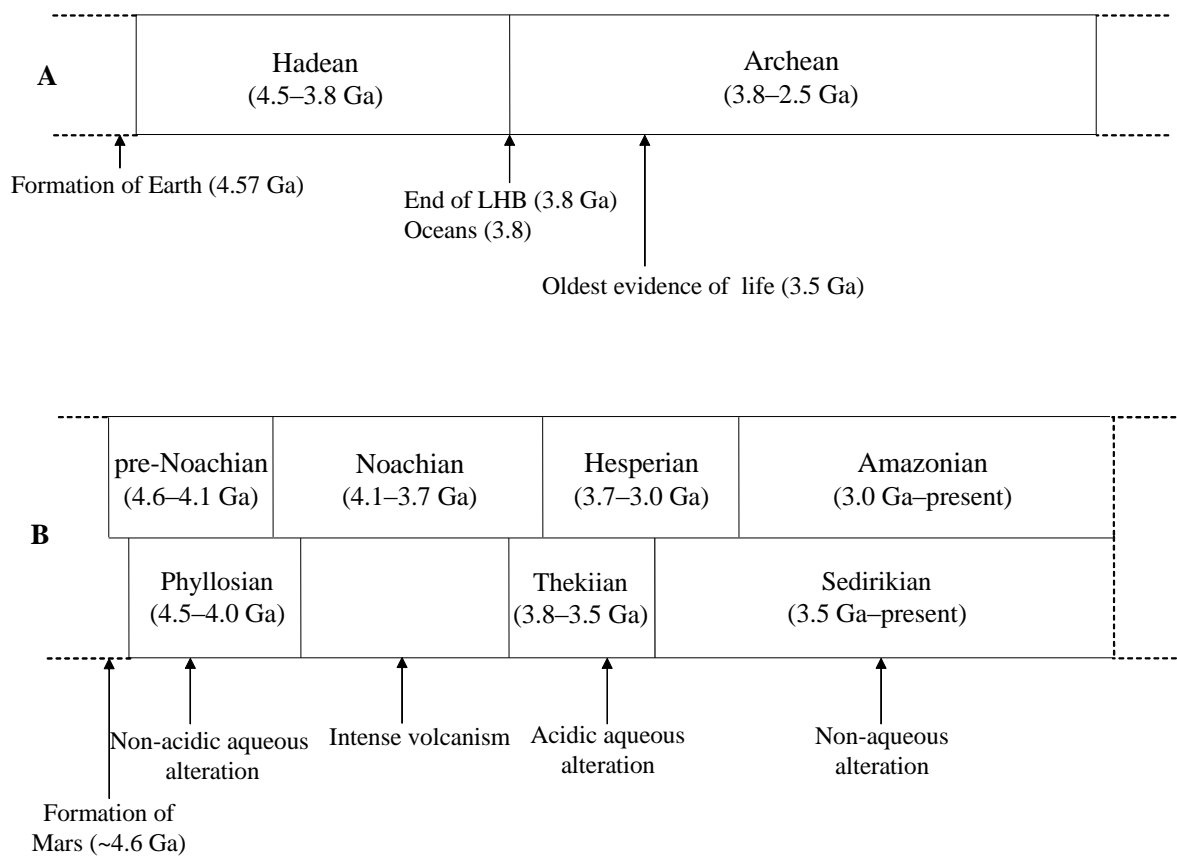


Fig. 3: Geological time scales and important events on (A) Earth and (B) Mars. LHB = Late heavy bombardment

1.2.3 Volcanism on Earth and Mars

Volcanism was more intense in the early history of Earth and Mars (Nimmo and Tanaka, 2005; Martin et al., 2006). On the present Earth, volcanism is mainly caused by the movement of tectonic plates (e.g. the Pacific Ring of Fire volcanoes). In addition, hot-spot volcanoes also exist (e.g. Hawaiian volcanoes). Hot-spot volcanoes rise from mantle plumes

and lithospheric extensions that allow the shallow melt to rise. Mars has shield volcanoes that are mainly present in the Tharsis and Elysium Planitia regions. The large shield volcanoes located in the Tharsis region include Olympus Mons, the largest volcano in the Solar System (Greeley and Spudis, 1981).

Volcanism could have played various important roles in prebiotic chemical evolution: (i) Volcanic heat is considered a significant source of energy available for prebiotic syntheses on the primitive Earth (Fox and Harada, 1961; Harada and Fox, 1964). (ii) In simulation experiments, various organic molecules were formed from a mixture of volcanic gases (Johnson et al., 2008). (iii) The dust particles and gases released by volcanic eruptions could have shielded the Earth's surface from short-wavelength UV radiation and thus prevented organic molecules from decomposition. (iv) Aqueous alteration of volcanic rock led to the formation of various clay minerals. Clay minerals are believed to be important in prebiotic organic syntheses.

1.3 Minerals of possible relevance to prebiotic chemistry

1.3.1 Clay minerals

Formation of clay minerals

Clay minerals have diverse properties and widespread appearance on Earth and Mars. For instance, montmorillonites, nontronites and kaolinite were recently found on Mars (Poulet et al., 2005, 2008; Mangold et al., 2007; Bishop et al., 2008; Mustard et al., 2008). Weathering and diagenesis of rocks and volcanic ash are major processes by which the clay minerals could have formed on the early Earth and Mars (Jackson, 1959; Fripiat and Cruz-Cumplido, 1974; Ponnampereuma et al., 1982; Righi and Meunier, 1995; Hillier, 1995; Ferris, 2006). Additionally, smectites can be formed by the interaction of hot brine in geothermal systems (Bischoff, 1972) and by hydrothermal alterations (Inoue and Utada, 1983; Çelik et al., 1999). The rate of formation of minerals is influenced by physical and chemical factors such as pressure, temperature, and pH (Hazen et al., 2008). Alkaline conditions favor the formation of smectites, whereas acidic conditions enhance the formation of kaolinite (Jackson, 1959). Recently, it has been reported that on Noachian Mars, Fe and Mg rich clays could have formed from water-rich magma by direct precipitation (Meunier et al., 2012).

Structures and properties of clays

Clay minerals are phyllosilicates having layered structures. The layers are composed of SiO_4 tetrahedral and AlO_6 octahedral units. Clay minerals have 1:1 layers or 2:1 layers (Fig. 4). In 1:1 layered clay, one tetrahedral silica layer is linked to the alumina octahedra (e.g. kaolinite). In 2:1 layered clays, the two tetrahedral silica layers sandwich an aluminium octahedral layer (e.g. montmorillonite and nontronite) (Brigatti et al., 2006). The octahedral layer is negatively charged, which is mainly due to isomorphous substitution. Isomorphous substitution is the replacement of metal ions by lower-charge cations of similar size (e.g. Al^{3+} for Si^{4+} , Mg^{2+} or Fe^{2+} for Al^{3+}). The negative charge is compensated by Na^+ , Ca^{2+} , Mg^{2+} , K^+ or Fe^{3+} cations present in the interlayer spaces (Fripiat and Cruz-Cumplido, 1974; Anderson and Banin, 1975).

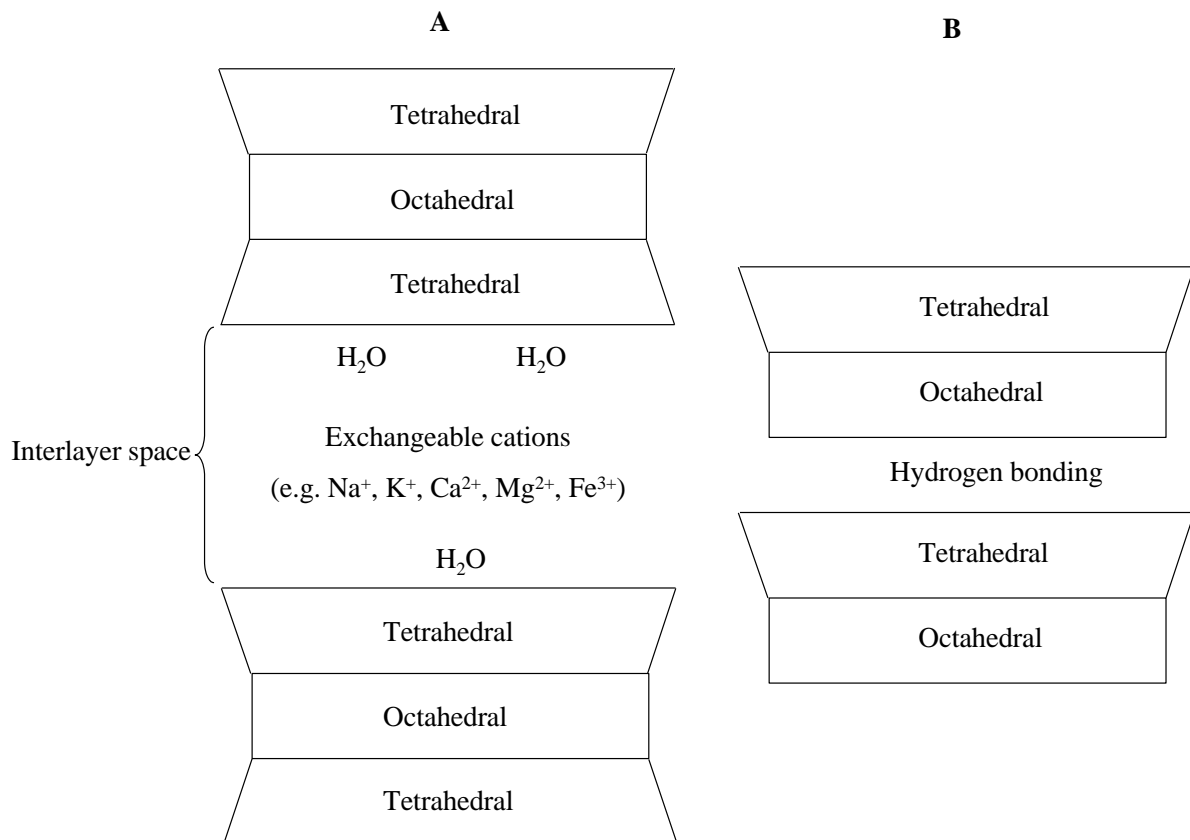


Fig. 4: Schematic diagram of (A) smectite and (B) kaolin clays.

Kaolinite is a non-swelling clay (Swartzen-Allen and Matijevic, 1974). The laminae (two or more layers) of kaolinite do not disperse readily in water due to strong hydrogen bonding. In contrast, smectites (e.g. montmorillonite) are swelling clays which refers to their ability to absorb large quantities of water in their interlayer spaces due to the absence of

hydrogen bonding. Moreover, the swelling behavior of clay minerals depends on the nature of exchangeable cations (Foster, 1954).

Kaolinite has low cation exchange capacity as compared to montmorillonite (Mitra and Rajgopalan, 1952). The cation exchange capacity of kaolinites can be enhanced by increasing the pH (Ma and Eggleton, 1999). Some important characteristic properties of montmorillonite and kaolinite are compared in Table 1.

Tab. 1: Surface characteristics of montmorillonite and kaolinite.

Characteristics	Montmorillonite	Kaolinite
Layer structure (tetrahedral:octahedral layer)	2:1	1:1
Total specific surface area ($\text{m}^2 \text{g}^{-1}$)	700–800	25–50
Cation exchange capacity (meq g^{-1})	0.8–1.2	0.02–0.1
Swelling in water ($\text{cm}^3 \text{g}^{-1}$)	0.5–20*	0–0.3

* Depending upon exchangeable cation

Data taken from Anderson and Banin, 1975

Cairns-Smith (1986) proposed a model, “the clay-locale hypothesis” for the origin of life. According to this model, a pre-existing inorganic matrix (e.g. clay minerals) acts as a template for the formation of organic molecules. Clay minerals are considered the first information-carrying genetic materials which were later replaced by RNA or DNA (Cairns-Smith, 2008). Clay minerals may have played a key role in various stages of prebiotic chemical evolution on the young Earth (Bernal, 1949, Ponnampereuma, 1982). Some important role of clay minerals are:

- 1) Clay minerals can catalyze the synthesis of organic molecules from a mixture of CO , H_2 , and NH_3 (Yoshino et al., 1971).
- 2) Clay minerals can absorb amino acids from a dilute solution and provide a matrix for polymerization (Lahav and White, 1980; Ponnampereuma, 1982).
- 3) Clays may have protected biomolecules such as polypeptides and nucleotides from hydrolysis and UV radiation (Paecht-Horowitz et al., 1970; Bernal, 1949; Scappini et al., 2004).
- 4) According to some reports, clays have been involved in the origin of homochirality of amino acids (Degens et al., 1970; Jackson, 1971 a, b; Julg and Ozias, 1988). The selective adsorption of D- and L-amino acids with subsequent polymerization may represent a possible mechanism for the production of homochiral peptides on the

prebiotic Earth (Hazen, 2001). However, chirality associated with the clay minerals is unclear.

1.3.2 Chlorides

The gaseous hydrogen chloride emitted by volcanoes can dissolve in water containing metal ions. The metal ions (e.g. Na^+ , K^+ , Ca^{2+} , Mg^{2+}) are released by the weathering of minerals. After the evaporation of water, chloride deposits remain. It has been reported that sublimates from the Kilauea volcano were composed of various metal chlorides. The sublimates could later form chloride deposits (Naughton et al., 1974).

It is generally accepted that various metal chlorides could have been present in the early ocean (Levine et al., 1982; Pinti, 2005). This, in turn, indicates the abundance of chloride deposits on the young Earth. The wide-spread presence of chlorides has been identified on Mars by infrared images from the Mars Odyssey Thermal Emission Imaging System (THEMIS) (Osterloo et al., 2008; Glotch et al., 2010). Moreover, sodium chloride was also reported in the Nakhla Martian meteorite (Gooding et al., 1991; Bridges and Grady, 2000). The identification of chloride deposits on Mars indicates the presence of liquid water in the early Martian history.

Salts are known to play an important role in the formation of smaller peptides in Salt-Induced Peptide Formation (SIPF) experiments (Schwendinger and Rode, 1989, 1991; Rode and Schwendinger, 1990). The SIPF reaction occurs in concentrated NaCl solutions that also contain a relatively high concentration of CuCl_2 . Sodium chloride acts as a dehydrating agent that enables the polymerization process in aqueous medium. It was predicted that at high concentrations, the hydration shells of Na^+ and Cl^- ions are “unsaturated” and thus bind with water molecules that are released during the condensation reaction (Limtrakul and Rode, 1985, Limtrakul et al., 1985). Thus, NaCl can shift the equilibrium towards the peptide formation (Schwendinger and Rode, 1981, 1989; Rode and Schwendinger, 1990). In a recent study, formation of peptides has been found in the presence of other chlorides such as SrCl_2 and BaCl_2 (Kitadai et al., 2011).

1.3.3 Carbonates

A high concentration of CO_2 on the early Mars was estimated because of frequent volcanic outgassing. CO_2 dissolves in water to form carbonic acid (H_2CO_3), which can cause the weathering of minerals thereby releasing ions (e.g. Ca^{2+} , Mg^{2+}) into water. Afterwards, these metal ions can precipitate as their carbonates (Gooding, 1978; Harvey, 2010). On early Mars,

the green-house effect caused by CO₂ may have raised the surface temperature to values considerably higher than today. As a consequence, liquid water could have existed on the surface of Mars (Kahn, 1985; Harvey, 2010). The presence of carbonates indicates a wet and warm climate in early Martian history (Pollack et al., 1987; Kasting, 1991; Harvey, 2010). According to Morse and Marion (1999), the precipitation of carbonates on the early Mars might have been similar as in the Earth's Hadean eon.

Magnesium carbonates are widely distributed in the Martian dust and were especially detected on the outcrops of Gusev crater and in the Nili Fossae region (Lellouch, 2000; Bandfield, 2003; Ehlmann et al., 2008; Palomba et al., 2009; Cloutis et al., 2010; Morris et al., 2010). They are also present in Martian meteorites such as EETA79001 and ALH84001 (Gooding et al., 1988; Clayton and Mayeda, 1988; Harvey, 1996; Bridges et al., 2001). In some cases, carbonates were found in association with sulfates (Gooding, 1988). However, only trace amounts of carbonates are reported. This may indicate that the formation of carbonates was inhibited or their deposits have been destroyed by the acidic water (H₂SO₄) produced through the volcanic degassing of SO₂ (Fairén et al., 2004; Bullock and Moore, 2007; Halevy et al., 2007). Hidden carbonate deposits at depth and/or embedded inside other minerals could also be the reason for the detection of carbonates in trace amounts (Harvey, 2010).

Carbonates might have been important for prebiotic chemical evolution. For instance, Saladino et al. (2001) have obtained a high yield of purine from formamide in the presence of CaCO₃. In another work, it has been shown that calcite selectively adsorbed one enantiomer from a solution containing a racemic amino acid (Hazen et al., 2001).

1.3.4 Sulfates

H₂O (water vapor), CO₂, SO₂, and H₂S are the major gases released during volcanic eruptions. The sulfur containing gases SO₂ and H₂S could have been oxidized by OH and O radicals to sulfate aerosols (sulfuric acid) under early Earth's anoxic atmosphere (DeWitt et al., 2010). These radicals were produced by the photolysis of H₂O, CO₂, and SO₂ (Kasting et al., 1989; Pavlov and Kasting, 2002). Subsequently, the sulfate aerosols could have dissolved in water to form acidic solutions. The acidic water then reacted with metal ions released by the weathering of minerals. The solutions gradually became concentrated by evaporation, and eventually sulfate deposits have formed (Fan et al., 2006). Wang et al. (2006) have suggested that similar conditions could have occurred on the early Mars.

Sulfate deposits are expected to have accumulated in the late Noachian and Hesperian eon due to intense volcanic activity. In fact, sulfates have been detected on the Martian surface by the Viking landers (Clark et al., 1981), Mars Pathfinder (Rieder et al., 1997), OMEGA (Observatoire pour la Minéralogie, l'Eau, les Glaciers, et l'Activité) on Mars Express (Bibring et al., 2005) and Mars exploration rovers (Wang et al., 2006). Calcium sulfates (gypsum and bassanite) have been identified in several regions on Mars (Langevin et al., 2005; Gendrin et al., 2005; Bibring et al., 2005, 2006; Fishbaugh et al., 2007; Kuzmin et al., 2009; Wray et al., 2010). Magnesium sulfate minerals (polyhydrated magnesium sulfate and kieserite) have been detected in Valles Marineris (Noe Dobrea et al., 2008). The presence of sulfates also indicates a warm and wet early Mars.

1.3.5 Other minerals

Other non-clay minerals (e.g. zeolites, feldspar, pyrite, borates and zircon) may have also been important in prebiotic chemical evolution. Zeolites and feldspar are formed by the process of crystallization of the volcanic ash (Smith, 1998 a). Zeolites have various cations in their porous structures. These cations can be readily exchanged for other ions present in the surrounding solution (cation-exchange). Moreover, zeolites can provide surfaces for the adsorption of reactants. Therefore, zeolites can act as catalysts for polymerization (Zamaraev et al., 1997). Feldspar has honeycomb-like structures that can function as micro-reactors. These organized structures can host the reactant molecules and foster the formation of products (Parsons et al., 1998; Smith 1998a, b). Furthermore, they may also function as a primitive cell wall that can protect biomolecules from hydrolysis and UV radiation (Parsons et al., 1998). Wächtershäuser (1988, 1990, 1993) has proposed the “Iron–Sulfur World” hypothesis according to which pyrite formation could have provided energy for a primitive metabolism. The synthesis of pentose sugars from formaldehyde and glyceraldehyde under alkaline conditions has been demonstrated in the presence of various borate minerals (Ricardo et al., 2004). Saladino et al. (2010) have shown the synthesis of nucleic acid bases and their derivatives (e.g. adenine, isocytosine) in the presence of various zirconium minerals (e.g. ZrO_2 and $ZrSiO_4$). The experiments described by Ricardo et al. (2004) and Saladino et al. (2010) may be, however, of limited prebiotic relevance.

1.4 Prebiotic amino acids

It is generally accepted that simple molecules such as H₂O, N₂, CO₂ and CH₂O were present on the young Earth. These simple molecules could have been the precursors of more complex organic molecules such as amino acids. Solar UV radiation, electric discharge, and geothermal energy were the possible sources of energy available on the primitive Earth (Deamer and Weber, 2010). In addition to endogenous (terrestrial) sources, amino acids were also available on the young Earth through exogenous delivery.

1.4.1 Amino acid sources

Endogenous sources

Amino acids may have been formed on the prebiotic Earth by Urey–Miller type syntheses (Miller, 1953, 1955; Schlesinger and Miller, 1983). Miller (1953) has demonstrated the production of amino acids in the presence of reducing gases (CH₄, H₂, NH₃) and electrical discharges. Various energy sources such as UV radiation, cosmic rays, X-rays, shock energy impacts, and simulated volcanic lightning were also used (Bar-Nun et al., 1970; Lemmon, 1970; Sagan and Khare, 1971; Miller, 1987; Johnson et al., 2008). Some common amino acids formed during discharge experiments are shown in Figure 5. It is generally believed that the Earth's early atmosphere was mainly composed of CO₂ and N₂. The dominance of these gases suggests that the atmosphere was not strongly reducing, but redox neutral (Kasting, 1993). According to some reports, the synthesis of amino acids under redox neutral atmospheric conditions is difficult (Abelson, 1966; Folsome et al., 1981; Schlesinger and Miller, 1983; Plankensteiner et al., 2004). In contrast, Cleaves et al. (2008) have shown the effective synthesis of amino acids from a mixture of redox-neutral gases (CO₂, N₂ and H₂O) in the presence of the antioxidant ascorbic acid. Later, Kuwahara et al. (2012) have used ¹³C-labeled CO₂ to identify the carbon source for the amino acids. The experiments were performed with redox-neutral gases in the presence of spark discharge and ascorbic acid. The results strongly indicated that the amino acids were hydrolysis products of ascorbic acid and were not formed from ¹³CO₂. Thus, the synthesis of amino acids seems unlikely from a mixture of redox-neutral gases. Additionally, the results were supported by the fact that aminoacetonitrile, the precursor of glycine, was also not detected in the spark discharge experiments with redox-neutral gases (Kuwahara et al., 2011, 2012).

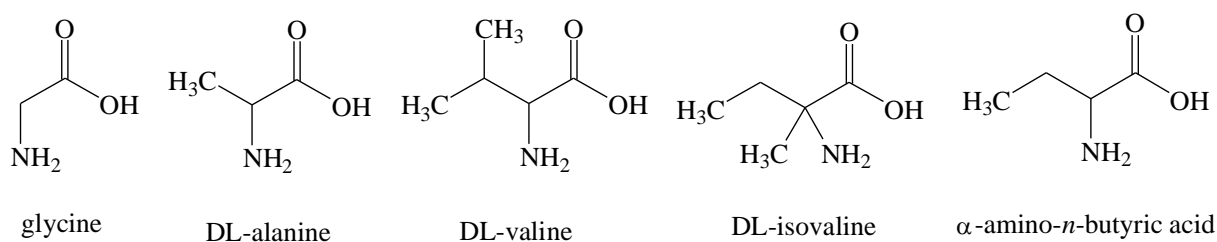


Fig. 5: Some common amino acids found in electric discharge experiments.

Furthermore, amino acids may have been formed under hydrothermal conditions (Hennet, 1992; Marshall, 1994; Alargov et al., 2002; Simoneit, 2004; Holm and Andersson, 2005). Amino acids and their corresponding oligopeptides were reported as products in simulation experiments for hydrothermal systems (Imai et al., 1999; Kawamura et al., 2005). However, amino acids produced under hydrothermal conditions of high temperature and pressure would probably decompose faster than they form. Thus, hydrothermal systems may act more as a sink than a source of amino acids (Miller and Bada, 1988; Bada et al., 1995).

Exogenous sources

Amino acids are also delivered to the Earth by meteorites and comets (Cronin and Pizzarello, 1983; Botta et al., 2002; Llorca, 2004, 2005). For instance, glycine was detected in samples from the Stardust space mission (Glavin et al., 2008; Elsila et al., 2009). Moreover, oligopeptides such as 2,5-diketopiperazine (DKP) and linear diglycine were also reported from the meteorites Yamato-791198 and Murchison (Shimoyama and Ogasawara, 2002). This indicates a possible mode of delivery of organic molecules to the prebiotic Earth's surface.

Micrometeorites are another important extraterrestrial source of abiotic amino acids (Glavin and Bada, 2001). Every year about 40,000 tons of micrometeorites with size $\leq 200 \mu\text{m}$ reach the Earth's surface (Love and Brownlee, 1993). Various amino acids have been found in micrometeorites from Antarctica. Among them, α -aminoisobutyric acid (AIB) is considered especially important. However, AIB was detected only in one sample out of five samples studied (Brinton et al., 1998). Subsequent studies by Glavin et al. (2004) have also suggested that the Antarctica micrometeorites are not a potential source of AIB. Therefore, AIB was regarded as a terrestrial contaminant. In contrast, Matrajt et al. (2004) have found significant amounts of AIB in micrometeorite samples collected from various regions of Antarctica. According to them, micrometeorites were important sources of AIB and other amino acids on the early Earth.

Amino acids have not yet been detected in the interstellar medium (ISM) in contrast to their nitrile precursors (Kalenskii et al., 2000; Pankonin et al., 2001). However, the synthesis of amino acids was demonstrated in different experiments simulating the ISM (Bernstein et al., 2002; Brack, 2007; Elsila et al., 2007). The availability of various amino acids from endogenous and exogenous sources and their relative abundances are summarized in Table 2.

Tab. 2: Relative abundances of amino acids from various prebiotically relevant sources.

Amino acid	Endogenous source	Exogenous source	
	Miller-Urey synthesis (electric discharge experiments)	Murchison meteorite	Murray meteorite
Glycine	*****	*****	*****
Alanine	*****	*****	*****
β -Alanine	**	**	*****
α -Amino- <i>n</i> -butyric acid	*****	***	***
α -Aminoisobutyric acid	**	*****	—
Valine	**	***	—
Isovaline	**	**	*****
Norvaline	***	***	—
Aspartic acid	***	***	***
Glutamic acid	**	***	***
Proline	*	***	—
β -Amino- <i>n</i> -butyric acid	*	*	***
β -Aminoisobutyric acid	*	*	**

Mole ratio to glycine (= 100): * <0.5, **0.5 – 5, ***5 – 50, *****>50

—: not reported

Adapted from Miller (1987) and Zaia et al. (2008)

1.4.2 Possible origins of biomolecular homochirality of amino acids

Homochirality appears to be a key factor for the existence of life. Biomolecules (proteins and sugars) associated with the present life forms are homochiral. For instance, amino acids in proteins have only the L-configuration, while the sugars present in nucleotides are entirely of the D-configuration. D-amino acids are less common than the L-forms, but are nevertheless important for living organisms. For example, a bacterium releases D-amino acids during its non-growth phase (stationary phase) to decrease the cell wall formation (Lam et al., 2009).

D-amino acids are also important for the osmoregulation in marine invertebrates (Friedman, 1999) and for the neurotransmission in mammals (Wolosker et al., 2008). Therefore, the biological importance of D-amino acids must not be neglected. However, a racemic mixture of biomolecules usually is a problem for present life forms. For example, the chiral purity of nucleotides is important for the double-stranded helical structure of DNA because the presence of any L-sugar in place of D-sugar would prevent the hydrogen bonding between nucleic acid bases (Goldanskii et al., 1986). Similarly, homochiral peptides are preferred (Schmidt et al., 1997) as the inclusion of D-amino acid disrupts their helical arrangement (Krause et al., 2000).

Biotic and abiotic theories have been proposed for the origin of homochirality (Fig. 6). According to the biotic theory, D- and L-organisms may have appeared together on the young Earth, and chance events eliminated one of the forms (Balasubramanian, 1983, 1985). Biotic theories for the origin of homochirality are less common as compared to abiotic ones. According to abiotic theories, the development of homochirality preceded the origin of life on Earth.

Abiotic theories can be further classified into chance and determinant mechanisms (Bonner, 1991a, 1991b, 1995). In chance mechanisms, there is an equal probability for the appearance of either D- or L-enantiomers. Frank (1953) proposed a model where chiral molecules can catalyze the production of their own enantiomer while they inhibit the synthesis of the other enantiomer. Soai's group (Soai et al., 1990, 1995) have demonstrated the enantioselective autocatalytic formation of pyridyl alkanol and pyrimidyl alkanol. Kondepudi (1990), for the first time, demonstrated the chiral symmetry breaking or total spontaneous resolution in the formation of sodium chlorate (NaClO_3) crystals. In his experiments, homochiral crystals (either left- or right-handed) of NaClO_3 were found when crystallized from an aqueous solution that was stirred. A role of clay minerals in the origin of homochirality has also been assumed. It was reported that some clay minerals (e.g. kaolinite, bentonite) exhibit stereoselectivity for L-aspartic acid, L-leucine, L-alanine, and D-glucose (Degens et al., 1970; Jackson, 1971a, 1971b; Bondy and Harrington, 1979; Yamagishi, 1987). However, the validity of these results has been questioned (McCullough and Lemmon, 1974; Flores and Bonner, 1974). Thus, chirality associated with clay minerals is ambiguous. A small enantioselective adsorption of alanine was also observed for quartz crystals (Bonner et al., 1974, 1975; Bonner and Kavasmaneck, 1976; Kavasmaneck and Bonner, 1977). Quartz crystals exist as d- and l-enantiomorphs. Initially, it was believed that l-quartz has a predominance of ~1 % over its d-enantiomorph on the surface of the Earth (Tranter, 1985).

However, this finding was later discarded, and it was instead suggested that there is an equal abundance of both enantiomorphs (Klabunovskii and Thiemann, 2000; Klabunovskii, 2001). Hazen et al. (2001) have demonstrated the preferential adsorption of D- or L-aspartic acid from a racemic solution on different surfaces of calcite crystals.

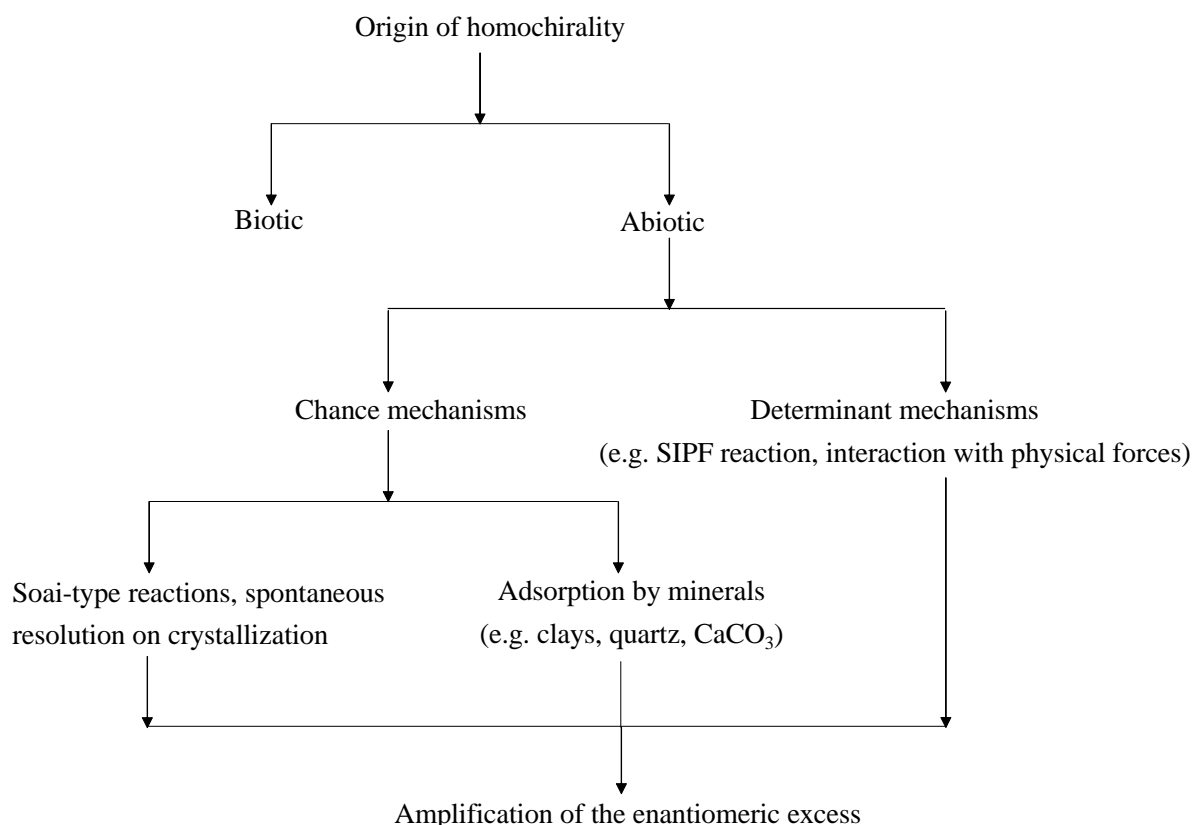


Fig. 6: Theories for the origin of homochirality.

Determinant mechanisms include enantioselective synthesis of chiral molecules due to the interaction with physical forces such as electric, magnetic and gravitational fields and circularly polarized light (CPL) (Norden, 1977; Gilat, 1985; Bonner and Rubenstein, 1987; Bonner, 1995; Bailey et al., 1998; Nishino et al., 2001). However, in many cases significant enantiomeric excess was not found (Bonner, 1991a). Determinant mechanisms also include Salt-Induced Peptide Formation (SIPF) where homochiral peptides are formed in the presence of NaCl and CuCl₂ (Plankensteiner et al., 2005). Sandars (2003) proposed a “toy model” for the growth of homochiral polymers. According to this model, polymer growth can only be catalyzed by monomers of the same chirality. The polymerization process is terminated by the monomers of the opposite chirality. The revised toy model by Brandenburg

et al. (2005) includes the breaking of the polymer at a point after reaching an appreciable length.

Amplification of enantiomeric excesses by sublimation

Abiotically synthesized amino acids are racemic. However, considerable L-enantiomeric excesses of some amino acids from meteorites have been reported (Cronin and Pizzarello, 1999; Pizzarello and Cronin, 2000; Pizzarello et al., 2008). Amino acids with small enantiomeric excess were found in less altered meteorites (CR meteorites), whereas amino acids with large enantiomeric excess were observed in less pristine meteorites (CM and CI meteorites) (Glavin and Dworkin, 2009). The mechanism responsible for the production of L-enantiomeric excess of amino acid could be sublimation (Perry et al., 2007; Fletcher et al., 2007). During the atmospheric entry, the surface of a meteorite is comparatively more heated than its core. This creates a temperature gradient which facilitates the sublimation of amino acids. As a result, the L-ee of amino acids can increase in different parts of a meteorite or asteroid by partial sublimation. Fletcher et al. (2007) studied the effect of sublimation on a wide range of amino acids with different initial enantiomeric excesses. They found that partial sublimation gave enantiomerically enriched sublimates. For instance, ~82 % L-enantiomeric excess in the sublimate was observed for leucine. While Perry et al. (2007), under different experimental conditions, have found no change in the enantiomeric excess of amino acids except for serine which forms octamers in the gas phase.

The different experimental results can be explained on the basis of the phase behavior of amino acids (Blackmond, 2007; Blackmond and Klussmann, 2007). Usually, the vapor pressures of enantiomeric (L or D) and racemic (LD) crystals of an amino acid are different. Some amino acids show so called conglomerate crystallization. Every crystal in a conglomerate is composed of either L- or D-enantiomers with no direct intermolecular interaction (Blackmond and Klussmann, 2007). With the onset of sublimation, both L- and D-crystals starts subliming together as they have identical vapour pressures. In contrast, if LD crystals exist, samples can be prepared that consist of enantiomerically pure L-crystals and racemic crystals. Such samples can show a difference in the rate of sublimation due to the different vapour pressures of L- and racemic crystals. Thus, samples that have the same L-enantiomeric excess but were prepared by different methods (either by mixing L- and D-crystals or L- and LD-crystals) exhibit differences in the sublimation behavior of the amino acid.

Amino acids such as isovaline and isoleucine were found to have significant L-enantiomeric excesses in carbonaceous chondrites. Isovaline was reported to have L-enantiomeric excesses of ~18.5 % in Murchison meteorite, ~6.0 % in the Murray and ~15.2 % in the Orgueil meteorite (Cronin and Pizzarello, 1999; Pizzarello et al., 2003; Glavin and Dworkin, 2009). In recent studies, Pizzarello et al. (2012) have found a large enantiomeric excess of ~60 % for isoleucine diastereomers. Meteoritic L-enantiomeric excesses of some α,α -dialkyl- α -amino acids are summarized in Table 3. In contrast to α,α -dialkyl- α -amino acids, amino acids with α -H (e.g. alanine, valine) were found to exist as racemic mixtures in meteorites, possibly because they can be easily racemized under aqueous conditions by the action of heat. The lack of an α -H atom prevents the racemization in α,α -dialkyl- α -amino acids (Pollack et al., 1975). The amplification of L-enantiomeric excess has been shown on the basis of the solubility difference between pure L and DL crystals (Levine et al., 2008; Breslow and Cheng, 2009).

Tab. 3: L-enantiomeric excess (%) of α,α -dialkyl- α -amino acids from the meteorites Murchison and Murray.

Amino acid	Murchison	Murray
2-Amino-2-methylbutanoic acid (Isovaline)	18.5	6.0
2-Amino-2,3-dimethylbutanoic acid	2.8	1.0
2-Amino-2-methylpentanoic acid	2.8	1.4
2-Amino-2,3-dimethylpentanoic acid	7.0	1.0

Adapted from Cronin and Pizzarello (1999); Pizzarello et al. (2003); Glavin and Dworkin (2009)

1.4.3 Thermal properties of amino acids

Various processes can occur during the thermal treatment of amino acids. For instance, glycine, alanine, and serine can sublime without complete decomposition (Gross and Grodsky, 1954). In addition, cyclic dipeptides were also formed during the sublimation process (Ostwald et al., 1952). Further, amino acids can undergo decarboxylation (loss of a carboxyl group by release of CO₂) producing amines with one carbon atom less than in the original carbon chain. Additionally, amino acids such as asparagine, aspartic acid, cysteine and glutamine can release large amounts of ammonia by deamination processes (Sohn and Ho, 1995). Moreover, amino acids can be completely pyrolyzed at higher temperatures (Ratcliff et al., 1974). Merritt and Robertson (1967) have analyzed the pyrolysis products of amino acids and peptides by gas chromatography–mass spectrometry. Complete pyrolysis of

glutamic acid was observed at 400 °C, whereas glycine, alanine, valine, leucine and AIB did not completely decompose even at 500 °C (Douda and Basiuk, 2000). In addition to amino acids, their respective cyclic dipeptides were also found at these temperatures. These results are relevant to the survivability of amino acids and peptides during their extraterrestrial delivery (Basiuk and Navarro-González, 1998; Douda and Basiuk, 2000). Amino acids are not only interesting as building blocks of proteins, but they may have also been the starting material for the prebiotic formation of other organic molecules such as pyrroles and porphyrins (Yusenko et al., 2008; Fox and Strasdeit, 2013). Another possible mode of decomposition of amino acids is “homolysis” that leads to the formation of saturated and unsaturated hydrocarbons (Ratcliff et al., 1974). Additionally, there are other significant secondary decomposition processes which include the formation of N-alkylaldimines and nitriles. N-alkylaldimines and nitriles are formed from aldimines which are the decomposition products of amines or cyclic dipeptides (Ratcliff et al., 1974).

1.5 Aims and objectives

The climatic and geological conditions of the early Earth and Mars might have been similar on both planets. For instance, both Earth and Mars had active volcanism and liquid water in their history. Various clay minerals and amino acids are believed to have been present on Earth during the time of prebiotic chemical evolution. Recently, clay minerals (phyllosilicates) were also identified on Mars. Therefore, it can be expected that Earth and Mars might had similar chemistry in the early times. Amino acids probably played an important role on the young Earth. For instance, amino acids might have interacted with the clay minerals near volcanic coasts. In addition, amino acids could have also come in contact with sea water in the rock pools. The aim of the present work is to elucidate the thermal behavior of amino acids, especially in inorganic matrices (phyllosilicates, salt crusts and sea salt mixtures, terrestrial and Martian soil simulants). The specific objectives of the thesis are to study:

1. The thermal behavior of glycine and glycine homopeptides in the absence of any inorganic matrices at different temperatures. Glycine was primarily chosen because it is the simplest amino acid and comparatively reactive.
2. The protection of glycine by various salts and salt mixtures at different temperatures.

3. The influence of various clay minerals on the chemical behavior of prebiotically relevant amino acids, such as glycine, alanine, valine, and isovaline. These amino acids are commonly found in carbonaceous meteorites and Urey–Miller–type syntheses.
 - 3.1 To study and compare the loading rates of glycine in different phyllosilicates.
 - 3.2 To investigate the possible role of phyllosilicates in the protection of glycine when exposed to high temperatures. Such temperatures could be possible at volcanic coasts and near the meteorite impacts.
 - 3.3 To compare the efficiency of the phyllosilicates in the polymerization of glycine.
 - 3.4 To compare the results obtained from objectives 3.2 and 3.3 with those obtained with terrestrial volcanic rock and Martian soil simulants.
 - 3.5 To study the influence of montmorillonite on chiral amino acids (e.g. alanine, valine, and isovaline) at different temperatures and durations of thermal treatment. The results were also to be compared with the experiments obtained in the absence of montmorillonite.

2 Results and Discussion

2.1 Thermal treatment of neat glycine and glycine homopeptides

2.1.1 Thermal treatment of neat glycine

It has been reported that a black residue was formed when glycine was heated at 260–280 °C (Heyns and Pavel, 1957a, 1957b). The authors assumed that this black residue was a polymeric substance which had properties similar to humic acid. Therefore, it was named thermo-melanoid. In this section, the results of a re-investigation of the thermal properties of glycine (Hgly) will be presented and discussed. The heating experiments were performed with neat glycine from 120 to 350 °C. All experiments were conducted under an atmosphere of pure nitrogen. Nitrogen was used to simulate an early atmosphere of the Earth, which was non-oxidizing and probably contained nitrogen as the major constituent (Kasting, 1993; Kasting and Howard, 2006; Shaw, 2008). Moreover, it acted as a carrier gas to transport the volatile products, which formed during the experiment, out of the furnace. The properties of residues obtained after the thermal treatment of neat glycine at different temperatures are summarized in Table 4 (see page 30). The residues were analyzed by infrared spectroscopy, chromatography (HPLC and GC-MS), and powder X-ray diffractometry.

The residues obtained after heating glycine at 120 and 150 °C after two days and two weeks were white. The infrared spectra of these residues were identical to the infrared spectrum of starting glycine (Fig. 7). For instance, the infrared absorption bands for glycine were found at 1609, 1583, 1500, 1409, 1331, 1314, 1131, 1111, 1033, 909, 891, 696, 606, and 500 cm^{-1} in the residues. Moreover, 2,5-diketopiperazine (DKP) was also identified along with unreacted glycine in the HPLC chromatograms of all residues. A negligible mass loss of 0.4–2.0 % was observed in the samples after two days (Tab. 4). This indicates that sublimation and the condensation reaction to DKP had occurred to a lesser extent. A very thin layer of sublimates which consists of glycine and DKP was found at the end of the quartz tube outside the furnace.

In the temperature range 160–200 °C, glycine turned grey to black after two days. The infrared spectra of the residues formed at 160 °C and 175 °C show the presence of unreacted glycine (Fig. A-1). In contrast, the infrared spectrum of the residue formed at 200 °C does no longer show any absorption bands of glycine. The residues (160, 175, and 200 °C) were washed with double distilled water to remove the readily water-soluble glycine. As the

complete dissolution of the thermo-melanoid in cold water takes a much longer time, glycine-free residues could be obtained. The infrared spectra of the washed residues formed at 160 °C and 175 °C clearly differ from the infrared spectrum of the washed residue formed at 200 °C, but also show similarities. For instance, the absorption bands at 1627, ~1530, ~1430, and ~1016 cm^{-1} were found in all three residues (for details see Fig. 7). In this thesis, the black residue formed at 200 °C is referred to as “thermo-melanoid”. From the above results it can be concluded that the formation of the thermo-melanoid starts at ~160 °C. The infrared spectrum of the glycine residue formed at 200 °C (thermo-melanoid) has been used as a reference spectrum for comparison with the spectra of other residues. The absence of infrared absorption bands of glycine in the residue obtained after heating at 200 °C means that only a small amount of glycine (<5 %) can be present.

In contrast, a small peak of unreacted glycine was detected in the HPLC chromatogram (Fig. 8). This suggests that the transformation of glycine into the thermo-melanoid and DKP was not entirely complete. With increasing temperature a greater decrease in the mass was observed (Tab. 4). At 200 °C, a mass loss of 42.6 % occurred. This considerable decrease was mainly due to the loss of water during the formation of DKP and thermo-melanoid. In addition, the sublimation of glycine and DKP also contributed to the mass loss.

For further investigations, temperatures from 250 to 350 °C were selected. The residues obtained at these temperatures appeared metallic black. The infrared analysis showed that these residues were chemically different from the thermo-melanoid formed at 200 °C (Fig. 9). The absorption bands of glycine, DKP or thermo-melanoid were not found in the infrared spectra of the high-temperature residues. However, DKP was identified in the residues by HPLC analysis. This indicates that glycine has been transformed into a product of unidentified chemical structure and small amounts of DKP. A greater mass loss (43.0 to 64.9 %) was observed at these temperatures, probably because of intense sublimation, condensation and polymerization (Tab. 4). Furthermore, a prominent pale yellow layer was also observed at cooler parts of the quartz tube outside the furnace. The layer that formed at 270 °C was analyzed by infrared spectroscopy and gas chromatography. The infrared spectrum clearly showed the presence of DKP (Fig. A-2). The methanol extract of the condensed layer was analyzed by GC-MS. Acetamide and 2,5-pyrrolidinedione (succinimide) were identified using reference substances.

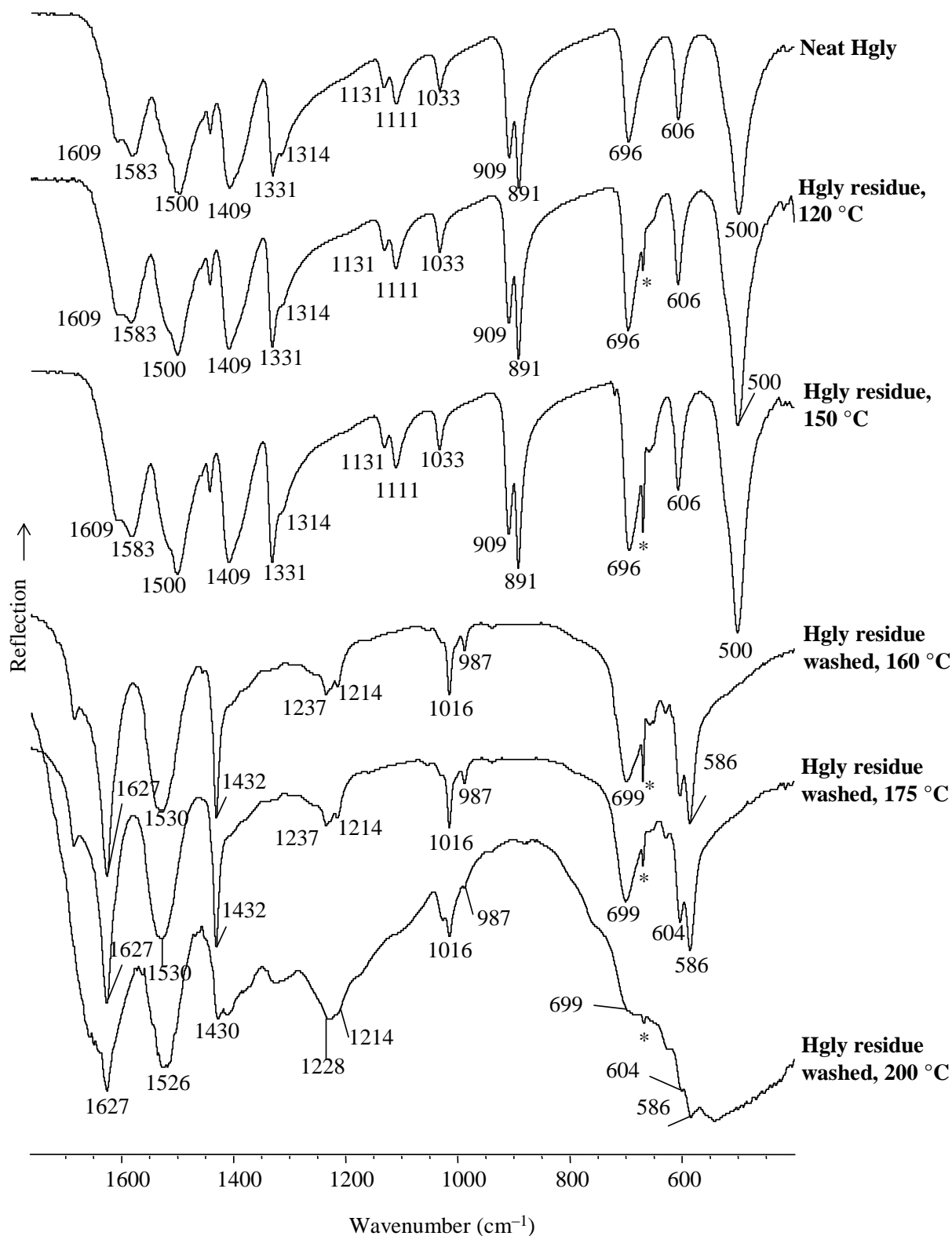


Fig. 7: Infrared spectra of neat glycine and the residues formed by treatment of glycine at various temperatures (120–200 °C) for two days. * Signal due to incomplete background correction.

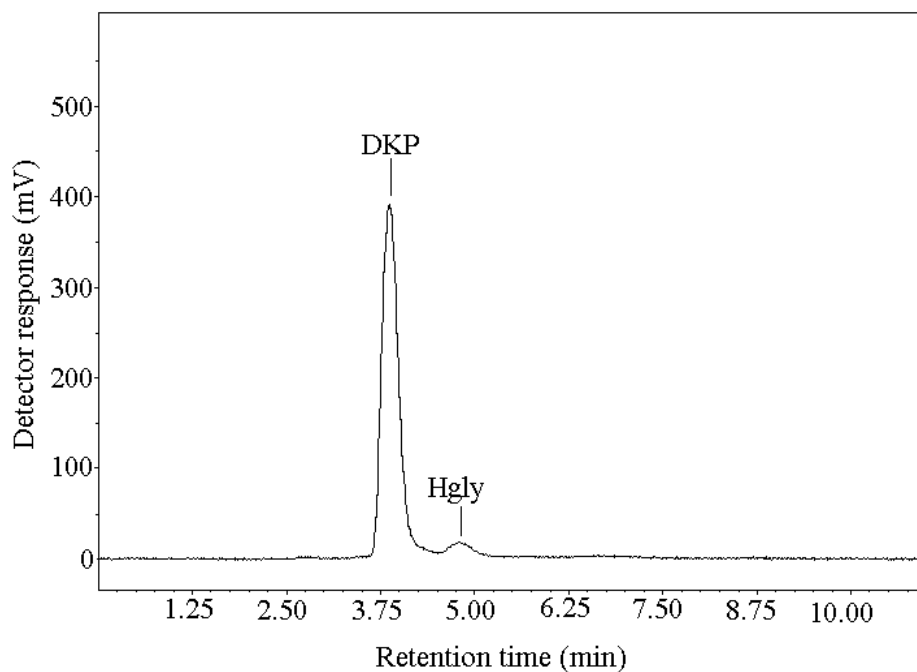


Fig. 8: HPLC analysis of the water extract of the residue obtained after heating neat glycine at 200 °C for two days.

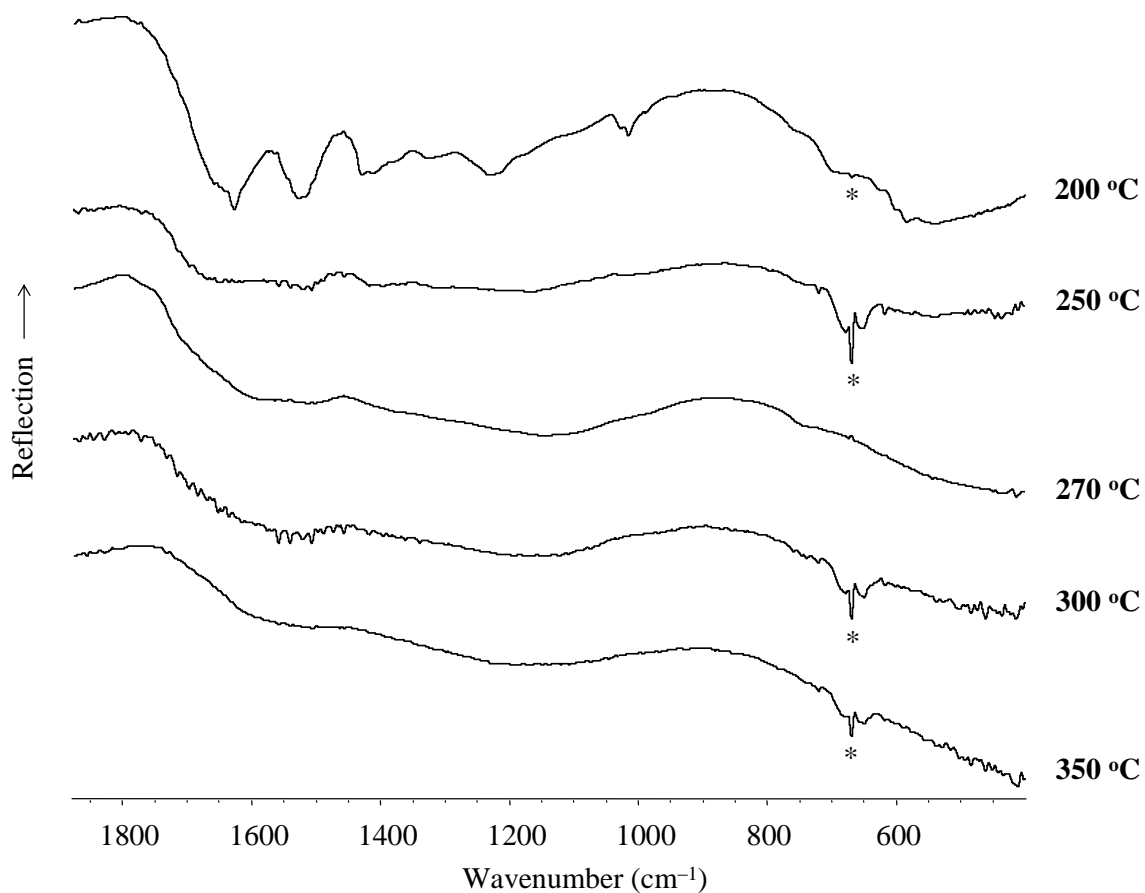


Fig. 9: Comparison between the infrared spectra of the glycine residues formed at 200 °C (thermo-melanoid) and at higher temperatures (250–350 °C). The heating time was 48 hours.
* Signal due to incomplete background correction.

In addition to the analytical methods mentioned (infrared spectroscopy, HPLC and GC), powder X-ray diffraction studies were performed on the residues obtained from glycine at 200 °C (thermo-melanoid) and 270 °C. The powder X-ray diffractogram of the thermo-melanoid at 200 °C has two relatively sharp signals with d values of 3.431 and 4.375 Å (Fig. 10 A). These signals indicate that the residue has retained at least some crystalline ordering. However, the residue obtained at 270 °C has only one very broad signal with a d value of ~3.468 Å (Fig. 10 B). The overall broad diffraction pattern of both the residues formed at 200 °C (thermo-melanoid) and 270 °C indicates that their major part has been transformed into amorphous material. This is in contrast to the diffraction pattern of the starting glycine which has sharp and narrow signals typical of crystals (Fig. 10 D).

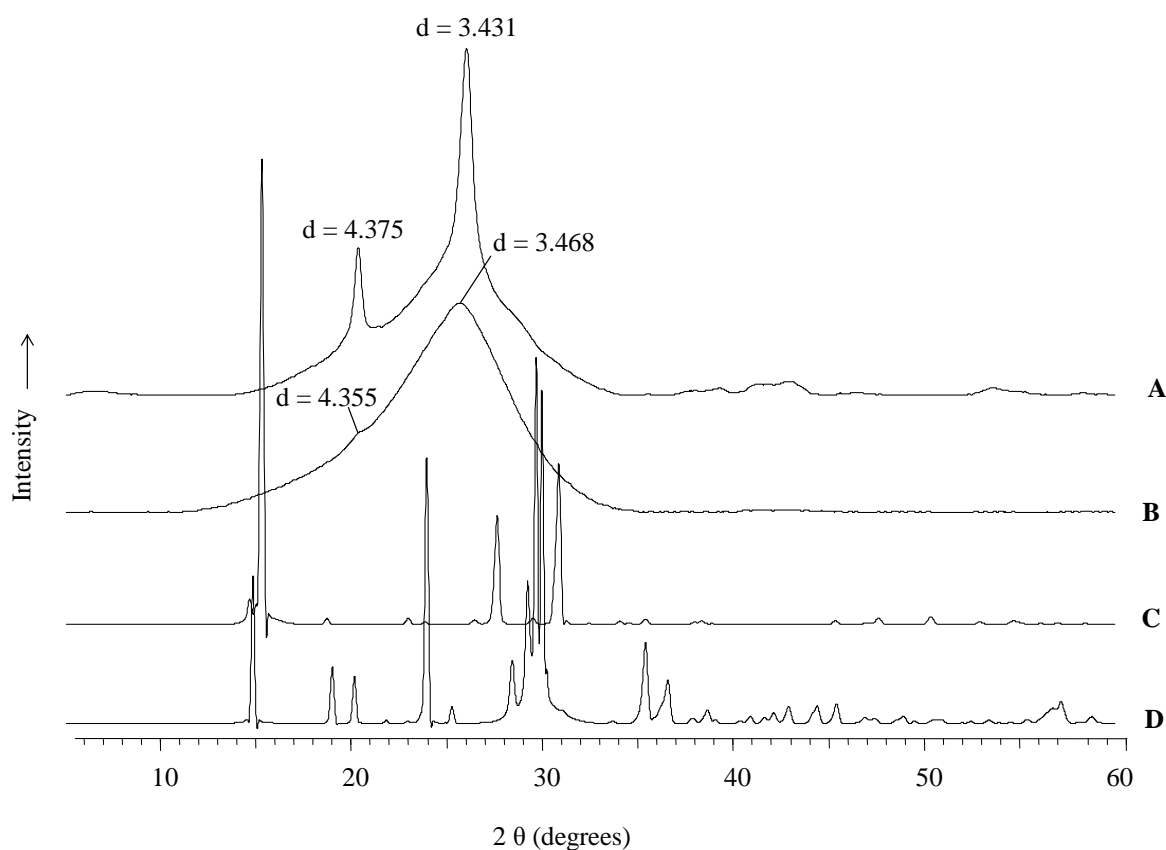


Fig. 10: Background subtracted powder X-ray diffractograms of: (A) the thermo-melanoid obtained after heating glycine at 200 °C for two days, (B) the residue obtained after heating glycine at 270 °C for two days, (C) DKP (reference), and (D) α -glycine (reference). The d values are given in Å.

Tab. 4: Mass loss and properties of the residues obtained by thermal treatment of neat glycine at different temperatures for two days.

Temperature (°C)	Initial amount	Mass loss (%)	Residue color	Residue composition*
120	500 mg	0.4	White	Hgly and DKP
140	500 mg	0.8	White	Hgly and DKP
150	500 mg	2.0	White	Hgly and DKP
160	500 mg	7.2	Light grey	Hgly, DKP, and thermo-melanoid
175	500 mg	8.4	Grey	Hgly, DKP, and thermo-melanoid
200	500 mg	42.6	Black	Hgly, DKP, and thermo-melanoid
250	2.000 g	43.0	Metallic black	DKP and residue different from thermo-melanoid
270	500 mg	47.2	Metallic black	DKP and residue different from thermo-melanoid
300	2.000 g	58.6	Metallic black	DKP and residue different from thermo-melanoid
350	2.000 g	64.9	Metallic black	DKP and residue different from thermo-melanoid

* Thermo-melanoid refers to the product obtained at 200 °C.

2.1.2 Thermal treatment of DKP and linear homopeptides of glycine

In the previous section, the thermal behavior of glycine has been investigated (see 2.1.1). It was found that a black product (thermo-melanoid) was obtained by heating glycine at 200 °C. The experiments described in the present section were aimed to study the thermal behavior of oligopeptides of glycine at 200 °C. The heating experiments were performed for two days under a nitrogen atmosphere to simulate the Earth's early oxygen-free atmosphere. The analysis of the residues was performed by infrared spectroscopy and HPLC.

First the residues obtained after the thermal treatment of DKP and diglycine were studied. The infrared absorption bands found for these residues were in accordance with the bands of the reference DKP (Fig. 11). Only a few weak absorption bands (~ 1626 , ~ 1526 , and ~ 1234 cm^{-1}) may belong to unreacted diglycine in the residue of the linear peptide. This indicates that the starting diglycine has been cyclized to DKP. The formation of the thermo-melanoid could also be assumed because the residues were dark grey.

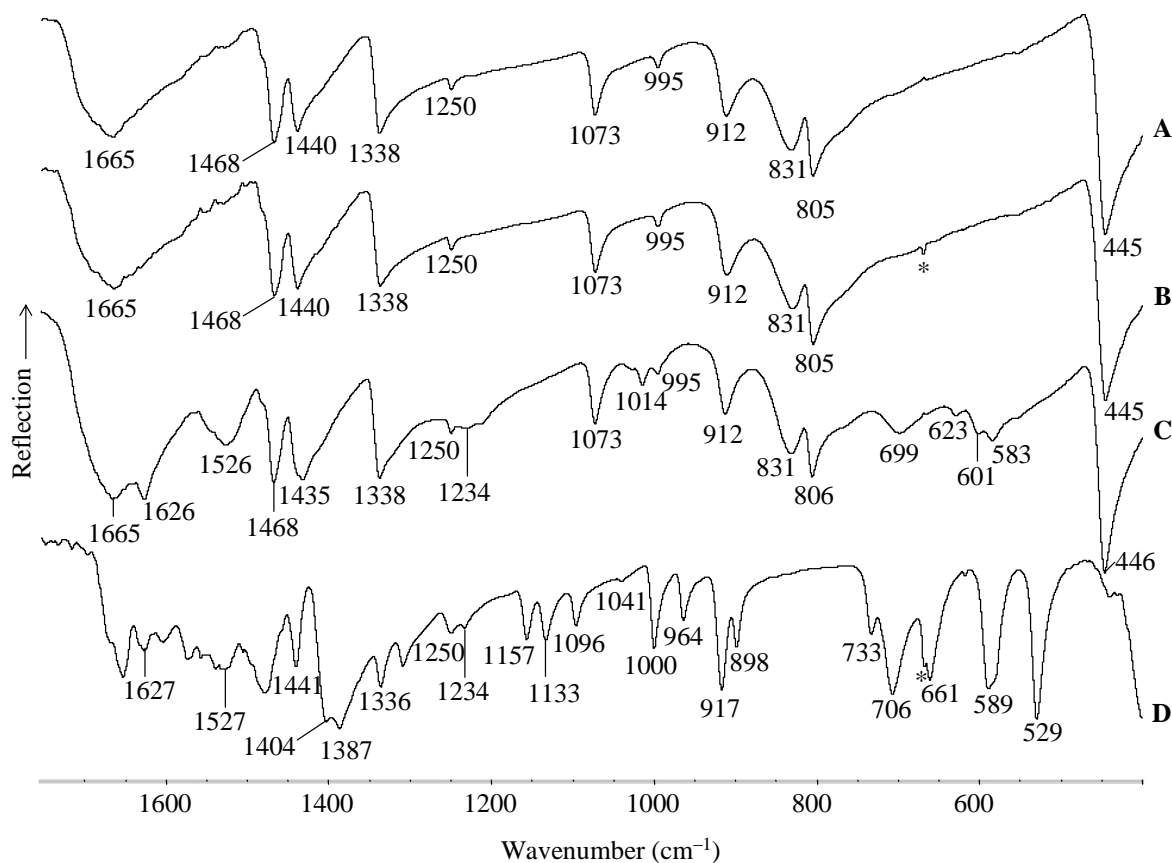


Fig. 11: Comparison between the infrared spectra of: (A) DKP (reference), (B) DKP residue after two days at 200 °C, (C) diglycine residue after two days at 200 °C, and (D) linear diglycine (reference). * Signal due to incomplete background correction.

For further investigations, the residues were washed with double distilled water to remove the water soluble peptides. In contrast to the peptides, the thermo-melanoid dissolves much slower in water. The infrared spectra of these washed residues exhibit close similarities with the thermo-melanoid (black residue of glycine formed at 200 °C) (Fig. 12). These results indicate that the starting peptides (DKP and linear diglycine) were present as DKP and thermo-melanoid in the residues.

The residues obtained after the thermal treatment of triglycine and tetraglycine were dark grey and light grey, respectively. The infrared analysis of the residues showed the presence of unreacted starting peptides, but DKP and thermo-melanoid signals were not detected. It could be, however, that the infrared absorption bands of the linear peptides obscured the absorption signals of small amounts DKP and thermo-melanoid. Thus, the residues were washed with double distilled water to remove the starting peptides. In fact, thermo-melanoid was found in the washed residues (Fig. 12). Moreover, DKP was also identified by HPLC in the water extract of the residues along with the respective starting peptide (Fig. 13 and Fig. A-3). It may be assumed that during the heating process, triglycine

or tetraglycine were broken into smaller units which were converted into DKP and the thermo-melanoid.

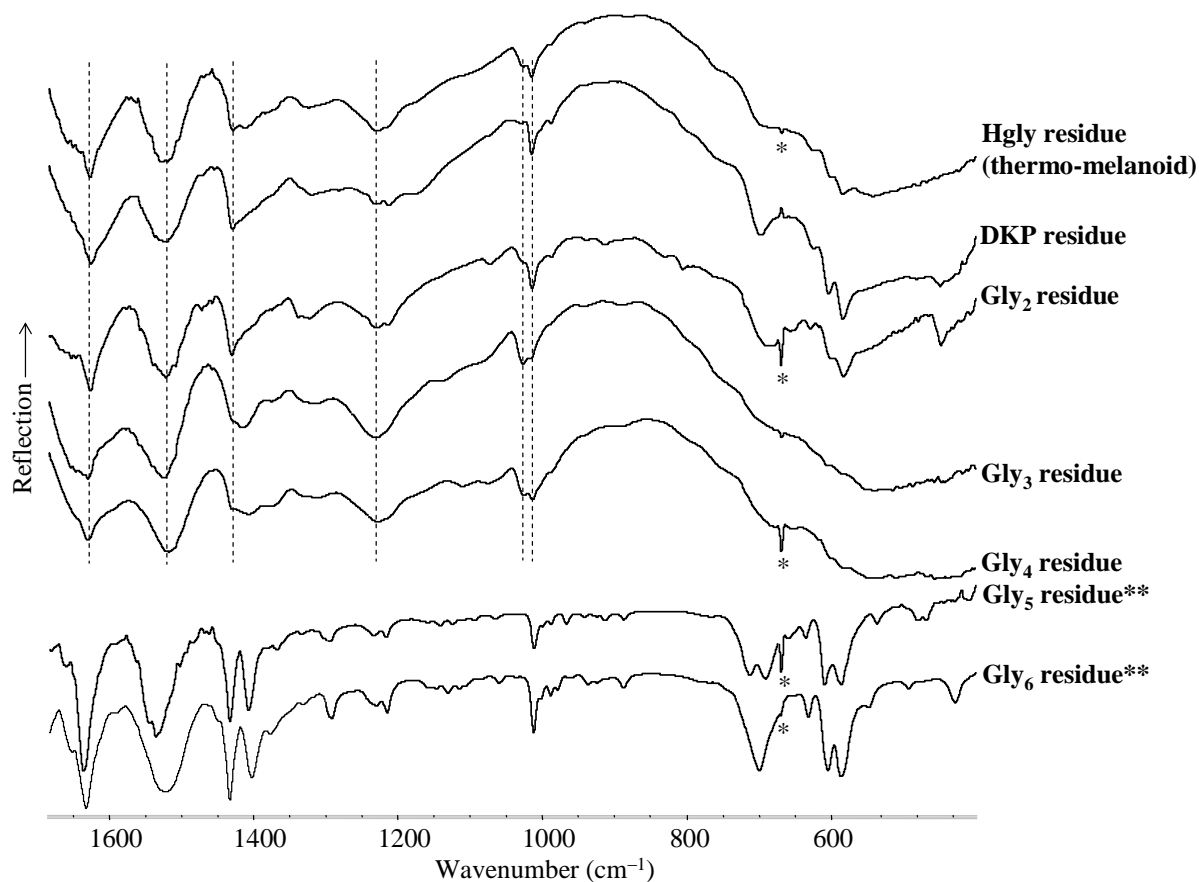


Fig. 12: Comparison between the infrared spectra of the thermo-melanoid and the washed residues from the thermal treatment of glycine oligomers at 200 °C for two days. Dashed lines show same band positions in the thermolysis residues. * Signal due to incomplete background correction, ** Unwashed.

The sublimates obtained after heating of DKP, diglycine, and triglycine were also analyzed by infrared spectroscopy and HPLC. It turned out that the sublimates were only composed of DKP (Figs. A-4 and A-5). The sublimation of DKP is easier than that of glycine and its homopeptides because DKP has no charged groups such as $-\text{NH}_3^+$ and $-\text{COO}^-$ (Fig. 14). Therefore, the intermolecular forces between DKP molecules are weaker. No sublimate was observed in the case of tetraglycine.

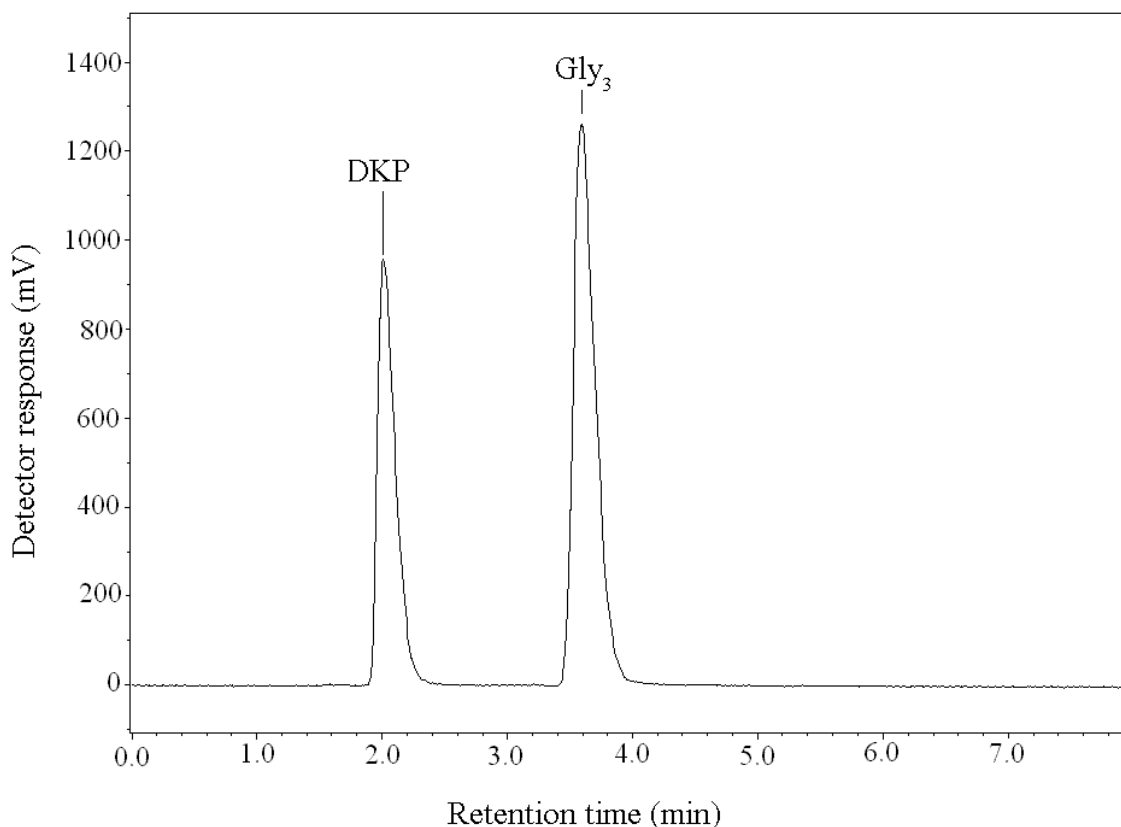


Fig. 13: HPLC analysis of the water extract of the residue obtained after heating triglycine at 200 °C for two days.

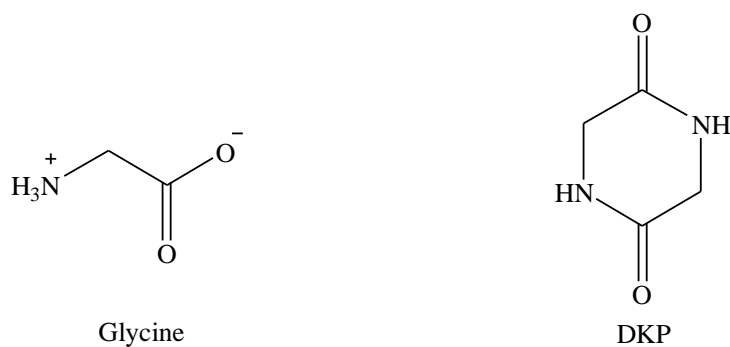


Fig. 14: Comparison of the structures of glycine and DKP.

Pentaglycine and hexaglycine were almost unreacted after heating at 200 °C. Particularly, the thermo-melanoid was not found in their residues. Obviously, in the case of these higher oligomers, the temperature of 200 °C is not sufficient for the condensation reaction to occur. This fact was supported by a negligible decrease in the mass of pentaglycine (1.3 %) and hexaglycine (1.4 %) samples (Tab. 5). Furthermore, no sublimation was observed during the heating of pentaglycine and hexaglycine. These results clearly show that pentaglycine and hexaglycine are more stable than smaller peptides (DKP, diglycine, triglycine, and tetraglycine) at 200 °C. However, it may be assumed that the formation of the

thermo-melanoid from pentaglycine and hexaglycine can occur at higher temperatures (for details see 2.2.1).

Tab. 5: Mass loss and properties of the residues after thermal treatment of glycine oligomers at 200 °C for two days.

Peptides*	Initial amount (mg)	Mass loss (%)	Residue color	Residue composition**
DKP	500.6	15.5	Dark grey	DKP and thermo-melanoid
Gly ₂	500.1	22.4	Dark grey	DKP and thermo-melanoid
Gly ₃	500.1	21.3	Dark grey	DKP, gly ₃ , and thermo-melanoid
Gly ₄	500.0	3.7	Light grey	DKP, gly ₄ , and thermo-melanoid
Gly ₅	100.4	1.3	Light brown	Gly ₅
Gly ₆	100.6	1.4	Light brown	Gly ₆

* Gly₂: diglycine, Gly₃: triglycine, Gly₄: tetraglycine, Gly₅: pentaglycine, and Gly₆: hexaglycine

** Thermo-melanoid refers to the product obtained after heating glycine at 200 °C.

It can be hypothesized that the thermo-melanoid may have played a role in prebiotic chemistry on the primitive Earth. For instance, the thermo-melanoid can be regarded as a storage form of glycine and its oligopeptides. It has been detected in the residues obtained after the thermal treatment of glycine and its oligopeptides DKP, diglycine, triglycine, and tetraglycine at 200 °C. Thus, its formation could have served as a possible mechanism for the protection of glycine and its oligopeptides against complete destruction on the primitive Earth. Moreover, the thermo-melanoid has a lower solubility in water as compared to glycine and glycine oligopeptides. This property may have influenced the distribution of glycine units on the young Earth. Further investigations on the properties of the thermo-melanoid and its possible role on the young Earth are described in the next chapter.

2.2 Analysis and properties of the glycine thermo-melanoid

2.2.1 Thermogravimetric analysis of glycine and homopeptides of glycine

Thermogravimetric analysis (TGA) was performed to get a deeper insight into the thermal behavior of neat glycine. A comparison was made between the effects observed in the preparative heating apparatus (furnace) and in the thermal balance. First of all, a temperature difference of ~70 degrees was found for thermal processes in TGA measurements and in the heating apparatus. For instance, a mass loss of 42 % was found at 200 °C when the glycine was heated in the furnace, whereas the nearly identical value of 44 % was observed only at

270 °C in the TGA (Fig. 15 A). The mass loss increased with temperature. For example, a mass loss of 65 % was found at 350 °C for glycine in the heating apparatus (see Tab. 1). A similar decrease of 61 % was found at 410 °C, i.e. 60 degrees higher in the TGA curve. In the previous section (see 2.1.1), it was found that the products formed above 250 °C were different from the thermo-melanoid obtained after heating glycine at 200 °C. Therefore, it can be concluded that the continuous mass loss of glycine in the TGA curve (Fig. 15 A) reflects a gradual transformation of the thermo-melanoid that results in a different product.

In contrast to glycine, 2-aminoisobutyric acid showed only one sharp step in the TGA curve. At 275 °C, almost all (~98 %) of 2-aminoisobutyric acid has been sublimed (Fig. 15 B). Therefore, the formation of a thermo-melanoid was not possible from this amino acid.

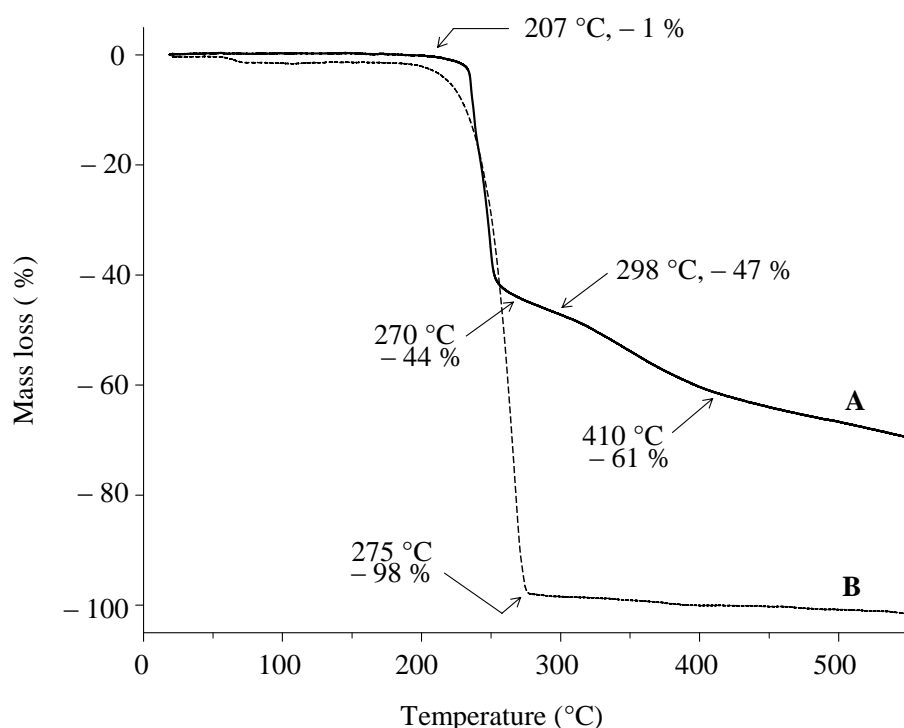


Fig. 15: Comparison between the thermogravimetric curves of (A) glycine and (B) 2-aminoisobutyric acid.

It can be seen in the TGA curves of the glycine oligomers that as the peptide chain length increases, the mass loss at 270 °C becomes negligible (Fig. 16). The mass loss of the oligopeptides in the thermal balance can be directly compared with the values obtained in the furnace at 200 °C (after considering the difference between thermal processes in TGA measurements and in the heating apparatus). For instance, triglycine had a mass loss of 21.3 % in the heating apparatus at 200 °C, which is in good agreement with the mass loss

observed in the TGA curve at ~ 270 °C (~ 21 %). Pentaglycine and hexaglycine were almost unreacted at 200 °C (mass loss of only 1.3 and 1.4 %, respectively; Tab. 5). Similarly, a negligible mass loss was also observed in the TGA curves of these two peptides at ~ 270 °C. However, a mass loss of ~ 30 % was found for these peptides above 300 °C in the TGA plot (Fig. 16). As the thermo-melanoid is not stable above ~ 270 °C (see curve A in Fig. 15), it can be concluded that the product formed from penta- and hexaglycine is probably not identical to the original thermo-melanoid.

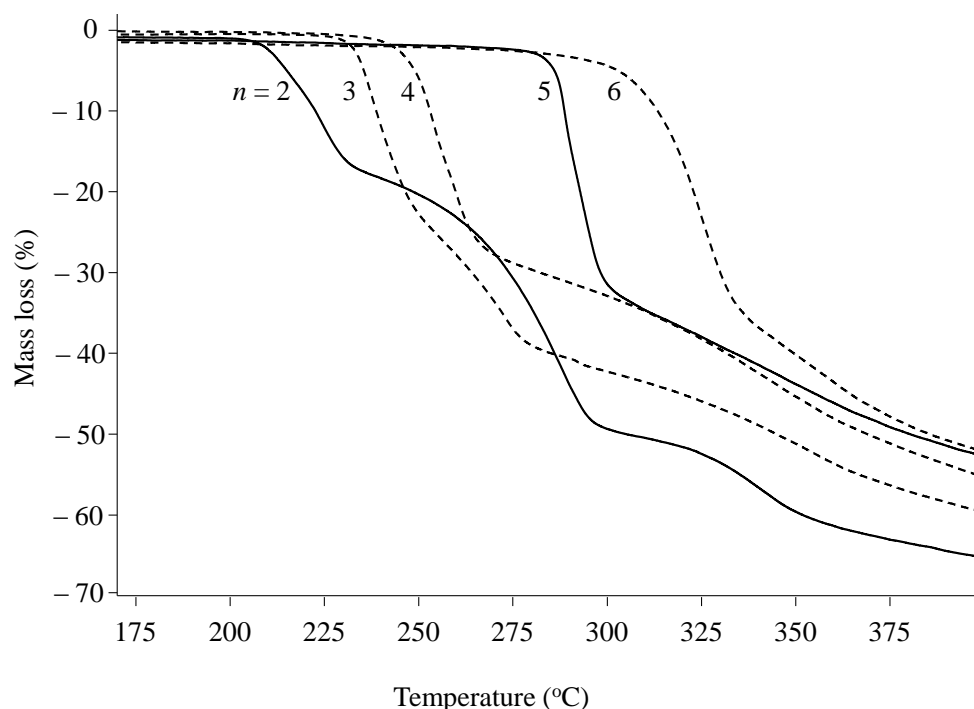


Fig. 16: Thermogravimetric curves of glycine homopeptides, where n represents the number of glycine units in a peptide.

2.2.2 Solubility and hydrolysis of the thermo-melanoid

The thermo-melanoid was insoluble in a number of organic solvents. However, it slowly dissolved in 0.1 mol L^{-1} of HCl and 0.1 mol L^{-1} of NaOH. It was found that the thermo-melanoid had relatively better solubility in NaOH than in HCl. Moreover, the thermo-melanoid also dissolved in hot water. For the experiment, 300 mg of the thermo-melanoid were added to 300 mL of water at 100 °C. After 10 days, only 76.5 mg of the thermo-melanoid was recovered which means that 75.4 % of the thermo-melanoid has been dissolved. The thermo-melanoid is probably formed by the condensation of glycine molecules by the continuous loss of water molecules as depicted in Fig. 17 A. Glycine, DKP and diglycine were released during the hydrolysis of thermo-melanoid with hot water

(Fig. A-6). Interestingly, the diglycine was not detected in the residue after heating neat glycine at 200 °C. This finding ensures that it was really a hydrolysis product. The pH of the solution was 4.3 after 10 days hydrolysis.

In addition to the water hydrolysis, the thermo-melanoid was also hydrolyzed by acid. The thermo-melanoid (5 mg) was mixed with 500 μL of 6 mol L^{-1} of HCl and heated at 110 °C for 1–6 hours. Thermo-melanoid was also hydrolyzed using deuterated acid (DCI/D₂O) (Fig. 17 B). Acid hydrolysis of the thermo-melanoid was followed by the derivatization of amino acids for GC-MS analysis. The detailed process of derivatization is described under Materials and Methods (see 4.1.3). Deuterated derivatizing reagents were used for the products of the hydrolysis with DCI/D₂O. This was done to minimise the possibility of H–D exchange. The GC-MS analysis led to the model shown in Figure 17. The analysis revealed that C=C bonds are a characteristic structural feature of the thermo-melanoid. These bonds form by an unusual condensation reaction between C=O and CH₂ groups.

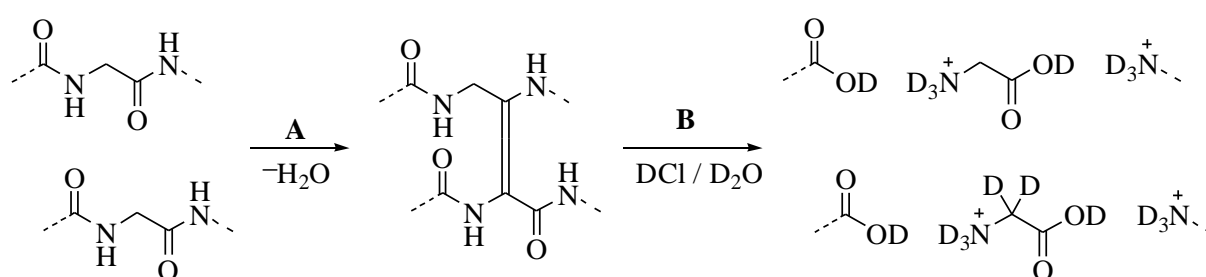


Fig. 17: (A) Suggestion for the key step in the formation of the thermo-melanoid and (B) Hydrolysis of thermo-melanoid in DCI/D₂O. The experiments and interpretation of the results were performed by Dr. Stefan Fox.

2.2.3 Biodegradability of the thermo-melanoid in soil

The biodegradability of the thermo-melanoid was traced through soil respiration experiments. For these experiments, thermo-melanoid has been produced by heating glycine at 200 °C for two days (see 4.4.2). During the experiment, CO₂ was released by the metabolism of microorganisms present in the soil. This CO₂ was dissolved in NaOH (as Na₂CO₃) and titrated with HCl. The experiment was performed in 14 “microcosmos” chambers. The detailed methodology of analysis is described under Materials and Methods (see 4.4.2).

The results indicate that the samples containing thermo-melanoid have produced a higher amount of CO₂ than the samples without the thermo-melanoid. The thermo-melanoid was decomposed in the soil. The decomposition was probably caused by microorganisms. Carbon dioxide production was very high in the beginning. However, it attains a stable value

after about two weeks (Fig. 18). It could be that the microorganisms were initially active due to the change in the surroundings and were slowly adapted to this change. Therefore, it can hypothesize that the thermo-melanoid could also have been utilized as a nutrient source by microorganisms on the early Earth.

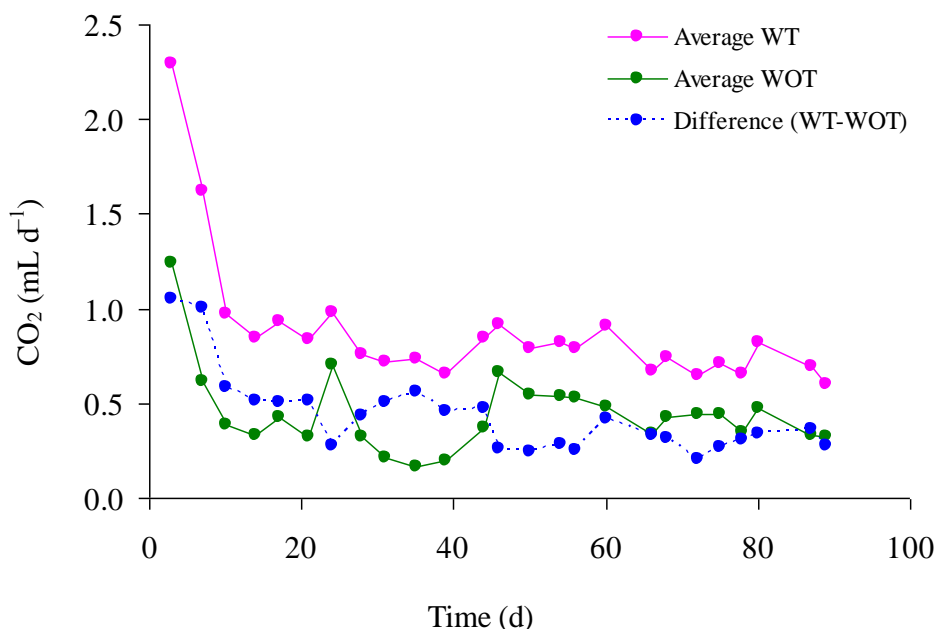


Fig. 18: Comparison between the CO₂ production rates of soil samples containing thermo-melanoid (WT) and samples without thermo-melanoid (WOT). The experiment was performed by Melanie Wagner.

2.3 Protection of glycine by different matrices

In this section, experiments are described that investigate the protection of glycine from decomposition and transformation into the thermo-melanoid. The protective effects of metal ions and minerals were studied on mixtures of glycine with various salts and clays. The heating experiments were performed in a tube furnace under pure nitrogen gas to simulate the Earth's early anoxic atmosphere.

2.3.1 The influence of salts and salt mixtures

Thermal treatment of glycine embedded in NaCl (NaCl-Hgly)

A solution containing equimolar amounts of NaCl and α -glycine was evaporated and finally dried to constant weight in vacuo (see 4.5.1). The infrared spectrum of pure NaCl has no absorption bands in the measured range. All absorption bands of glycine embedded in the

NaCl crust are shifted with respect to the positions for pure α -glycine (Fig. 19). For instance, some strong infrared signals of reference glycine at 1583, 1409, 1111, 1033, 909, 891, and 696 cm^{-1} were clearly shifted to 1575, 1390, 1126, 1043, 928, 888, and 685 cm^{-1} after evaporation in the presence of NaCl (for details, see Fig. 19). Interestingly, it was found that the α -modification of the starting glycine had been transformed into the γ -modification during the crystallization process. This observation was in accordance with various studies that have described the formation of γ -glycine in the presence of sodium salts (Bhat and Dharmaprakash, 2002a, 2002b). The infrared absorption bands of γ -glycine at approximately 1390, 685, and 501 cm^{-1} were attributed to the $-\text{COO}^-$ group, while signals at 1576, 1494, 1155, and 1126 cm^{-1} were assigned to the $-\text{NH}_3^+$ group (Ambujam et al., 2006; Balakrishnan et al., 2008; Peter and Ramasamy, 2010). Obviously, glycine was present in the zwitterionic form. Further, in the literature the absorption signals at 1043, 930, and 888 cm^{-1} were assigned to vibrations involving C–N, C–H and C–C groups, respectively. The infrared absorption bands of γ -glycine reported in the literature were in excellent agreement with the signals of glycine embedded in the NaCl crust (Ambujam et al., 2006; Balakrishnan et al., 2008; Peter and Ramasamy, 2010). In addition, the powder X-ray diffractogram of NaCl–Hgly was compared with the diffractogram of γ -glycine, which was calculated from single-crystal X-ray data (DIAMOND – Crystal and Molecular Structure Visualization, Version 3.1, Crystal Impact). The comparison also showed that glycine was exclusively present in the γ -modification when crystallized from NaCl solution and embedded in the NaCl crust.

The influence of NaCl on the thermal behaviour of glycine was studied on samples of NaCl–Hgly that contained 3.00 mmol glycine and NaCl each. The samples were heated at 200 °C for two days or seven days. In both cases, the residues were black. Infrared analyses of the washed residues indicated the presence of the thermo-melanoid (i.e. the product obtained from pure α -glycine at 200 °C) (Fig. A-7). The powder X-ray diffractogram is also consistent with the formation of the thermo-melanoid (Fig. A-8). Further, DKP and unreacted glycine were detected in the water extract of both residues by HPLC (Fig. 20). The HPLC quantification revealed that only 0.24 mmol (8.0 %) of glycine had survived after two days of heating. Only 0.15 mmol (4.9 %) of glycine was found after seven days of heating. Additionally, 0.03 mmol of the newly formed DKP was detected after two days and seven days. These values clearly show that the major portion (>90 %) of the starting glycine was transformed into the thermo-melanoid and DKP. Sublimation of DKP and glycine and water

loss by condensation reactions contributed to a mass loss of 21.5 % and 23.5 % of the samples after two days and seven days, respectively.

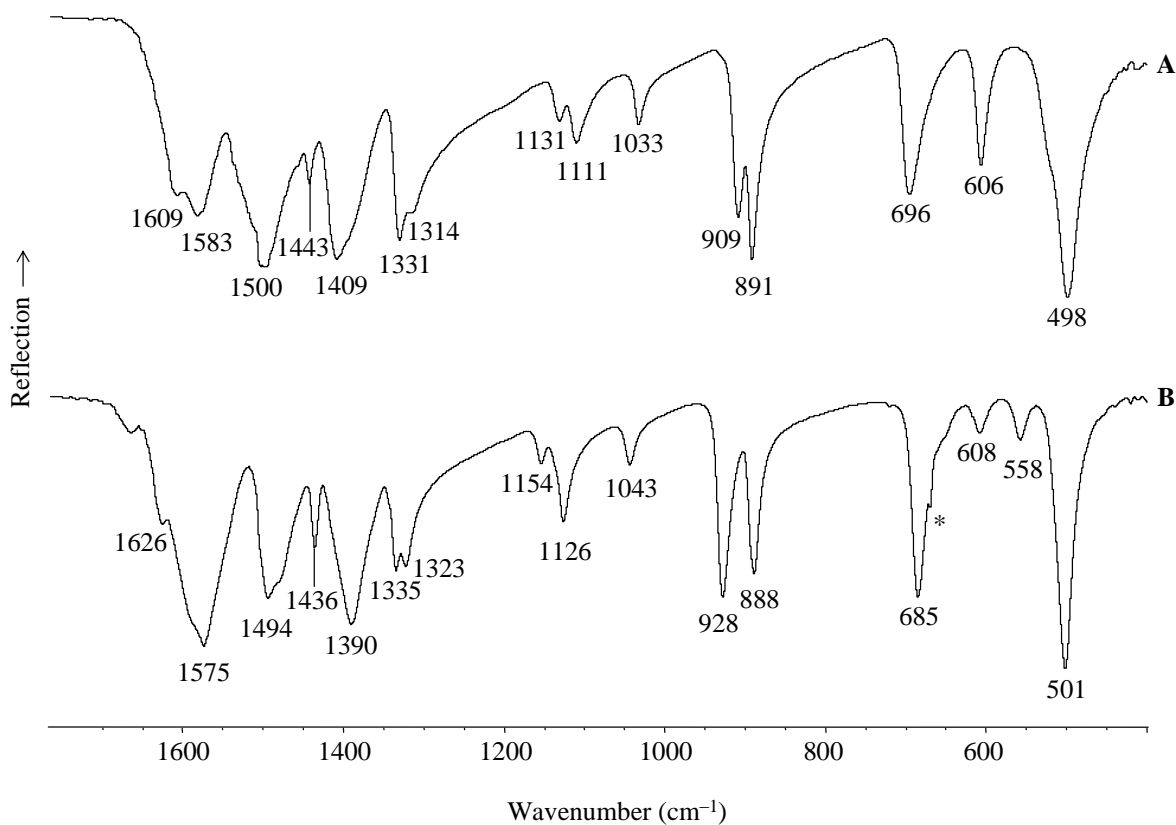


Fig. 19: Infrared spectra of (A) α-glycine (reference) and (B) NaCl-Hgly (for preparation: see 4.5.1). * Signal due to incomplete background correction.

In solution, glycine molecules only very weakly coordinate to sodium ions; they do not form solid sodium complexes. Therefore, at 200 °C, glycine embedded in the NaCl crust showed a very similar thermal behavior as the neat amino acid (see 2.1). For instance, formation of the thermo-melanoid and sublimation were observed in both cases. However, the mass loss was nearly twice as high (42.6 %) in the case of neat glycine. This could be due to the mechanical effects caused by the presence of NaCl. It has been reported that the γ-modification of glycine is transformed back into the α-form on heating above 165 °C (Iitaka, 1961). However, the α-glycine was not observed in the residues by infrared and powder X-ray diffraction studies. The experiments have demonstrated that NaCl is not very effective in protecting glycine from transforming into the thermo-melanoid.

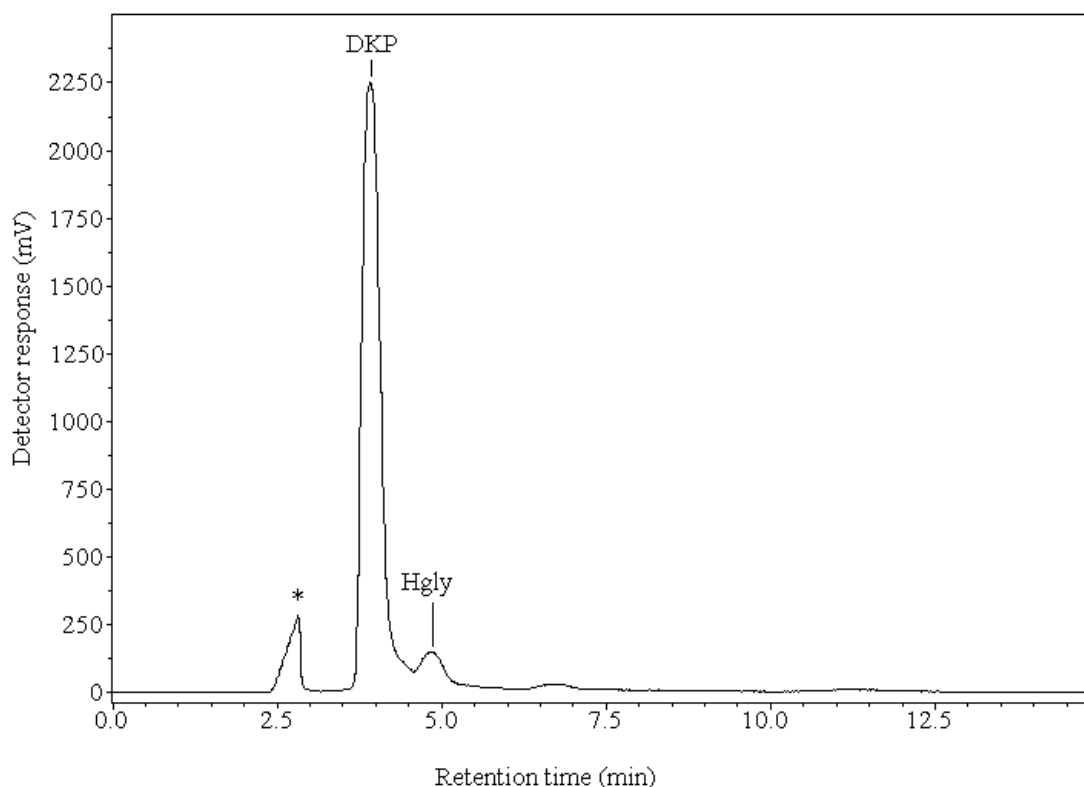


Fig. 20: HPLC analysis of the water extract of the residue obtained by heating NaCl–Hgly at 200 °C for two days. * Solvent peak

Thermal treatment of glycine embedded in NaCl–KCl

A solution of NaCl (705 mmol), KCl (15 mmol), and α -glycine (10 mmol) was prepared. The sodium-to-potassium ratio used is the one found in the present-day sea water. This mixture was evaporated and finally dried in vacuo. Both pure NaCl and KCl have no absorption bands in the measured range. The infrared spectrum of reference α -glycine was different from the spectrum of glycine in the NaCl–KCl crust. For instance, the infrared absorption bands of reference glycine found at 1583, 1409, 1111, 1033, 909, 891, and 696 cm^{-1} were shifted to 1575, 1390, 1126, 1043, 928, 888, and 685 cm^{-1} in the presence of NaCl–KCl (for details see Fig. 21 A and C). The infrared spectra of glycine in NaCl–KCl–Hgly and NaCl–Hgly were practically identical (Fig. 21 B and C). This again indicated the presence of γ -glycine. This conclusion was also supported by the comparison between the powder X-ray diffractograms of NaCl–Hgly and NaCl–KCl–Hgly.

The residue obtained by heating NaCl–KCl–Hgly at 200 °C for seven days was dark grey. The infrared spectroscopic analysis of the washed residue showed the presence of the thermo-melanoid, as in the case of NaCl–Hgly (Fig. A-7). As both sodium and potassium

cations do not form complexes with glycine in the solid state, the amino acid remained in its free form in the salt crust. The absence of any additional chemical interaction resulted in the transformation of glycine into the thermo-melanoid. Furthermore, DKP and unreacted glycine were detected by HPLC analysis of the residue. 1.20 mmol of glycine were found in the residue as compared to the initial amount of 2.78 mmol, whereas the amount of DKP was not sufficient for quantification. The percentage of glycine that had survived after seven days (43.2 %) was ~9 times more in NaCl–KCl as compared to NaCl (4.9 %). This was probably caused by the higher salt-to-glycine (70.5:1) molar ratio in the NaCl–KCl–Hgly experiment which might have provided a kind of mechanical protection to glycine. A thin layer of sublimate composed of glycine and DKP was found at the end of the quartz tube outside the furnace.

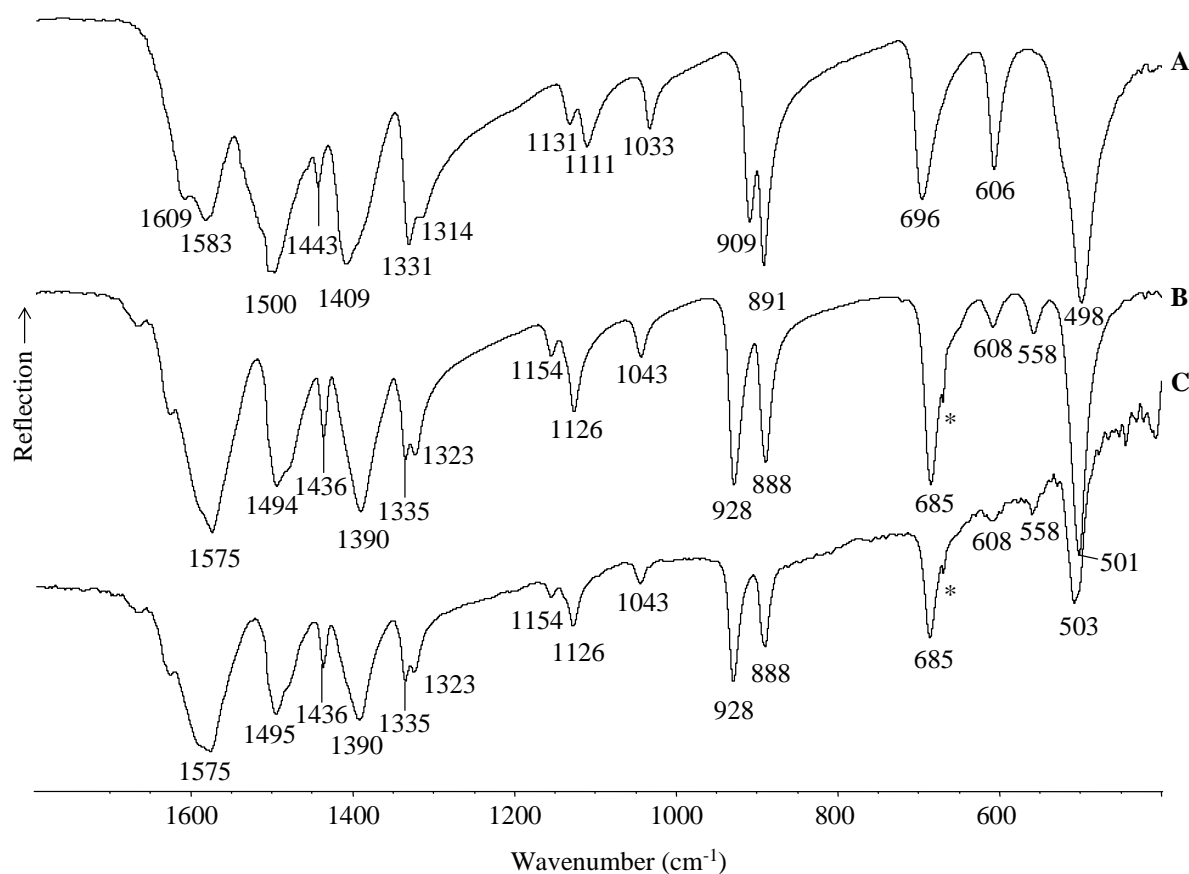


Fig. 21: Infrared spectra of (A) α -glycine (reference), (B) NaCl–Hgly and (C) NaCl–KCl–Hgly (for preparation: see 4.5.1). * Signal due to incomplete background correction.

Thermal treatment of the coordination compound $\text{CaCl}_2(\text{Hgly}) \cdot \text{H}_2\text{O}$

The coordination compound $\text{CaCl}_2(\text{Hgly}) \cdot \text{H}_2\text{O}$ was prepared from an aqueous solution of equimolar amounts of $\text{CaCl}_2 \cdot 2\text{H}_2\text{O}$ and glycine (Yusenko et al., 2008). The solution was evaporated and finally dried to constant weight under vacuum. As expected for a coordination compound, the infrared spectrum of $\text{CaCl}_2(\text{Hgly}) \cdot \text{H}_2\text{O}$ clearly differs from the spectrum of the non-coordinated glycine ligand (Fig. 22). For instance, some strong absorption bands of neat α -glycine were found at 1500, 1331, 909, 891, 696, and 498 cm^{-1} , whereas the corresponding bands of glycine in $\text{CaCl}_2(\text{Hgly}) \cdot \text{H}_2\text{O}$ occurred at 1561, 1353, 923, 901, 681, and 509 cm^{-1} (for details see Fig. 22). In addition, the powder X-ray diffraction pattern of $\text{CaCl}_2(\text{Hgly}) \cdot \text{H}_2\text{O}$ differed clearly from the diffraction patterns of the three polymorphs of glycine (α , β and γ). Thus, there is practically no doubt that glycine is coordinated to Ca^{2+} in $\text{CaCl}_2(\text{Hgly}) \cdot \text{H}_2\text{O}$ (Yusenko et al., 2008), though for a final confirmation a crystal structure analysis would be needed.

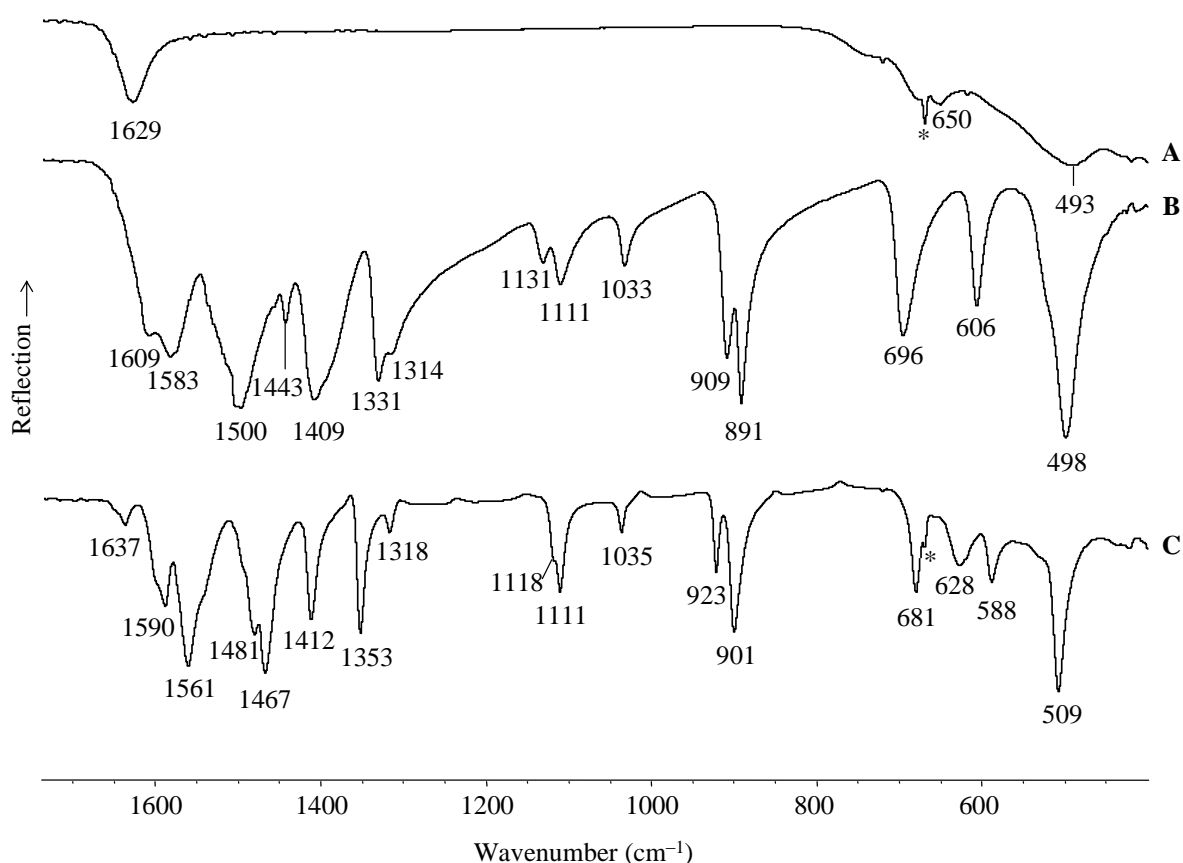


Fig. 22: Infrared spectra of (A) $\text{CaCl}_2 \cdot 2\text{H}_2\text{O}$, (B) α -glycine (reference), and (C) $\text{CaCl}_2(\text{Hgly}) \cdot \text{H}_2\text{O}$ (for preparation: see 4.5.1). * Signal due to incomplete background correction.

The residues were peach at 200 °C, light orange at 230 °C, brown at 250 °C, and black at 350 °C. As the temperature was raised, the Ca and Cl content increased (Tab. 6). However, due to the hygroscopic nature and brown color of the 250 °C residue, Ca and Cl content could not be accurately determined. All HPLC measurements showed the presence of DKP and unreacted glycine in the residues (Fig. 23). After seven days at 200 °C, 93.6 % of the glycine was still present. This value decreased to 85.2 % after thermal treatment at 230 °C (Tab. 6). At 250 and 350 °C, however, the amount of glycine in the residue was too small to be quantified by titration and HPLC. These results show that glycine in the compound $\text{CaCl}_2(\text{Hgly}) \cdot \text{H}_2\text{O}$ is fairly stable up to 200 °C. Interestingly, the thermo-melanoid, i.e. the residue that is formed from neat glycine at 200 °C, was not found in the residues obtained at 200, 230, and 250 °C. Obviously, the coordination of glycine to Ca^{2+} prevents the transformation of glycine into the thermo-melanoid up to 250 °C.

Tab. 6: Analytical data determined after heating $\text{CaCl}_2(\text{Hgly}) \cdot \text{H}_2\text{O}$ for seven days.

Temperature (°C)	Initial glycine (mmol)	Calcium and chlorine content (%)		Glycine* (mmol)	Glycine** (mmol)
200	7.24	Ca	21.7	6.75	6.81
		Cl	36.6		
230	48.29	Ca	21.7	41.06	41.23
		Cl	38.0		
250	48.29	Ca [#]	24.8	n.d.	n.d.
		Cl	–		

* determined by titration, ** determined by HPLC, # for Ca^{2+} titration, the sample was weighed in the glove box because the residue formed at 250 °C was highly hygroscopic, n.d. too less for quantification, – not determined because the residue at 250 °C was brown making end point determination for Cl^- difficult

The infrared spectroscopic analysis of the residue that formed at 350 °C showed the presence of the thermo-melanoid. At this temperature, a mass loss of 39.0 % was observed due to the formation of volatiles. In the volatile fraction, N-heterocycles (pyrroles), N-methylacetamide, and acetamide were detected by GC-MS (this work; Yusenko et al., 2008).

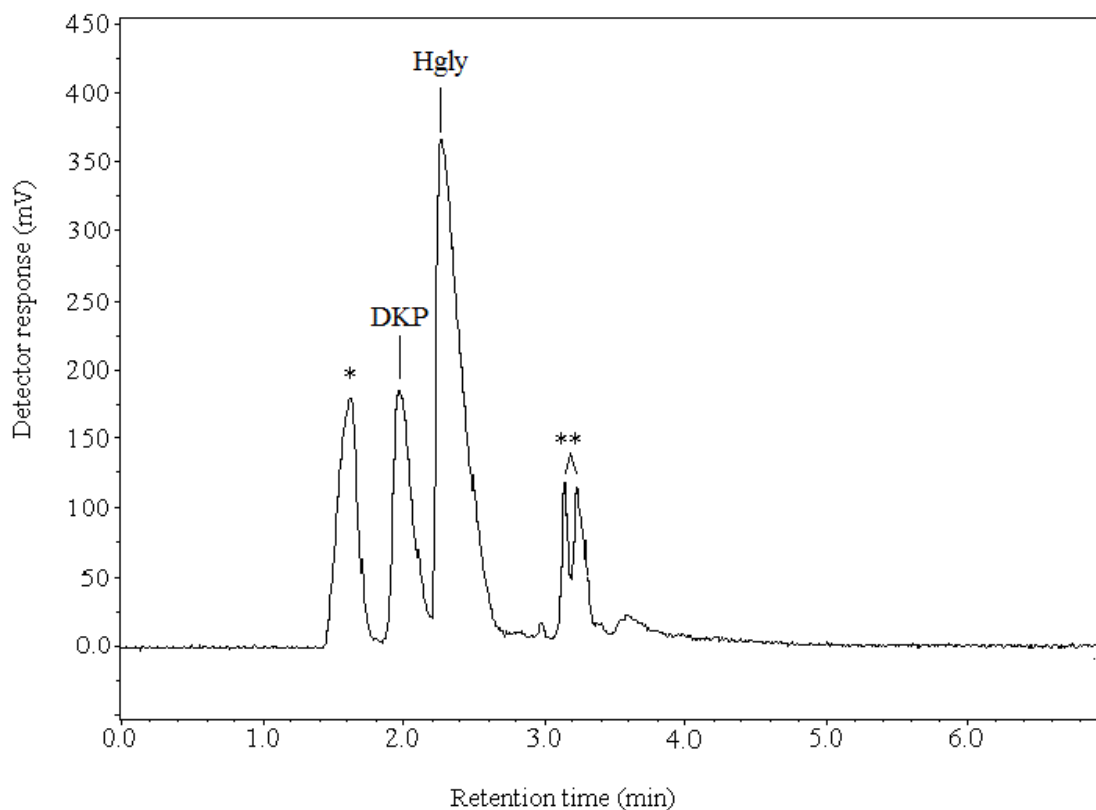


Fig. 23: HPLC analysis of the water extract of the residue obtained by heating $\text{CaCl}_2(\text{Hgly}) \cdot \text{H}_2\text{O}$ at 200 °C for seven days. * Solvent peak, ** Unidentified decomposition products.

Thermal treatment of glycine embedded in artificial sea salt

A mixture of artificial sea salt and glycine (AS–Hgly) was prepared by dissolving NaCl (705 mmol), KCl (15 mmol), $\text{MgCl}_2 \cdot 6\text{H}_2\text{O}$ (80 mmol), $\text{CaCl}_2 \cdot 2\text{H}_2\text{O}$ (15 mmol), and glycine (10 mmol) in 225 mL of double distilled water. The solution was completely evaporated and dried in vacuo to constant weight. The cation ratio in the artificial sea salt corresponds to the average one in present-day sea water. The exact composition of the late Hadean/early Archean sea water is unknown. However, the presence of sulfates and phosphates can probably be neglected because the early atmosphere was anoxic. Thus, sulfates and phosphates may not have formed. The infrared spectrum of dried AS–Hgly was clearly different from the spectrum of α -glycine (Fig. 24 A and C). The artificial sea salt mixture contains single (Na^+ and K^+) and double (Ca^{2+} and Mg^{2+}) charged ions. However, the metal ions had not transformed the modification of glycine. Instead, the infrared absorption bands of glycine embedded in the artificial sea salt and those of $\text{CaCl}_2(\text{Hgly}) \cdot \text{H}_2\text{O}$ were at nearly identical positions (for details, compare Fig. 24). Moreover, $\text{CaCl}_2(\text{Hgly}) \cdot \text{H}_2\text{O}$ was also identified in AS–Hgly by powder X-ray diffractometry. These results showed that

$\text{CaCl}_2(\text{Hgly}) \cdot \text{H}_2\text{O}$ was the main and probably the only binding form of glycine in AS–Hgly. Therefore, it can be assumed that glycine embedded in artificial sea salt will show a similar thermal behavior as $\text{CaCl}_2(\text{Hgly}) \cdot \text{H}_2\text{O}$.

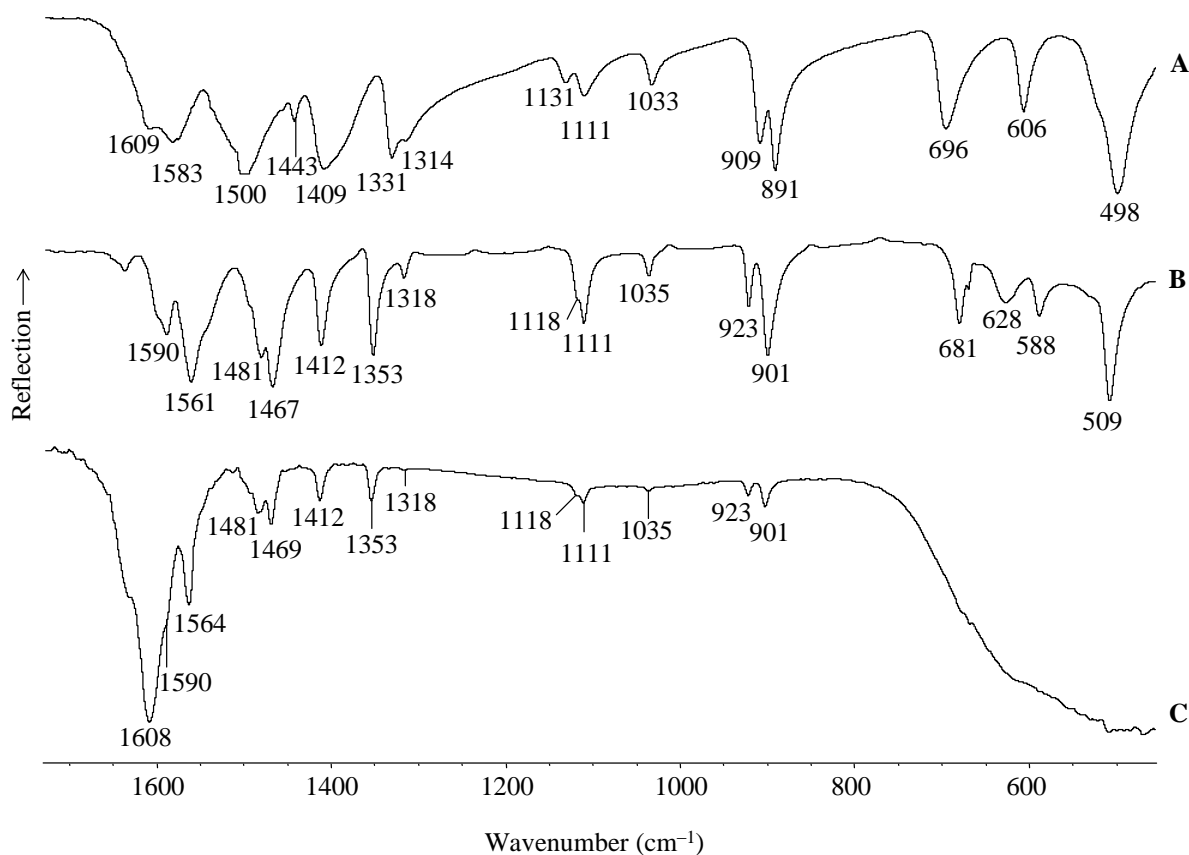


Fig. 24: Infrared spectra of (A) α -glycine (reference), (B) $\text{CaCl}_2(\text{Hgly}) \cdot \text{H}_2\text{O}$, and (C) artificial sea salt with embedded Hgly (for preparation: see 4.5.1).

The residue was still white after heating AS–Hgly at 200 °C for seven days. This indicated that AS–Hgly, in contrast to neat glycine, did not form the thermo-melanoid at this temperature. The absence of the thermo-melanoid in the residue was also supported by infrared spectroscopy. Glycine and DKP were detected in the water extract of the residue by HPLC analysis. Interestingly, 0.48 mmol of glycine were present in the residue as compared to the starting 0.57 mmol. This showed that a large portion (84.2 %) of glycine was still available after seven days of heating. Sublimation was not observed during the thermal treatment of AS–Hgly. As in the case of $\text{CaCl}_2(\text{Hgly}) \cdot \text{H}_2\text{O}$, the coordination to Ca^{2+} protected the amino acid glycine from sublimation and transformation into the thermo-melanoid. A mass loss of 14.6 % was observed in the sample due to the loss of crystal water and water of condensation.

Thermal treatment of glycine embedded in $\text{CaSO}_4 \cdot 2\text{H}_2\text{O}$ (gypsum–Hgly)

First, 2 mmol of gypsum ($\text{CaSO}_4 \cdot 2\text{H}_2\text{O}$) were dissolved in 200 mL of double distilled water. Gypsum dissolves slowly in water. To this solution, glycine (0.4 mmol) was added, and the mixture was evaporated to dryness. The absorption bands of neat $\text{CaSO}_4 \cdot 2\text{H}_2\text{O}$ could be clearly observed in the infrared spectrum (Fig. 25 A). The infrared signals of glycine occurred at 1517, 1413, 1334, 1041, 912, 893, 697, and 502 cm^{-1} in gypsum–Hgly (Fig. 25 C). These positions are slightly shifted with respect to neat α -glycine (1500, 1409, 1331, 1033, 909, 891, 696, and 498 cm^{-1}). However, the intensities of the glycine signals in gypsum–Hgly were weak. Further, their positions were different from those of glycine in NaCl–Hgly, NaCl–KCl–Hgly, and $\text{CaCl}_2(\text{Hgly}) \cdot \text{H}_2\text{O}$ (Fig. 19 B, 21 C, and 22 C). Therefore, it is likely that there was no change in the modification of glycine and also no complex formation in the gypsum–Hgly mixture. In addition to infrared spectroscopy, powder X-ray diffraction analysis was also performed on the sample. Glycine signals were not detected in the diffractogram. This is probably due to the low amount of glycine used.

Gypsum is dehydrated to anhydrite (CaSO_4) at 160–240 °C (Elbeyli et al., 2003; http://www.thass.org/DOWN/applications/App_SIINT/TA022.pdf, Strydom and Potgieter, 1999). When gypsum–Hgly was heated at 200 °C for seven days, the residue was dark grey. The grey color might be due to the presence of the thermo-melanoid. However, the thermo-melanoid could not be detected in the washed and unwashed residues by infrared spectroscopy. It seems possible that the broad infrared signals of CaSO_4 may have obscured the thermo-melanoid signals. The presence of CaSO_4 even after washing is due to its low solubility in water. DKP and glycine were detected both in the residue and the sublimate by HPLC (Fig. A-9). It was found that only 0.02 mmol (9.5 %) of glycine was found in the residue as compared to the starting 0.21 mmol. DKP was present in small amounts and was not quantified. A mass loss of 23.3 % was found for the sample. This weight loss agrees well with the reported TGA values (19 % after complete dehydration of gypsum) (Elbeyli et al., 2003). Therefore, the mass loss was due to the loss of crystal water from $\text{CaSO}_4 \cdot 2\text{H}_2\text{O}$, loss of water by the condensation reaction that formed DKP and sublimation of DKP.

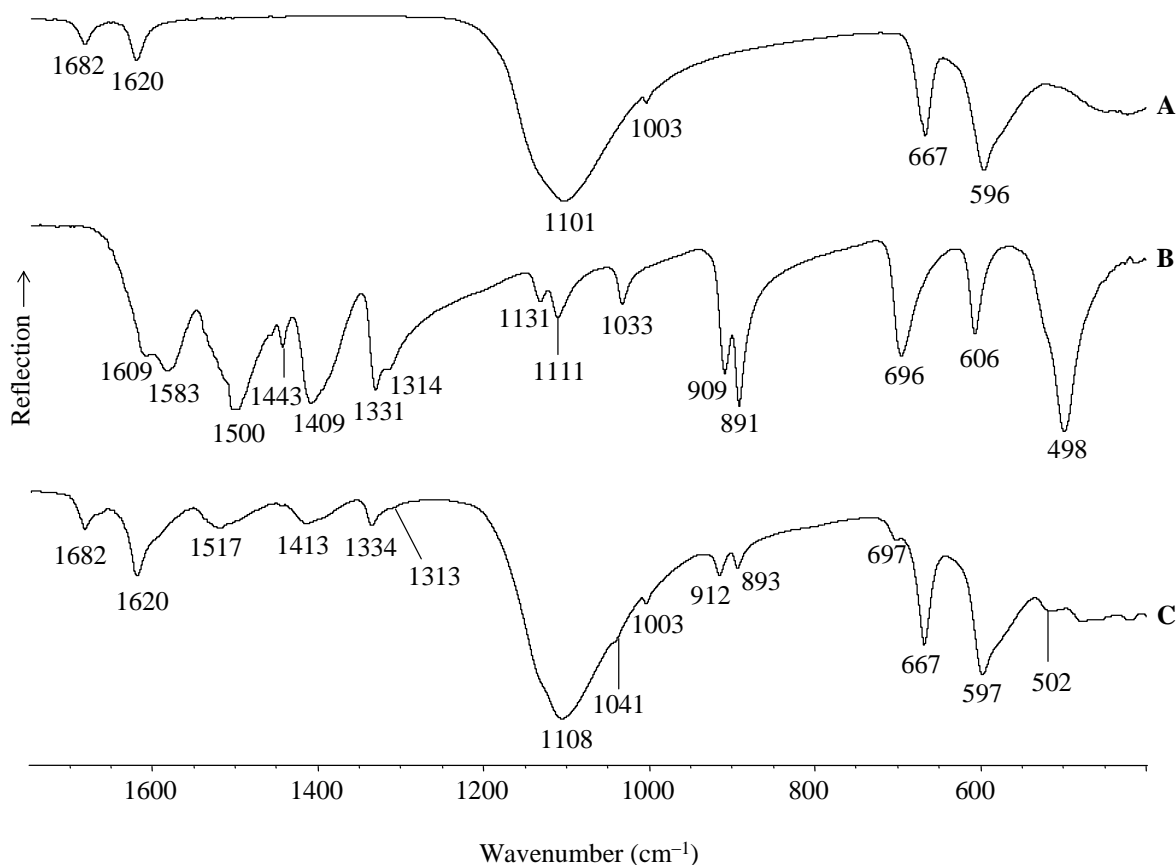


Fig. 25: Infrared spectra of (A) $\text{CaSO}_4 \cdot 2\text{H}_2\text{O}$ (gypsum), (B) α -glycine, and (C) gypsum–Hgly mixture (for preparation: see 4.5.1).

Thermal treatment of glycine embedded in MgCO_3 (MgCO_3 –Hgly)

MgCO_3 –Hgly was prepared by dry mixing of MgCO_3 (2 mmol) and glycine (0.4 mmol). Dry mixing was used because of the low solubility of MgCO_3 in water (0.001 mol L^{-1}). The detailed method of preparation is described under Materials and Methods (see 4.5.1). As expected, the infrared absorption bands of glycine in MgCO_3 –Hgly were at the same positions as in neat α -glycine, for example at 1331, 1131, 1033, 909, 606, and 498 cm^{-1} (Fig. A-10). This indicated the presence of free glycine and the absence of a coordinative interaction between Mg^{2+} and glycine. After heating MgCO_3 –Hgly at $200 \text{ }^\circ\text{C}$ for seven days, the residue was light grey. The formation of the thermo-melanoid was assumed because, in the starting material, glycine was present in its free form. However, it could not be detected in the residue by infrared spectroscopy. This may be due to: (i) the presence of too small amounts of the thermo-melanoid, and/or (ii) the broad infrared absorption bands of MgCO_3 that may have obscured the bands of the thermo-melanoid. The dark material could not be separated from the residue by washing with water because of the low solubility of MgCO_3 . Glycine and DKP were detected in the water extract of the residue by HPLC analysis

(Fig. A-11). However, their quantification was not possible because of the presence of other signals, possibly from decomposition products. Also, a thin layer of sublimate composed of glycine and DKP was found at the end of the quartz tube outside the furnace. These observations may demonstrate a small extend of thermal protection of glycine by MgCO_3 .

2.3.2 Thermal treatment of glycine embedded in clay minerals

In this section, the thermal behavior of glycine in the presence of various clay minerals (phyllosilicates) is described. For these studies, Ca-montmorillonite (SAz-1 and STx-1), Na-montmorillonite, nontronite (NAu-1), and kaolinite (KGa-1) were used. The Na-montmorillonite was prepared from Ca-montmorillonite by ion exchange in our laboratory (see 4.5.2). All other clay minerals were purchased from the Clay Minerals Society. It was found that nearly all Ca^{2+} ions in the interlayer spaces of Ca-montmorillonite were replaced by Na^+ ions during the process of ion exchange (Tab. 7). Note that one Ca^{2+} ion must be replaced by two Na^+ ions to balance the charge.

Tab. 7: Calcium and sodium content in Ca- and Na-montmorillonite.*

Metal	Ca-montmorillonite (SAz-1)	Na-montmorillonite**
Ca	2.82 %	0.023 %
Na	0.063 %	2.89 %

* Samples were vacuum dried at room temperature.

** Prepared by ion exchange from Ca-montmorillonite.

The loading of the clay minerals Ca-montmorillonite, Na-montmorillonite, and nontronite was performed by suspending 9.00 g of clay in 0.50 mol L^{-1} glycine solution (2.82 g of glycine in 75 mL of double distilled water). The clay minerals had been stored at 51 % relative humidity prior to use. Mixtures of kaolinite and glycine were prepared by directly mixing the two components in a small sample container. For this, 10 mg of glycine, dissolved in a minimum amount of double distilled water were added to 200 mg of kaolinite, and the suspension was dried. The detailed process of loading is described under Materials and Methods (see 4.5.2).

Analysis of glycine-loaded clay minerals

The clay minerals loaded with glycine were characterized by various analytical methods such as titration, HPLC, infrared spectroscopy and powder X-ray diffractometry.

The amount of glycine in the loaded clay minerals was determined by conductometric titration and HPLC quantification (see 4.5.4). The glycine content was 6.2 % in the Ca-montmorillonite SAz-1. The glycine content of Ca-montmorillonite STx-1 was 5.2 % and thus slightly lower. The lower absorption of glycine by STx-1 can be attributed to the lower negative charge on the interlayer surface of this clay mineral (Tab. 8). The lower interlayer charge corresponds to a smaller number of interlayer cations that are required as counterions. This, in turn, results in a lower absorption of glycine, which is supposed to be coordinated by the Ca^{2+} ions.

Tab. 8: Some properties of the Ca-montmorillonites SAz-1 and STx-1.

Property	SAz-1	STx-1
Cation exchange capacity (meq g^{-1})	1.20	0.84
Interlayer charge	-1.08	-0.68

Data taken from <http://www.clays.org/SOURCE%20CLAYS/SCdata.html>

The glycine contents found by both methods, titration and HPLC, were in good agreement with each other (Tab. 9). These values were averaged and formed the basis for the calculation of the yields of glycine after thermal treatments. The absorption of glycine depends on the nature of the cations in the interlayer spaces. It was found that nearly twice the amount of glycine was intercalated in Na-montmorillonite as compared to Ca-montmorillonite (Tab. 9). Na-montmorillonite has a higher interlayer swelling by H_2O molecules in comparison to Ca-montmorillonite (Foster, 1954; Odom, 1984). One reason for this is the absence of strong bridges between the interlayers when Na^+ is present. Therefore, more water can enter between the layers. In contrast, Ca^{2+} holds the layers together more strongly (Foster, 1954). Thus, during the loading process more water can be displaced by glycine molecules in the interlayer spaces of Na-montmorillonite. Similar results were obtained by Benincasa et al. (2000). The glycine content in nontronite was 7.7 % and thus comparable to the values found in the Ca-montmorillonites (Tab. 9).

Tab. 9: Content of glycine in clay minerals.

Clay mineral type	Glycine (%)		
	from titration	from HPLC	average of both methods
Ca-montmorillonite (SAz-1)	6.3	6.1	6.2
Ca-montmorillonite (STx-1)	5.3	5.1	5.2
Na-montmorillonite	12.2	11.6	11.9
Nontronite	7.6	7.7	7.7

The infrared spectra of glycine-loaded clay minerals showed only few absorption bands of the amino acid. These signals were found at 1501, 1412, and 1332 cm^{-1} . They occurred at similar position as for glycine (Fig. A-12). The other glycine signals were obscured by broad absorption bands of the clays.

Additionally, powder X-ray diffraction was employed to investigate the effect of glycine intercalation on the clay minerals. The powder X-ray diffraction patterns of the glycine-loaded clays were compared with those of the unloaded clays. The most significant information lies in the region of small diffraction angles. An increase in the interlayer space, mirrored by the $d(001)$ value, could be assumed for the clay minerals loaded with amino acids. However, a decrease in the interlayer space was observed both for Ca-montmorillonite and nontronite loaded with glycine (Tab. 10). This finding is in accordance with the report by Khan et al. (2009). The decrease is probably due to the replacement of water by glycine molecules in the interlayer spaces. Signals of free glycine present on the clay surface were not found. Therefore, it can be concluded that only a small amount of glycine (probably less than 10 %) was non-intercalated. In contrast, no change in the $d(001)$ position was observed for kaolinite–glycine mixtures (Tab. 10). Thus, glycine was mainly present on the surface of the kaolinite particles or not at all associated to the mineral. Due to the presence of strong hydrogen bonds between the repeating layers, intercalation of glycine was not possible.

Tab. 10: Position of the reflection 001 in the X-ray diffractograms of clay minerals before and after loading with glycine.

Mineral	Unloaded (Å)	Glycine loaded (Å)
Ca-montmorillonite SAz-1	15.01	14.57
Nontronite	14.90	13.13
Kaolinite	7.17	7.17

Thermal treatment of Ca-montmorillonite SAz-1 loaded with glycine

Ca-montmorillonite (SAz-1) was purchased from the Clay Minerals Society. To exclude artifacts caused by contaminations, a blank experiment was performed with neat Ca-montmorillonite under pure nitrogen atmosphere at 200 °C for two days. HPLC analysis of the water extract of the residue did not show the presence of amino acids or peptides. Therefore, it can be concluded that these compounds do not occur as contaminations under the experimental conditions.

Glycine-loaded Ca-montmorillonite was heated under a nitrogen atmosphere at 200 and 250 °C for two days. HPLC and MALDI–TOF/TOF MS analyses of the water extracts of the residues revealed the formation of several organic products. The results showed that Ca-montmorillonite enables glycine to survive these temperatures as unreacted glycine and glycine homopeptides. Besides glycine, at both temperatures DKP and peptides up to hexaglycine were detected by HPLC (Fig. 26). However, peptides higher than hexaglycine were not found in the chromatograms. This could be because of the low concentrations of higher peptides which were below the detection limit. The unambiguous identification of peptides was performed through “spiking”. For spiking, a known amount of reference substance is added to the analyte sample by which the height of the respective peak increases in comparison to others.

Furthermore, MALDI–TOF/TOF MS measurements were performed on the residue that remained after heating glycine-loaded Ca-montmorillonite at 200 °C for two days. For this, the water extract of the residue was mixed with a matrix solution (α -cyano-4-hydroxycinnamic acid) and dried on a target plate. The analysis showed the presence of glycine homopeptides from tetra- to decaglycine in their Na^+ forms (Tab. 11). Their corresponding protonated forms were not found. Peptides smaller than tetraglycine could not be unambiguously identified because too many intense signals of the matrix appear in the low mass region. The glycine homopeptides were identified by comparing their masses with those of reference substances.

The amounts of glycine, DKP, diglycine, and triglycine were determined by HPLC with the help of calibration curves. It should be mentioned that the experimental procedure involves several steps where inaccuracy in the quantification may occur, for example during sample preparation, extractions, volume measurement, and calibration. The process of extraction and calibration is described in detail under Materials and Methods (see 4.5.4).

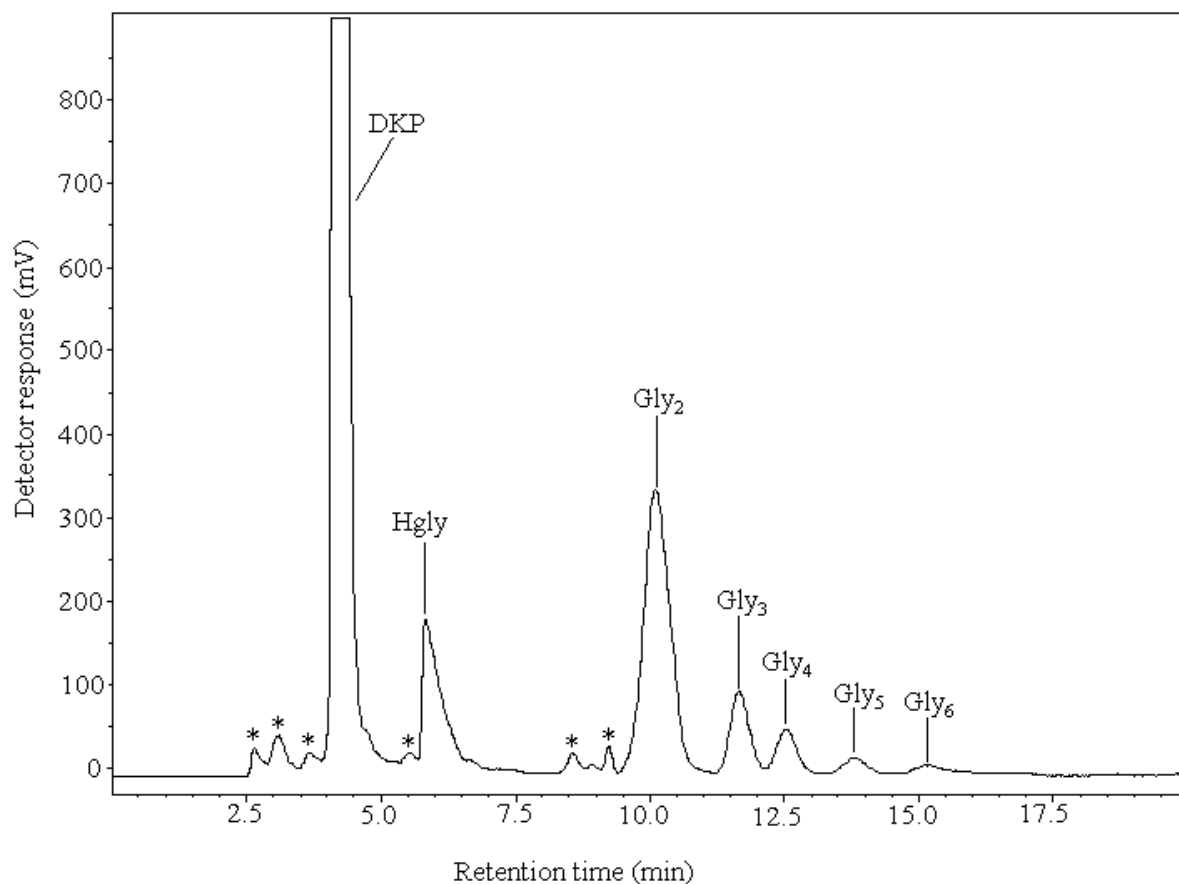


Fig. 26: HPLC analysis of the water extract of the residue obtained by heating glycine-loaded Ca-montmorillonite SAz-1 at 200 °C for two days. * Unidentified reaction products.

Tab. 11: Peptides identified by MALDI-TOF/TOF MS in the residue obtained by heating glycine-loaded Ca-montmorillonite SAz-1 at 200 °C for two days.

Species	Calculated mass	Observed mass
$[\text{Gly}_4 + \text{Na}]^+$	269.1	268.8
$[\text{Gly}_5 + \text{Na}]^+$	326.1	325.8
$[\text{Gly}_6 + \text{Na}]^+$	383.1	382.9
$[\text{Gly}_7 + \text{Na}]^+$	440.1	439.9
$[\text{Gly}_8 + \text{Na}]^+$	497.2	497.0
$[\text{Gly}_9 + \text{Na}]^+$	554.2	554.0
$[\text{Gly}_{10} + \text{Na}]^+$	611.2	611.0

After heating at 200 °C, the amount of glycine was found to be 0.258 mmol in the residue as compared to the starting value of 0.413 mmol. This represents 62.5 % of the initial content. Most of the remaining 37.5 % was transformed into the homopeptides: DKP

(0.054 mmol), diglycine (0.011 mmol), and triglycine (0.001 mmol). The quantification results showed that nearly all the starting glycine was still present in the unreacted form or had been transformed into peptides. After heating at 250 °C, the residue contained 0.029 mmol of glycine, which corresponded to 7.0 % of the initial content, 0.141 mmol of DKP, 0.009 mmol of diglycine, and 0.001 mmol of triglycine.

The results showed that (i) the amount of glycine that survived unreacted was about 9 times higher at 200 °C than at 250 °C; (ii) the formation of DKP increased with increasing temperature: the amount of DKP was about 2.6 times higher at 250 °C than at 200 °C; (iii) the thermo-melanoid was not found at both temperatures; and (iv) interestingly, no sublimation was observed during the thermal treatments. Thus, the main conclusion is that the process of intercalation in Ca-montmorillonite protects glycine from transformation into the thermo-melanoid and sublimation.

Mass losses of 14.4 and 15.4 % were found after two days at 200 and 250 °C, respectively. They were mainly caused by the loss of water of condensation during the peptide bond formation and the loss of water from the interlayer spaces of Ca-montmorillonite. A small extent of decomposition was also seen as unidentified peaks in the HPLC chromatogram (Fig. 26).

Additionally, a seven-day experiment was also performed at 200 °C to study the influence of a prolonged heating period on glycine in Ca-montmorillonite. The HPLC analysis of the water extract of the residue showed the presence of glycine (0.064 mmol), DKP (0.014 mmol), diglycine (0.005 mmol), and triglycine, but no other peptides. The glycine amount corresponded to 38.8 % of the starting amount (0.165 mmol) and was approximately 1.6 times less than in the two-days residue. Triglycine was not quantified because of the improper base line separation in the HPLC chromatogram. The results indicated that (i) more glycine has reacted and (ii) higher glycine homopeptides (tetraglycine to decaglycine), which were formed after two days, have been decomposed during the longer heating period.

Thermal treatment of Ca-montmorillonite STx-1 loaded with glycine

For comparison, the Ca-montmorillonite STx-1 was loaded with glycine and also heated at 200 °C for two days and seven days. The HPLC analyses of the water extracts of the residues showed the presence of only glycine, DKP, diglycine, and triglycine.

After two days of thermal treatment, 0.055 mmol of glycine were found which was 39.6 % of the initial amount of 0.139 mmol. DKP and diglycine were found in amounts of

0.002 mmol each. After seven days, 0.043 mmol of glycine (30.9 % of the initial content), 0.003 mmol of DKP, and 0.002 mmol of diglycine were found. The triglycine signal was not well resolved in the HPLC chromatogram. Thus, this peptide was not quantified. Some unidentified peaks due to decomposition were also found at both temperatures.

The comparison between the two types of Ca-montmorillonites (SAz-1 and STx-1) showed that: (i) SAz-1 provided better protection to glycine than STx-1 on heating at 200 °C for two days and seven days, (ii) the degree of polymerization of glycine was higher in SAz-1. The reasons for this different behavior are unclear. The two Ca-montmorillonites mainly differ in the negative charge on their interlayer surface (see Tab. 8).

Thermal treatment of Na-montmorillonite loaded with glycine

Glycine-loaded Na-montmorillonite was also heated at 200 and 250 °C for two days. The residues were extracted, and the extracts were analyzed with HPLC. Glycine, DKP, and glycine homopeptides up to the hexapeptide were found after treatment at 200 °C. At this temperature, 0.168 mmol of glycine had survived in the residue, which were 53.0 % of the initial 0.317 mmol. About half of the remaining glycine had been converted into 0.039 mmol of DKP and 0.002 mmol of diglycine. Other glycine homopeptides were not quantified.

The residue that was obtained after treatment at 250 °C contained unreacted glycine, DKP, and diglycine but no higher peptides. The glycine amount in the residue was 0.078 mmol, corresponding to 24.6 % of the initial glycine. The amount of DKP was found to be 0.062 mmol, whereas the amount of diglycine was too low for quantification. The mass loss of 13.0 % and 15.0 % observed at 200 and 250 °C, respectively, can be explained by the loss of water during peptide bond formation and from the interlayer spaces of the clay mineral.

The comparison between Ca- and Na-montmorillonite showed that (i) at 200 °C, the relative amount of glycine that had survived was slightly higher (nearly 1.2 times) in Ca-montmorillonite than in Na-montmorillonite, (ii) at 250 °C, the amount of glycine available was higher in Na-montmorillonite than in Ca-montmorillonite, and (iii) at 250 °C, the degree of polymerization of glycine was higher in Ca-montmorillonite.

Thermal treatment of nontronite NAu-1 loaded with glycine

500 mg samples of glycine-loaded nontronite NAu-1 were heated at 200 and 250 °C for two days. HPLC analysis of the water extract of the residue formed at 200 °C showed the presence of glycine, DKP, diglycine, and triglycine. The amount of glycine in the residue was

0.202 mmol, corresponding to 39.4 % of the initial content of 0.513 mmol. Glycine was converted into 0.004 mmol of diglycine. DKP was not quantified due to improper baseline separation and the amount of triglycine was too low to be quantified. Thus, about half of the initial amount of glycine was transformed into unidentified products.

The residue that remained at 250 °C contained 0.127 mmol of glycine which represents 24.8 % of the initial amount. DKP and diglycine were also present but were not quantified because of improper baseline separation in the HPLC chromatogram, which was probably caused by the presence of other signals lying under the DKP and diglycine peaks. Peptides higher than diglycine were not detected.

At both temperatures, peaks of unidentified decomposition products were also observed in the chromatograms. A mass loss of 10.5 % and 15.8 % was found at 200 and 250 °C, respectively. The results showed that: (i) a considerably smaller amount of glycine survived at 200 °C in nontronite as compared to the two smectite clay minerals SAz-1 and Na-montmorillonite, (ii) the degree of polymerization of glycine was lower in nontronite as compared to Ca- and Na-montmorillonite at both temperatures. The amount of glycine survived in Ca-montmorillonite at 200 °C was approximately 1.6 times higher as compared to nontronite under similar experimental conditions. Keeling et al. (2000) have reported that nontronite NAu-1 also contains kaolinite, goethite, quartz, and biotite. The presence of these minerals may lead to a decrease in the protection and polymerization of glycine.

Thermal treatment of a mixture of the kaolinite KGa-1 and glycine

For preparing a kaolinite–glycine mixture, 10 mg of glycine dissolved in a minimum amount of water were added to 200 mg of kaolinite. This suspension was prepared and dried in the quartz container as described under Materials and Methods (see 4.5.2). Direct mixing was preferred because intercalation of glycine in kaolinite was not expected. Instead, glycine was assumed to be mainly present on the surface of the kaolinite particles. Again, the heating experiments were performed at 200 and 250 °C for two days.

The HPLC analysis of the water extract of the 200 °C residue showed the presence of glycine, DKP, and glycine homopeptides up to pentaglycine (Fig. 27). At this temperature, 0.020 mmol of glycine were found (15.0 % of the initial 0.133 mmol). When compared, the amount of glycine survived in Ca-montmorillonite at 200 °C was four times higher under similar experimental conditions. In addition, 0.015 mmol of DKP, 0.003 mmol of diglycine, and 0.001 mmol of triglycine were found.

Glycine, DKP, diglycine, and triglycine were also found in the water extract of the residue formed at 250 °C. The glycine amount was 0.008 mmol, which was 6.0 % of the initial one. 0.005 mmol of DKP were formed. Diglycine and triglycine were not quantified as their peaks were not well resolved. This was possibly caused by interfering signals of decomposition products.

At both temperatures, a very thin layer of sublimate composed of glycine and DKP was found at the end of the quartz tube. This observation supported the assumption that glycine was not intercalated and was mainly on the surface of the kaolinite particles, in contrast to the situation with the other clay minerals Ca-montmorillonite, Na-montmorillonite, and nontronite .

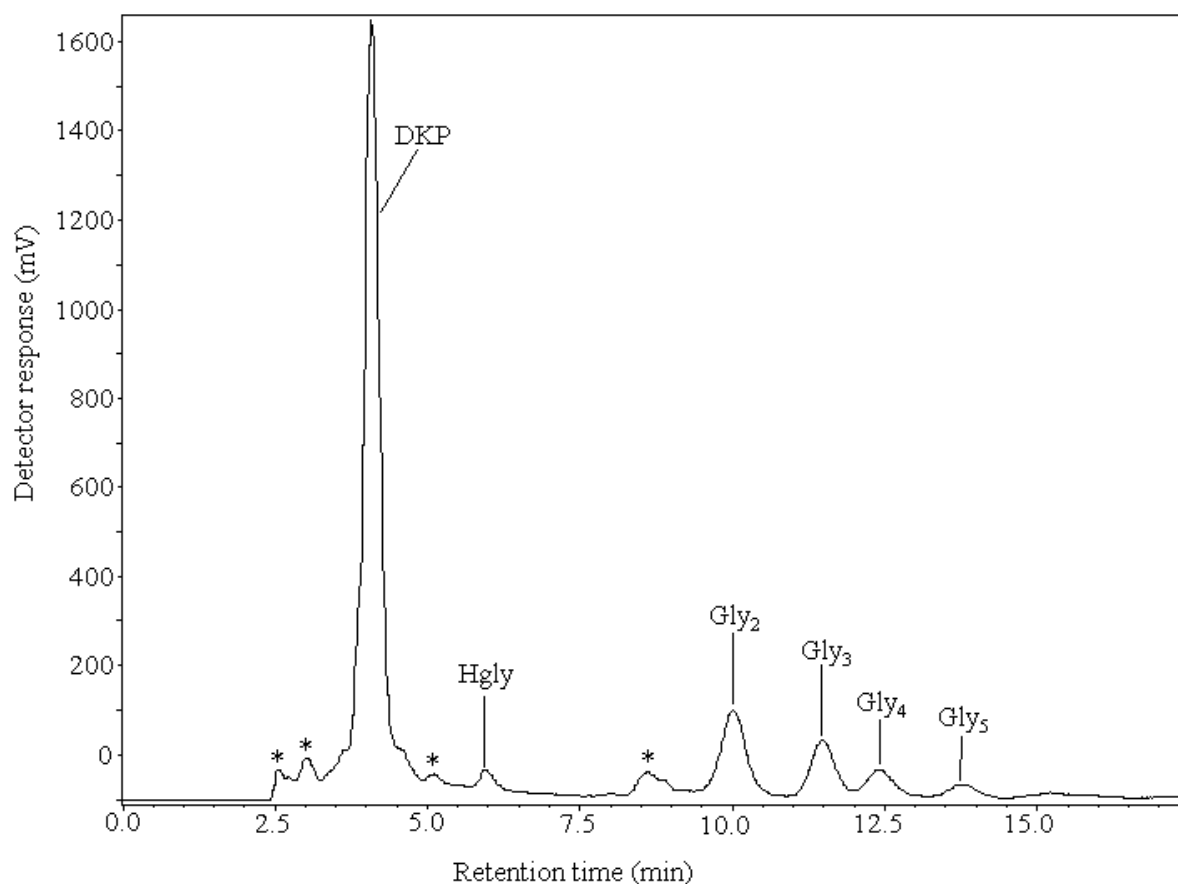


Fig. 27: HPLC analysis of the water extract of the residue obtained by heating a kaolinite–glycine mixture at 200 °C for two days. * Unidentified decomposition products.

Overview on the protection of glycine by salts and clay minerals

It is generally assumed that various salts and amino acids were present on the young Earth (see 1.4.1). In addition to the SIPF reactions (Schwendinger and Rode, 1989, 1991; Rode and Schwendinger, 1990) salts may have played an important role in altering the chemical and physical behavior of amino acids. In experiments described above, glycine was found to exist in its free form in the presence of NaCl, NaCl–KCl mixture, and MgCO₃. However, the initial α -modification had changed to the γ -form in the presence of NaCl and NaCl–KCl. At 200 °C, glycine embedded in NaCl or NaCl–KCl was mainly transformed into the thermo-melanoid. Small amounts of DKP were also formed but no other oligopeptides. The formation of the thermo-melanoid may have been of importance to prebiotic chemistry. For instance, it could have served as a possible mechanism for the protection of glycine and its peptides under early Earth's harsh conditions (see 2.1 and 2.2). Afterwards, the amino acid and peptides could have been released by hydrolysis (see 2.2.2).

In contrast, glycine was exclusively present as CaCl₂(Hgly) · H₂O in the mixtures prepared from glycine and CaCl₂ · 2H₂O or artificial sea salt (AS). At 200 °C, 93.6 and 83.8 % of the glycine remained unchanged in CaCl₂(Hgly) · H₂O and AS–Hgly, respectively (Tab. 12). The coordination of glycine to Ca²⁺ cations prevented the transformation of the amino acid into the thermo-melanoid up to 250 °C. At 350 °C, various alkylated pyrroles were detected in the volatile fraction formed from CaCl₂(Hgly) · H₂O (this work and Yusenko et al., 2008). It is interesting to note that pyrroles are building blocks of porphyrin-type biomolecules such as cytochromes and chlorophylls.

The thermal behavior of glycine was also studied in the presence of clay minerals. Clay minerals are formed by weathering of volcanic rock and are believed to have been present already at the time of prebiotic chemical evolution (see 1.3.1). Recently, they have also been found on Mars. The results of the heating experiments demonstrated that glycine could partly survive unreacted and as glycine homopeptides in the clay minerals at 200 and 250 °C (see 2.3.2). Glycine enters into the interlayer spaces of the smectites (Ca-montmorillonite, Na-montmorillonite, and nontronite) and probably binds to the metal ions which are present there. A higher degree of polymerization of amino acids has been reported in the presence of divalent cations (Remko and Rode, 2004; Constantino et al., 2009). Remko and Rode (2001, 2004) have shown that glycine polymers form more stable complexes than glycine with various cations due to strong binding energies. Similarly, calcium ions present in the interlayer spaces of Ca-montmorillonite probably form a coordination complex with

glycine. Thus, they may promote the polymerization of glycine to peptides because calcium–peptide complexes are more stable than calcium–glycine complexes. At 200 °C, 62.5 % of the initial amount of glycine was still present in Ca-montmorillonite. This was ca. 1.2 times more than in Na-montmorillonite, 1.6 times more than in nontronite, and 4 times more than in kaolinite under similar experimental conditions. It was found that Ca-montmorillonite, Na-montmorillonite, and nontronite have protected glycine from (i) transformation into the thermo-melanoid, (ii) sublimation, and (iii) complete decomposition. However, polymerization of glycine to homopeptides occurred during the thermal treatment at both 200 and 250 °C in the presence of clay minerals (Tab. 13).

Tab. 12: Behavior of glycine in different salt matrices when treated at 200 °C for seven days.

Sample	Binding form of glycine	Residue color	Mass loss (%)*	Glycine survived (%)	Organic components identified in the residue
NaCl–Hgly	Free (γ -Hgly)	Black	23.5	4.9	Thermo-melanoid, Hgly, and DKP
NaCl–KCl–Hgly	Free (γ -Hgly)	Dark grey	1.4	43.2	Thermo-melanoid, Hgly, and DKP
CaCl ₂ (Hgly) · H ₂ O	Metal coordinated	Peach	10.7	93.6	Hgly and DKP
AS–Hgly	Metal coordinated	White	14.6	84.2	Hgly and DKP
Gypsum–Hgly	Unknown	Dark grey	23.3	9.5	Thermo-melanoid [#] , Hgly, and DKP
MgCO ₃ –Hgly	Free (α -Hgly)	Light grey	9.0	n.q.	Thermo-melanoid [#] , Hgly, and DKP

*Note the different glycine contents of the starting materials (see text), AS: artificial sea salt, n.q.: not quantified, [#] tentatively assigned

In contrast, sublimation, formation of the thermo-melanoid, and no peptide formation (except DKP) were observed when neat glycine was heated at 200 °C (see 2.1.1). Thus, intercalation into the clay minerals, including the formation of interlayer metal–glycine complexes, could have been an important mechanism to protect glycine on the early Earth and Mars. In contrast, the repeating layers in kaolinite are connected through strong hydrogen

bonds. The outer layers have exposed oxygen and hydroxyl groups (Miranda-Trevino and Coles, 2003), with which glycine can interact. Therefore, the absorption of glycine was assumed to be limited to the surface of kaolinite particles, unlike to the situation with smectites.

Tab. 13: Overview on the peptide formation by thermal treatment of glycine-loaded clay minerals for two days.

Clay mineral	Temperature (°C)	Mass loss (%)	Glycine survived (%)	Peptides identified in the residue
Ca-montmorillonite SAz-1	200	14.4	62.5	DKP, Gly ₂ to Gly ₁₀
	250	15.4	7.0	DKP, Gly ₂ to Gly ₆
Ca-montmorillonite STx-1	200	13.2	39.6	DKP, Gly ₂ , and Gly ₃
	250	13.0	53.0	DKP, Gly ₂ to Gly ₆
Na-montmorillonite	200	13.0	53.0	DKP, Gly ₂ to Gly ₆
	250	15.0	24.6	DKP and Gly ₂
Nontronite NAu-1	200	10.5	39.4	DKP, Gly ₂ , and Gly ₃
	250	15.8	24.8	DKP and Gly ₂
Kaolinite KGa-1	200	3.8	15.0	DKP, Gly ₂ to Gly ₅
	250	7.8	6.0	DKP, Gly ₂ , and Gly ₃

2.3.3 Terrestrial volcanic rock and Martian soil simulants

Mixture of volcanic rock and glycine

The basaltic “sand” used was a product of the 2007 eruption of the Piton de la Fournaise volcano on the island of La Réunion, Indian Ocean. A few days after it had been collected in 2011 the basaltic sand was dried and sterilized (Fox and Strasdeit, unpublished results). Prior to use, it was pulverized (see 4.5.3). The mineral composition of the basaltic sand was studied by powder X-ray diffractometry. The basaltic sand was mixed with pure NaCl as an internal standard. The diffractograms of this mixture and of pure NaCl were recorded. Literature values for the d spacings of NaCl differ by no more than 0.003 Å (<http://www.handbookofmineralogy.org/pdfs/halite.pdf>, <http://rruff.geo.arizona.edu/AMS/download.php?id=12689.txt&down=dif>, http://database.iem.ac.ru/mincryst/s_carta.php?HALITE). The following mean values were used for calibration: 3.257, 2.820, 1.994, 1.701, 1.628, 1.410, 1.294, 1.261, and 1.152 Å. It

was found that the d values of the basaltic sand and the d values of forsterite (Mg_2SiO_4) reported in the literature were in good agreement with each other (Fig. 28 and Tab. A-1). However, fayalite (Fe_2SiO_4) signals did not match with the signals found. The presence of forsterite was also supported by infrared spectroscopy. The absorption bands found at 976, 891, 838, 601, 493, and 460 cm^{-1} were in accordance with the forsterite signals reported in the literature (<http://rruff.info/forsterite/display=default/R040018>). Therefore, forsterite (Mg_2SiO_4) is the major crystalline mineral in the basaltic sand. Olivine [$(\text{Mg,Fe})_2\text{SiO}_4$], which is a solid solution of forsterite and fayalite, may be present but was not unambiguously identified.

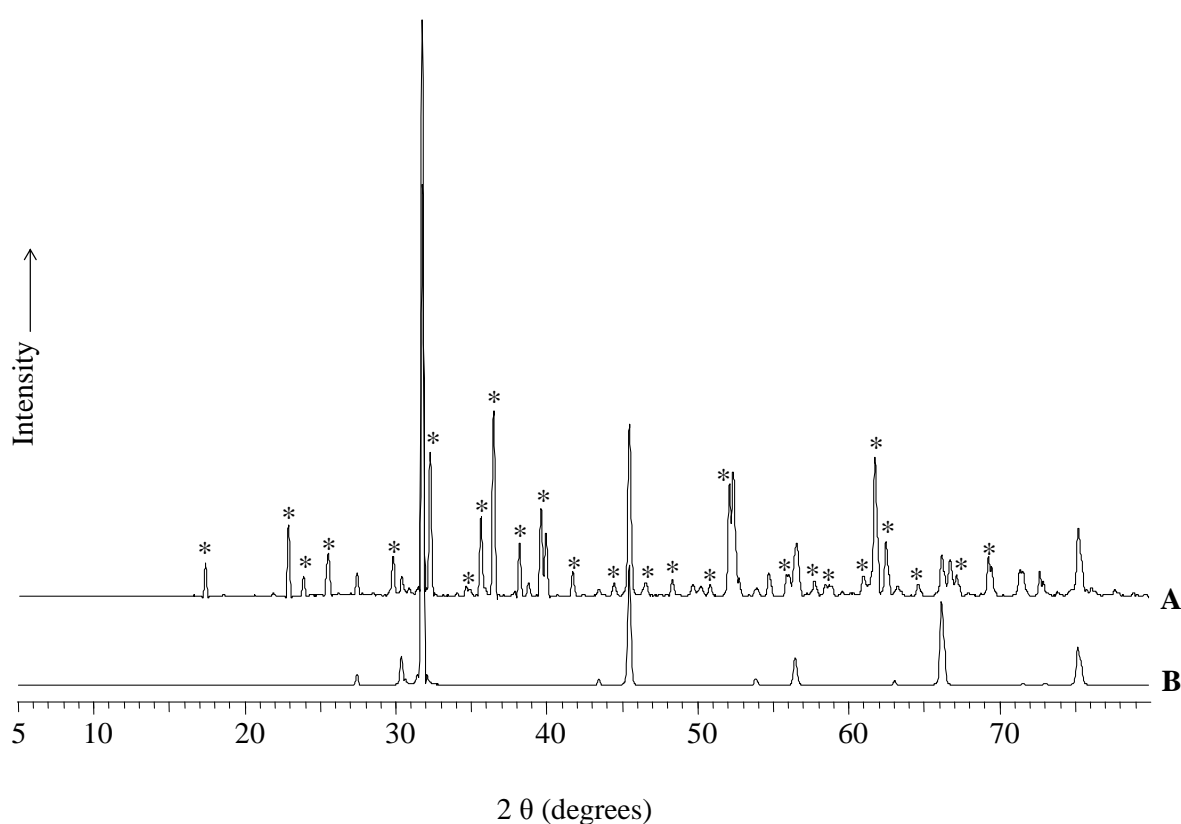


Fig. 28: Background subtracted powder X-ray diffractograms of (A) the basaltic sand mixed with NaCl and (B) neat NaCl. * Signals assigned to forsterite.

An experiment was performed to study the thermal behavior of glycine in the presence of basaltic sand. For this purpose, 465 mg of the basaltic sand (stored at 51 % relative humidity) was mixed with 35 mg (0.466 mmol) of glycine and heated at 200 °C for two days. HPLC analysis of the water extract of the residue showed the presence of 0.003 mmol of DKP, but no glycine and glycine peptides were found. To analyze for the presence of the thermo-melanoid, the residue was mixed with CCl_4 ($\rho = 1.59\text{ g cm}^{-3}$) and

shaken vigorously. By this the heavier basaltic sand was separated from the lighter thermo-melanoid particles ($\rho = 1.50 \text{ g cm}^{-3}$). The floating black particles were collected and dried. The infrared spectrum of these particles closely resembled that of the thermo-melanoid (Fig. A-13). A sublimate composed of glycine and DKP was also observed in the heating experiment. The results showed that at least a large portion of glycine had been transformed into the thermo-melanoid or sublimed.

Mixtures of Phyllosilicatic Mars Regolith Simulant (P-MRS) and Sulfatic Mars Regolith Simulant (S-MRS) with glycine

The Martian soil simulants P-MRS and S-MRS were obtained from the Museum für Naturkunde, Berlin. P-MRS simulates the soil that existed under the early hydrous conditions on Noachian Mars, and S-MRS is a model for the acidic Hesperian soil environment (Böttger et al., 2012). In the heating experiments, a mixture of P-MRS or S-MRS (465 mg) with glycine (35 mg) was heated at 200 °C for two days.

In the case of the P-MRS–glycine mixture, HPLC analysis of the water extract of the residue showed the presence of glycine, DKP, and diglycine to hexaglycine (Fig. A-14). These findings are comparable to the results obtained by heating various glycine-loaded clay minerals. In fact, P-MRS largely consists of clay minerals, e.g. montmorillonite (45 %), chamosite (20 %), and kaolinite (5 %) (Böttger et al., 2012). As discussed above, the intercalation of glycine in clay minerals promotes polymerization and protects glycine from complete decomposition and transformation into the thermo-melanoid (see 2.3.2). In particular, glycine homopeptides thermally form in the presence of clay minerals. In the experiment with P-MRS, a mass loss of 8.2 % was observed after heating. This loss was due to the partial sublimation of glycine and DKP, loss of water of condensation, and loss of interlayer water from the clay minerals. In the HPLC chromatogram, some unidentified peaks were also found, obviously from decomposition products. An incomplete protection of glycine from decomposition and sublimation may be explained by the presence of non-clay minerals such as quartz (10 %), mafic igneous rocks, siderite, and hydromagnesite (5 % each).

In contrast to the results obtained for P-MRS, HPLC analysis of the residue of S-MRS with glycine showed only the presence of unreacted glycine, DKP, and diglycine, but no higher peptides. Some unidentified decomposition products were also observed in the HPLC chromatogram. The major mineral components of S-MRS are mafic igneous rocks (47 %), gypsum ($\text{CaSO}_4 \cdot 2\text{H}_2\text{O}$) (30 %), and iron oxides (20 %), but no clay minerals

(Böttger et al., 2012). The formation of smaller peptides could have been promoted by iron oxides as reported by Shanker et al. (2012). However, the presence of gypsum can result in the decomposition and sublimation of glycine as seen before (see 2.3.1). In the heating experiment with glycine-loaded S-MRS, the sublimate consists of glycine and DKP.

Mixtures of the Martian regolith simulant JSC Mars-1A with glycine

JSC Mars-1A (2007) is a reproduction of the JSC Mars-1 (1997) Martian soil simulant. “JSC” refers to “NASA Johnson Space Center”. These soil simulants are the weathering products of volcanic ash from Pu’u Nene, a cinder cone on the Island of Hawaii. They have UV/NIR spectra comparable the bright regions of Mars (Mustard and Bell, 1994). A blank experiment was performed, in which JSC Mars-1A was heated at 200 °C for two days to test for relevant contaminations. No amino acids or peptides were detected by HPLC in the water extract of the residue.

A dried mixture of JSC Mars-1A (465 mg) and glycine (35 mg) was heated at 200 °C for two days (see 4.5.3). HPLC analysis of the water extract of the residue showed the presence of DKP and glycine. The DKP and glycine peaks were not well resolved and thus, were not quantified. Possibly signals of other decomposition products interfered with these peaks. JSC Mars-1A contains mainly amorphous palagonite (product of volcanic glass alteration) and trace amounts of clay minerals (<1 %), hematite, olivine and glass (Allen et al., 1997). Therefore, JSC Mars-1A, unlike clay minerals, does not intercalate amino acids. A mass loss of 15.3 % was found in the sample due to the sublimation of glycine and DKP, loss of water of condensation from DKP formation, and loss of water from JSC Mars-1A.

JSC Mars-1A contains a considerable amount of water (Allen et al., 1997). To measure the water loss, 500 mg of JSC Mars-1A in a quartz container (6.736 g) were heated at 200 °C for two days under a pure nitrogen atmosphere. The residue was immediately taken out of the furnace and kept in a desiccator for cooling. The combined mass of the residue and the container was 7.181 g. Therefore, the mass loss was 11.0 %.

2.4 Racemization of amino acids intercalated in Ca-montmorillonite

Batches of Ca-montmorillonite were loaded with α -amino acids having different L-enantiomeric excesses (ee). The amino acids studied were alanine [L-ee: 0 (i.e. racemic), 4, 20, 50, and 100 %], L-valine (i.e. 100 % L-ee), and L-isovaline (i.e. 100 % L-ee). The detailed process of loading is described under Materials and Methods (see 4.5.2). Additionally, experiments were performed with Ca-montmorillonite loaded with a mixture of

L-alanine and L-isovaline and Ca-montmorillonite loaded with a mixture of racemic alanine and L-isovaline (see 4.5.2). All samples were heated at 200 °C for eight weeks. Furthermore, one long-term experiment with Ca-montmorillonite loaded with L-alanine was performed at 200 °C for 24 weeks. To investigate the influence of the temperature on the rate of racemization, Ca-montmorillonite loaded with L-alanine was also heated at various temperatures (120, 150, 180, 200, and 220 °C) for eight weeks. Samples were collected in certain time intervals, extracted with double distilled water, dried, and derivatized for GC-MS and GC-FID analyses (for details see 4.5.2, 4.5.4, and 4.1.3).

The major mass-spectrometric fragments of the amino acid derivatives used corresponded to $m/e = 140$ for the alanine derivative and $m/e = 168$ for the valine derivative. These fragments represented $[M-CO_2CH_3]^+$ ions. Minor fragments were also observed at 168 and 196 for alanine and valine, respectively. They resulted from the loss of OCH_3 from the molecular ions (Manhas et al., 1970).

Special attention was paid to the precision and accuracy of the GC measurements. During the thermal treatment, ~200 mg aliquots of the sample were collected at certain intervals. Each aliquot was divided into two parts (replicates) that were separately extracted, derivatized, and analyzed. The two replicates usually gave values which deviated by no more than 0.5 % from each other, which showed that the whole procedure yielded sufficiently precise results. Therefore, the average value from the two replicates was used for each data point. The results were also reproducible under similar experimental conditions. Moreover, the GC results differed only by ≤ 1.0 % from the true value. For example, for racemic alanine an L-ee between -0.5 and $+0.5$ % was found by manual integration. However, in the case of isovaline, a deviation of 2–3 % from the true value was found because the base line separation between L- and D-form was not as good as for alanine.

2.4.1 Thermal treatment at 200 °C of Ca-montmorillonite loaded with alanine having different starting L-ee

Batches of Ca-montmorillonite loaded with alanine were heated at 200 °C for eight weeks. The products obtained after certain time intervals were analyzed for changes in the L-ee by GC-MS and GC-FID. In all experiments, it was found that the L-ee of alanine had considerably decreased during eight weeks of heating. The eighth-week residues contained 17.5–25.0 % of the initial L-ee (Tab.14). This relatively narrow range indicated that the normalized rate of racemization was independent of the starting L-ee. This is also obvious from Figure 29.

Tab. 14: Change of the L-ee of alanine intercalated in Ca-montmorillonite after eight weeks at 200 °C.

Ideal value of the starting L-ee (%)	Measured starting L-ee (%)	L-ee measured after eight weeks	
		Absolute (%)	% of the starting ee
100	99.6	20.4	20.5
50	50.2	11.7	23.3
20	19.2	4.8	25.0
4	4.0	0.7	17.5
0	-0.1	-0.1	- ^a

^a Normalization not appropriate

In aqueous solution, the process of racemization generally takes place via the abstraction of the α -H from the amino acid forming a carbanion (Smith et al., 1978). According to various reports, racemization is faster under aqueous conditions and is retarded in the complete absence of water (Schroeder and Bada, 1976; Bada et al., 1994; Cohen and Chyba, 2000). The experiments with 4–100 % L-ee showed a fast rate of racemization in the first 2–3 days, which thereafter slowed down (Fig. 29). There was a continuous increase in the relative concentration of the D-form over a time period of eight weeks (Fig. 30). The influence of Ca-montmorillonite on the rate of racemization of alanine is not clear, because comparative experiments with neat alanine could not be conducted due to technical problems (e.g. sublimation, decomposition). DL-alanine in Ca-montmorillonite did not change its racemic character during the eight weeks of thermal treatment. Therefore, it can be concluded that Ca-montmorillonite does not have any specific preference for the formation of either D- or L-alanine.

Additionally, HPLC analyses of the water extracts of some of the residues were performed. They showed the presence of unreacted alanine, the two diastereomers (DL and LL/DD) of the 2,5-diketopiperazine of alanine, and the open-chain dialanine (Fig. A-15).

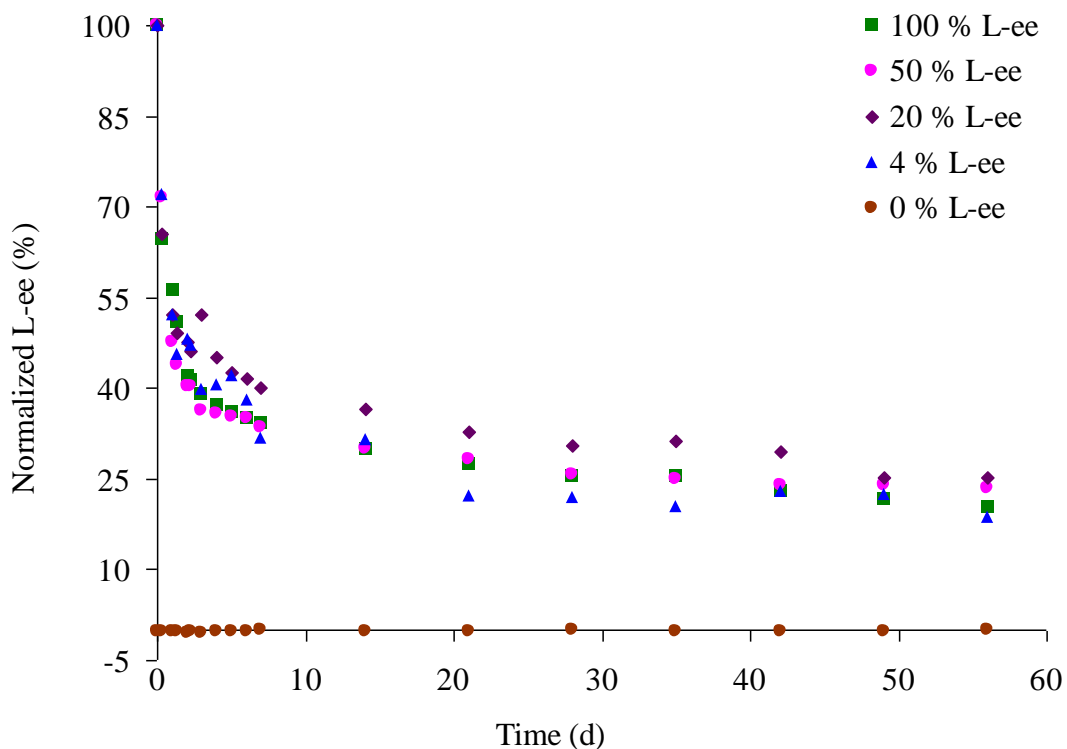


Fig. 29: Development of the L-ee of alanine intercalated in Ca-montmorillonite during eight weeks of heating at 200 °C. The L-ee percentage values were normalized to 100 % except for racemic alanine.

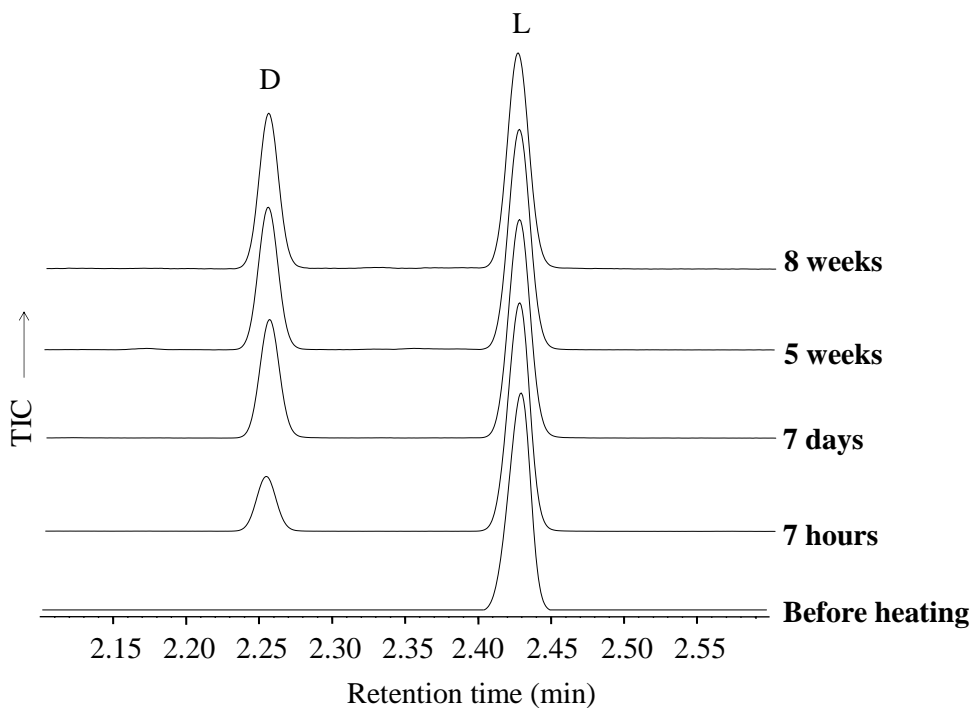


Fig. 30: Development of the gas chromatogram of a sample starting with 100 % L-ee of alanine intercalated in Ca-montmorillonite during heating at 200 °C. Detection: total ion current (TIC).

An additional heating experiment at 200 °C was performed with Ca-montmorillonite loaded with enantiopure L-alanine for 24 weeks. Its purpose was to investigate the influence of longer heating times on the racemization of alanine. As in the eight-week experiment, racemization was fast during the initial 2–3 days, and slowed down thereafter (Fig. A-16). The residues obtained after eight weeks contained 20.4 % and 25.4 % L-ee alanine in the eight-weeks and 24-weeks (long-term) experiment, respectively. These L-ee values are comparable but not identical. Thus, they give an idea about the limited reproducibility under heterogenous solid state conditions. After 24 weeks, 16.8 % L-ee was still found in the residue. This result also shows that Ca-montmorillonite protects alanine from complete decomposition and sublimation even after 24 weeks.

In another experiment, the racemization of alanine in Ca-montmorillonite loaded by two different methods was compared. These methods were the “distribution method” and the “direct loading method”. In the first method, an amino acid solution and Ca-montmorillonite were shaken overnight to allow the distribution of the amino acid between the solution and the solid phase. The suspension was then centrifuged. The sediment was dried and stored in a desiccator which contained a saturated solution of $\text{Ca}(\text{NO}_3)_2$ to maintain 51 % relative humidity (for details see 4.5.2). The amount of amino acid loaded into Ca-montmorillonite was 6.9–7.9 % when the distribution method was employed. Therefore, a similar amount of the amino acid (ca. 7.5 %) was used in the direct loading method. The direct loading simulates a prebiotic scenario where an amino acid-containing solution interacts with clay minerals and completely evaporates. In this method an amino acid and Ca-montmorillonite were dissolved and suspended, respectively, in a minimum amount of water. The suspension was air-dried to a muddy consistency. Afterwards, a small amount of water was added along the walls of the container to wash dried amino acid back into the clay mineral. Subsequently, the sample was completely air-dried, pulverized, and stored over a saturated solution of $\text{Ca}(\text{NO}_3)_2$. A sample prepared by the direct loading method was also heated at 200 °C for eight weeks. Independently of the method used to prepare the sample (distribution or direct loading), the racemization rate was fast only during first few days. The residues contained 28.5 % L-ee of alanine (direct loading) and 20.4 % L-ee (distribution method), respectively. It is not clear whether this difference is due to the different methods of loading or the limits of the reproducibility (see above).

2.4.2 Thermal treatment at various temperatures of Ca-montmorillonite loaded with L-alanine

In separate experiments, Ca-montmorillonite loaded with L-alanine was heated at 120, 150, 180, 200, and 220 °C. The results showed that the racemization process was strongly temperature-dependent. As expected, the racemization rate increased with increasing temperature (Fig. 31). The temperature-dependent formation of D-alanine is evident from the gas chromatograms shown in Figure 32. After eight weeks, a high L-ee of alanine (75.4 %) was still present at 120 °C, whereas only 15.3 % remained at 220 °C (Tab. 15). Sublimation of alanine did not occur at any of the temperatures employed. In contrast, neat alanine can sublime within a few hours (see 2.5). As already discussed in 2.3.2, Ca-montmorillonite can protect amino acids from sublimation and complete decomposition.

Tab. 15: Change of the L-ee of alanine intercalated in Ca-montmorillonite after eight weeks at different temperatures.

Temperature (°C)	Starting L-ee (%)	L-ee (%) after eight weeks
120	99.6	75.4
150	99.2	47.6
180	99.6	35.3
200	99.6	20.4
220	99.7	15.3

2.4.3 Thermal treatment of Ca-montmorillonite loaded with other amino acids

Ca-montmorillonite loaded with L-valine

Enantiopure L-valine embedded in Ca-montmorillonite was also heated at 200 °C for eight weeks. This experiment was performed in order to compare the racemization rates of alanine and valine in the presence of Ca-montmorillonite. As in the case of alanine, the L-ee of valine decreased rapidly during the initial few days but more slowly thereafter (Fig. A-17). After eight weeks, valine had 6.8 % L-ee, whereas 20.4 % L-ee had been found for alanine under similar experimental conditions.

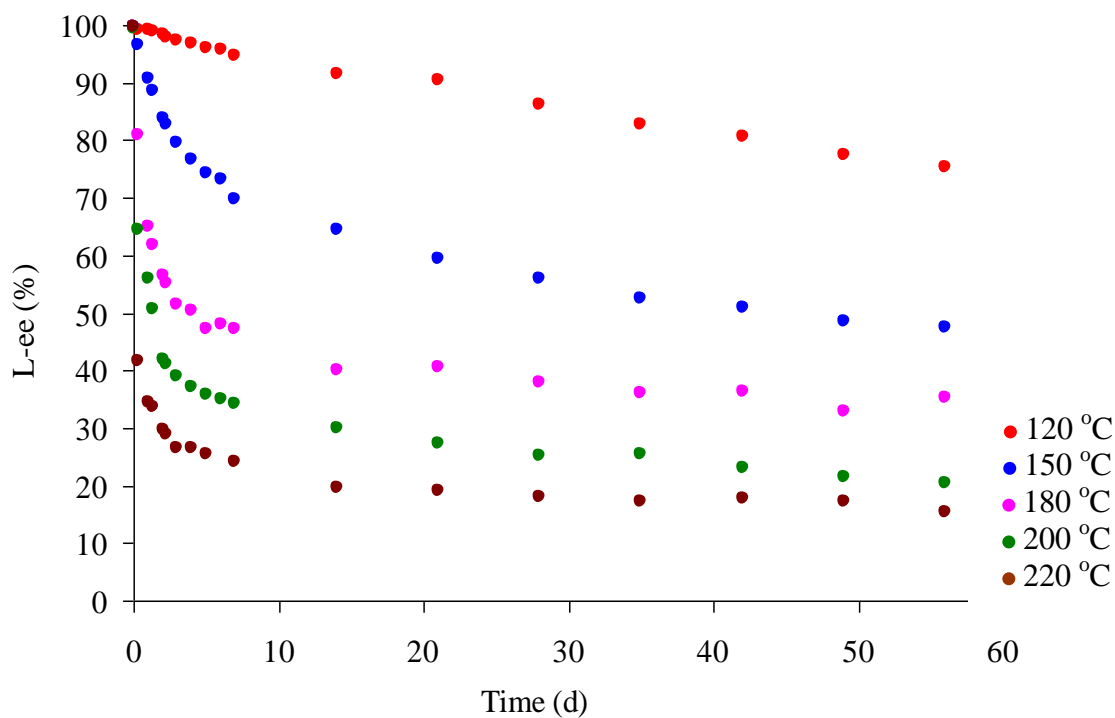


Fig. 31: Development of the L-ee of alanine intercalated in Ca-montmorillonite during eight weeks of heating at various temperatures. In each experiment, the starting L-ee was nearly 100 % (see Tab. 15 for the exact values).

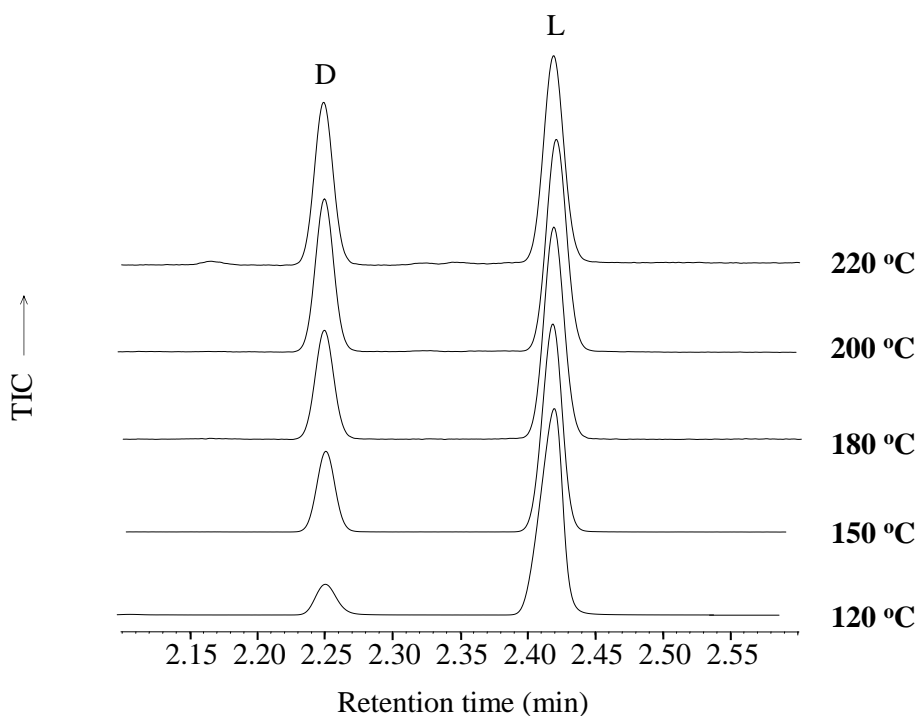


Fig. 32: D-to-L ratio of alanine after heating of L-alanine intercalated in Ca-montmorillonite at various temperatures for eight weeks. Gas chromatograms after derivatization (see 4.1.3); TIC: total ion current detection.

The rate of racemization of amino acids is related to the electronegativity and size of the functional group. In aqueous medium, alanine generally racemizes faster than valine due to the inductive effect which stabilizes the alanine carbanion more than valine carbanion (Smith et al., 1978; Smith and Reddy, 1989). The reverse behavior observed for the racemization of the amino acids in Ca-montmorillonite may be attributed to the heterogenous conditions provided by the mineral which, for example, can cause stacking or a special orientation of the amino acids in the interlayer spaces (Yamagishi, 1987).

The experiments with alanine and valine revealed the racemization behavior of α -alkyl- α -amino acids in Ca-montmorillonite. In subsequent experiments, the racemization of α,α -dialkyl- α -amino acids was studied on isovaline as an example. Concerning the rate and mechanism of racemization it is important to remember that isovaline possesses no α -hydrogen atom.

Ca-montmorillonite loaded with L-isovaline

Ca-montmorillonite that had been loaded with enantiopure L-isovaline (7.5 %) by the direct loading method was heated at 200 °C for eight weeks. Under these conditions, racemization of L-isovaline was not expected as the amino acid lacks the α -hydrogen atom. It should be mentioned that radioracemization and radiolysis of isovaline have been reported (Bonner et al. 1979). However, it was found in the present experiment that L-isovaline could also racemize thermally, but at a much slower rate than the monoalkyl- α -amino acids alanine and valine. After eight weeks, 95.0 % L-ee of isovaline was found in the residue, which means that the remaining 5.0 % have racemized. Further experiments were made to study the influence of L-isovaline on the racemization of alanine in the presence of Ca-montmorillonite.

Ca-montmorillonite loaded with a mixture of L-isovaline and L-alanine

Loading of Ca-montmorillonite with a mixture of L-isovaline (3.75 %) and L-alanine (3.75 %), both enantiopure, was performed by the direct loading method (see 4.5.2). The dried sample was heated at 200 °C for eight weeks. At the end of the experiment, the residue contained 90.9 % L-ee of isovaline and 3.5 % L-ee of alanine. Interestingly, the racemization of L-alanine was accelerated by the presence of L-isovaline in Ca-montmorillonite. In the absence of L-isovaline, 28.5 % L-ee of alanine was still present after eight weeks (see 2.4.1). In the first 2–3 days, no significant change was observed in the L-ee of isovaline (i.e. no formation of D-isovaline), afterwards L-isovaline slowly racemized. In contrast, L-alanine

underwent very fast racemization during the initial few days – much faster than in the absence of L-isovaline. Racemization slowed down thereafter (Fig. 33). This clearly indicated that L-isovaline increased the racemization rate of L-alanine. Levine et al. (2008) have demonstrated the transfer of chirality from α -methyl-amino acids to other amino acids. They have shown that enantiopure L- α -methylvaline can transaminate phenylpyruvate to L-phenylalanine with 37 % ee and pyruvate to L-alanine with 20 % ee. Though these observations cannot be directly transferred to the experiments with Ca-montmorillonite, it may be hypothesized that L-isovaline increases the formation of D-alanine. This would result in a faster racemization of L-alanine in the presence of L-isovaline.

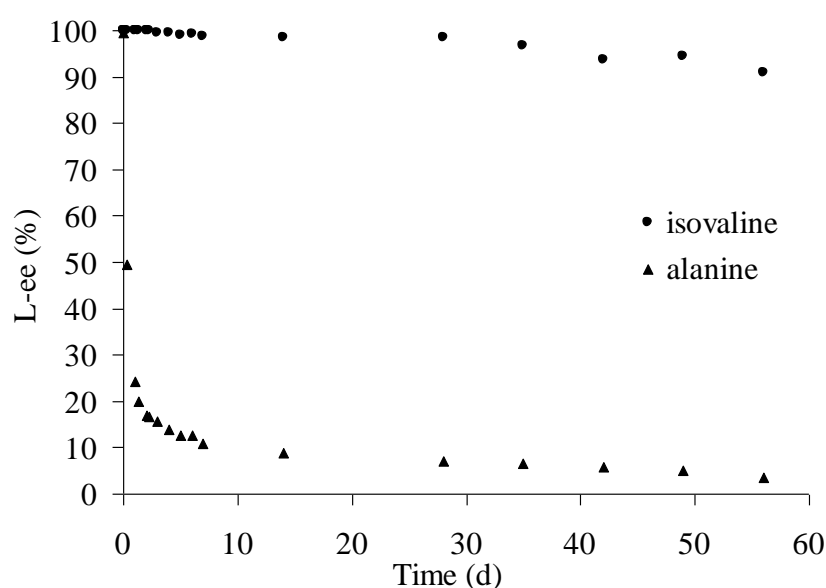


Fig. 33: Development of the L-ee values of alanine and isovaline jointly intercalated in Ca-montmorillonite during eight weeks of heating at 200 °C. Both starting L-ee values were 100 %.

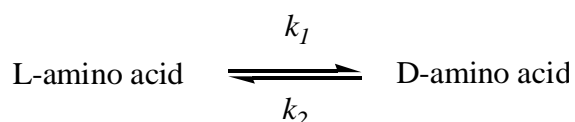
Ca-montmorillonite loaded with a mixture of L-isovaline and racemic alanine

Ca-montmorillonite loaded with a mixture of L-isovaline (3.75 %) and racemic alanine (3.75 %) was prepared by the direct loading method. The sample was also heated at 200 °C for eight weeks. It was found that 93.9 % L-ee of isovaline was present in the residue at the end of the experiment. Interestingly, a small D-ee of alanine (2.5 %) was measured after eight weeks (Fig. A-18). Thus, the presence of L-isovaline promoted the formation of D-alanine. In contrast, racemic alanine, i.e. without L-isovaline, did not develop an enantiomeric excess during eight weeks of thermal treatment (see 2.4.1). These results are also consistent with the observation that L-isovaline increases the rate of racemization of L-alanine (see above).

The experiments conducted with enantiopure L-isovaline demonstrated that (i) isovaline showed a small degree of racemization over a period of eight weeks, (ii) differences in the concentration of isovaline (3.75–7.5 %) did not result in significantly different degrees of racemization (L-ee = 90.9–95.4 %), and (iii) the presence of L-isovaline increased the formation of D-alanine relative to L-alanine.

2.4.4 Racemization kinetics of alanine in Ca-montmorillonite

In general, the racemization reaction of an amino acid can be expressed as:



where k_1 and k_2 are the forward and reverse rate constants, respectively.

The rate expression for the first order kinetics of racemization of amino acids with a single center of symmetry is:

$$\ln \left[\frac{(1+D/L)}{(1-D/L)} \right]_t - \ln \left[\frac{(1+D/L)}{(1-D/L)} \right]_{t=0} = 2kt \quad (1)$$

where k is the racemization rate constant, t is the time, and D and L are the percentage enantiomeric excesses of the D- and L-amino acid, respectively (Goodfriend, 1991; Cohen and Chyba, 2000).

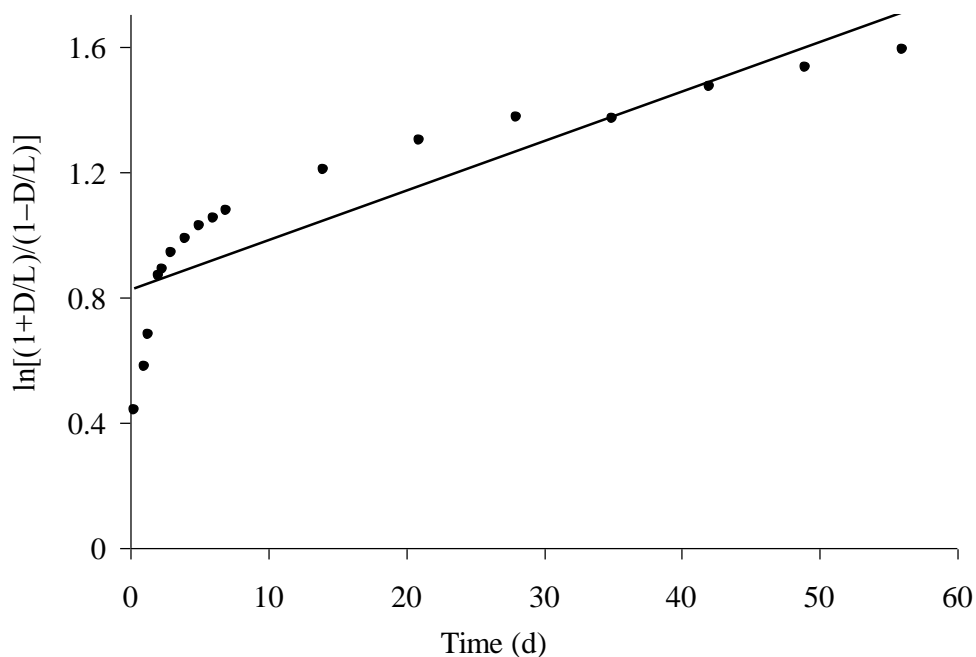


Fig. 34: Relationship between $\ln[(1+D/L)/(1-D/L)]$ and time for the racemization of alanine intercalated in Ca-montmorillonite. The temperature was 200 °C, the starting L-ee was 100 %.

If the process of racemization follows first order kinetics then there is a straight line for the plot of $\ln[(1+D/L)/(1-D/L)]$ over the time. However, at most temperatures, the first order kinetics model does not adequately describe the racemization of alanine in Ca-montmorillonite (Fig. 34), except at the lowest temperature employed (120 °C). Krishna et al. (2010) have observed that the racemization of aspartic acid in clay sediments from the southwestern Bay of Bengal did also not fit the first order kinetics model. Similar results were also reported by others (Mitterer and Kriausakul, 1989; Goodfriend, 1991; Goodfriend and Meyer, 1991). Therefore, a simple empirical best fit plot for 180, 200, and 220 °C was derived. It is described by a linear relationship between D/L and $\ln(t)$ (Fig. 35). Thus, the equation for racemization of alanine intercalated in Ca-montmorillonite can be written as:

$$D/L = a \cdot \ln(t) + b \quad (2)$$

where a and b are empirical constants.

Using this logarithmic model, the time for nearly complete racemization of alanine at a particular temperature can be roughly estimated (see below). These estimates rely on the assumption that the linear relationship is valid over time periods much longer than the duration of the experiments, which is not necessarily the case.

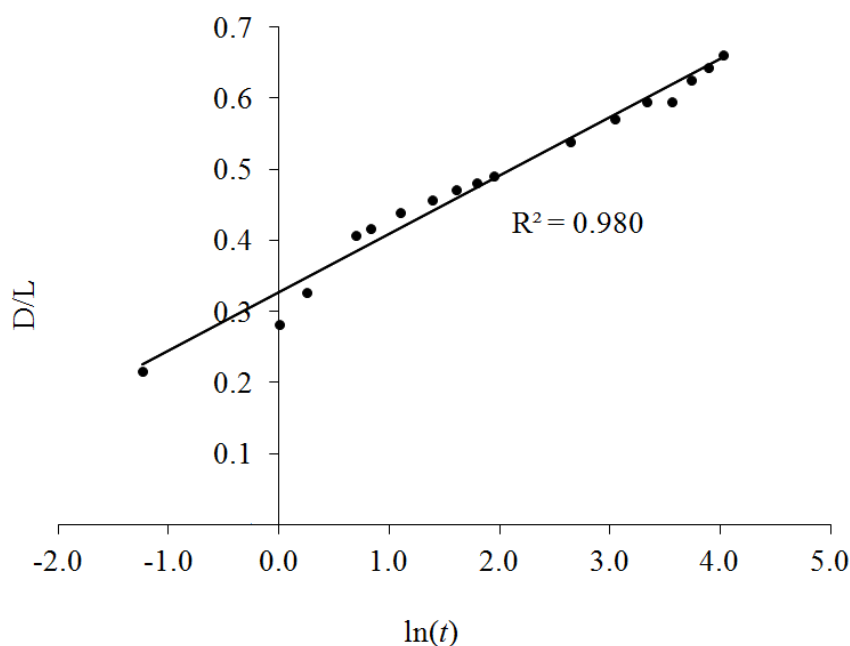


Fig. 35: Variation of the D/L ratio of alanine in Ca-montmorillonite with $\ln(t)$ during eight weeks at 200 °C. The starting L-ee was 100 %; t in days; R^2 : coefficient of determination indicating the quality of the fit.

In contrast, the relationship between D/L and $\ln(t)$ was not linear for 120 °C. Instead, the best fit plot for 120 °C was obtained using a linear relationship between D/L and time (Fig. 36). At this temperature, racemization of alanine was observed at a noticeable rate over eight weeks. It did not slow down during the duration of the experiment. The corresponding equation for the racemization of alanine at 120 °C is:

$$D/L = c \cdot t + d \quad (3)$$

where c and d are empirical constants.

At higher temperatures (180, 200, and 220 °C), the D/L ratio followed a linear trend only for the first 2–3 days when plotted against time (Fig. 37). Obviously, the initial development in racemization at high temperatures corresponds to the racemization process that was observed during the whole duration of the 120 °C experiment. It can be inferred from Figure 37 that the linear relationship found at 120 °C (Fig. 36) will persist until $D/L \approx 0.4$.

For 150 °C, the plots D/L vs. t (best fit for 120 °C) and D/L vs. $\ln(t)$ (best fit for 180, 200, and 220 °C) were compared (Fig. 38 A and B). The comparison showed that the racemization of alanine at 150 °C had an intermediate position between the situation at 120 °C and at high temperatures (180–220 °C). However, the plot of D/L vs. $\ln(t)$ clearly gave the best result (Fig. 38 A).

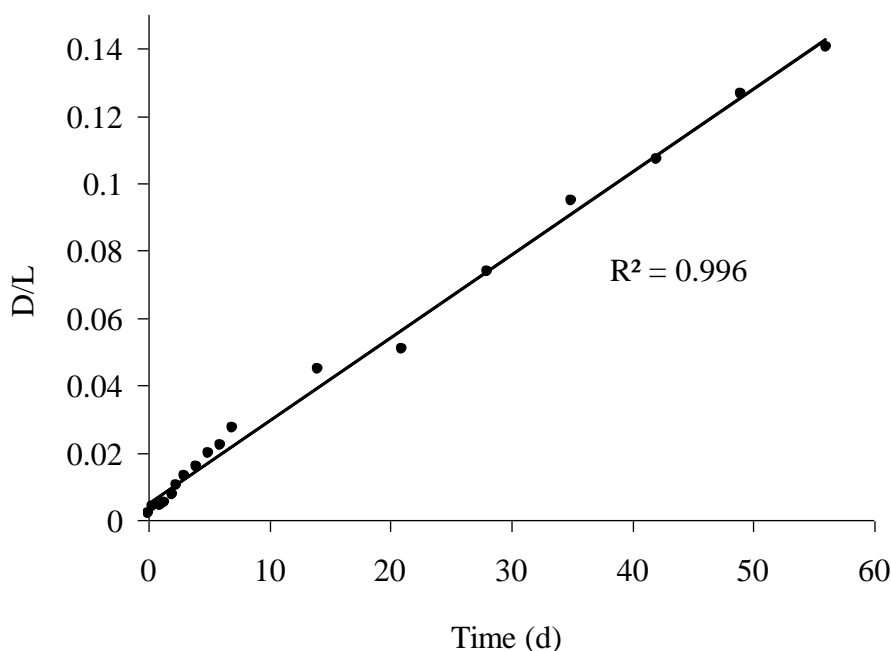


Fig. 36: Variation of the D/L ratio of alanine in Ca-montmorillonite with time during eight weeks at 120 °C. The starting L-ee was 100 %.

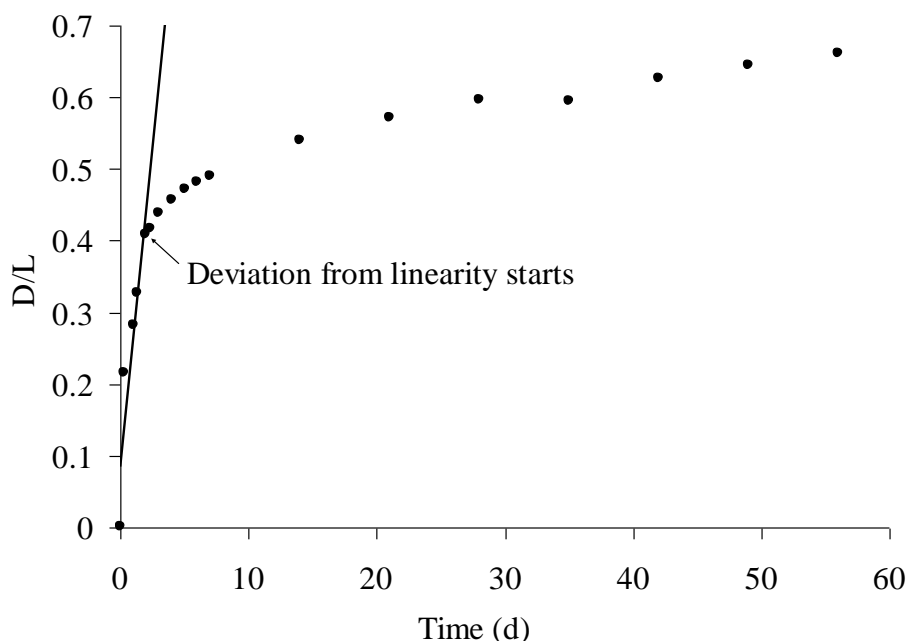


Fig. 37: Variation of the D/L ratio of alanine in Ca-montmorillonite with time during eight weeks at 200 °C. The starting L-ee was 100 %.

On the surface of the young Earth locally high temperatures occurred due to intense impacts of extraterrestrial objects and volcanic activity. Clay minerals and amino acids could have interacted with each other in the hotter regions. This scenario forms the prebiotic background of the above described experiments. These experiments yielded the following main results: (i) The relative rate of racemization of alanine was nearly independent of the starting L-ee. After eight weeks, the residues contained 17.5–25.0 % of the initial L-ee. (ii) It is well-known that the temperature is an important factor that determines the rate of racemization of amino acids (Schroeder and Bada, 1976). This could also be clearly observed in the experiments which started with 100 % L-ee of alanine in Ca-montmorillonite. After eight weeks at 120 °C, 75.4 % L-ee was still present, whereas only 15.3 % L-ee was found at 220 °C. (iii) The racemization rate depended on the type of amino acid that was intercalated in Ca-montmorillonite. (iv) The formation of D-alanine was probably enhanced by the presence of L-isovaline. (v) Ca-montmorillonite may have some influence on the faster racemization of valine as compared to alanine. (vi) Ca-montmorillonite protects amino acids from complete decomposition and sublimation. In the clay mineral, alanine, for example, was available for racemization even after 24 weeks at 200 °C. It can be estimated that the complete racemization of alanine intercalated in Ca-montmorillonite may take many years. However, the extrapolated time periods of ~2050 years at 150 °C to ~10 years at 200 °C

(see 2.4.4, equation 2) are rough estimates (see the discussion above). Nevertheless, it can be assumed that L-amino acids may have survived for years in clay minerals on the young Earth. Later, the L-ee of the enantio-enriched amino acids could have been amplified and induced homochirality (see 1.4).

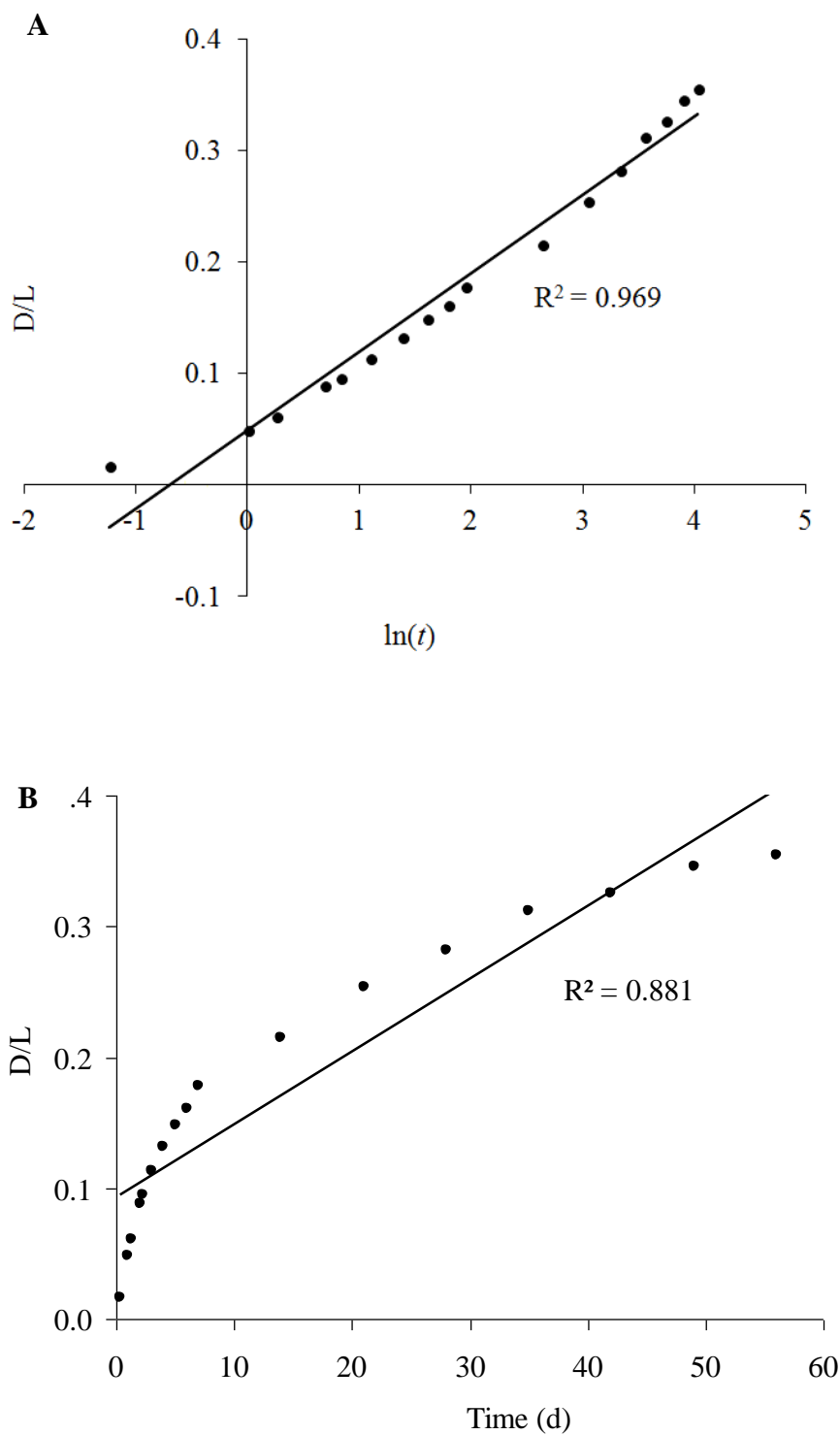


Fig. 38: Comparison between (A) D/L vs. $\ln(t)$ and (B) D/L vs. t for alanine in Ca-montmorillonite during eight weeks at 150 °C. The starting L-ee was 100 %.

2.5 Sublimation of neat alanine and valine

Neat amino acid mixtures with different L-ee were prepared by first dissolving the racemic amino acid together with the enantiomerically pure L-form in a minimum amount of water. These solutions were then completely air-dried at room temperature. In the following experiments, the solid samples were heated at 200 °C. Subsequently, the initial samples, residues, and sublimates were analyzed by gas chromatography.

Sublimation of neat alanine

This experiment was performed in a tube furnace under a pure nitrogen atmosphere (see 4.3). The initial L-ee of alanine had increased from 93.7 to 95.3% and from 93.0 to 99.3 % after 3 hours and 24 hours of heating, respectively. In contrast, no considerable change in the L-ee was found in experiments that started from racemic alanine. In addition, the L-ee of the sublimates were lower than the starting L-ee, but no regular pattern of the L-ee distribution in the sublimation tube was observed (Tab. 16). The irregularity could be due to turbulences in the nitrogen stream. Obviously, the vapour pressures of racemic and enantiopure alanine crystals are different. The results indicated that the racemic alanine crystals are more volatile than L-alanine crystals. However, experiments by others have shown an increase in the L-ee of the sublimate as compared to the starting sample (Fletcher et al., 2007; Viedma et al., 2012). In fact, according to Bellec and Guillemin (2010), the enantiomeric excess of either the residue or the sublimate could increase.

Tab. 16: Change of the L-ee of neat alanine at 200 °C.

Initial L-ee (%)	Duration of heating (h)	Initial amount (mg)	Residue left (mg)	L-ee (%) in the residue	L-ee (%) in the sublimate (hotter to colder region)
93.7	3	199.9	175.3	95.3	67.8, 66.7, 68.8
93.0	24	200.1	100.2	99.3	80.6, 85.5, 83.4
99.6	24	200.1	109.3	99.7	98.5, 98.9, 98.4
Racemic	24	200.5	88.7	0.6	1.1, 0.9, 0.7, 1.6

In another experiment, the influence of air on the thermal behavior of neat alanine was demonstrated. For this, two Wheaton reaction vials were filled with 1.5 mg of L-alanine each. One of the vials was purged with argon inside a glove box. Both the vials were tightly closed and kept in an oven at 200 °C for 24 hours. Afterwards, the samples were derivatized and analyzed by gas chromatography. After 24 hours of heating, the sample under argon was still white and had 99.8 % of L-ee of alanine. In contrast, the sample under air was completely brown. Alanine was not detected in this sample, indicating complete decomposition. This experiment showed that in a closed system an inert gas is necessary to protect alanine from decomposition at 200 °C.

Another experiment was performed to investigate the influence of quartz sand on the thermal behavior of alanine. For this, 1.0 g of enantiopure L-alanine was covered with 7.0 g of quartz sand in an open quartz container. Quartz sand with a particle size of ~355 µm was used. After heating at 200 °C under pure nitrogen gas for two days, the residue was brown. The mass loss was 49 %. The residue was extracted with water, and the extract was dried, derivatized, and analyzed by gas chromatography. The extract contained 96.5 % L-ee of alanine. Thus, there may have been a small degree of racemization. However, the possibility exists that signals of decomposition products interfered with the alanine signals in the gas chromatograms and the observed racemization was not real. Finally, it can be concluded that, in contrast to Ca-montmorillonite, quartz sand does not protect alanine from decomposition and sublimation. The sublimates collected from different locations in the thermolysis tube have 23.5, 54.4, 47.4, and 75.5 L-ee %, showing that in fact some racemization must have occurred.

Sublimation of neat valine

At 200 °C, the L-ee of valine increased from 93.1 to 99.7 % and from 92.9 % to 99.9 % after 3 hours and 24 hours of heating, respectively. In a control experiment with racemic valine, the amino acid had completely sublimed so that no GC analysis of the residue could be performed. As in the case of alanine, the results indicated that the racemic crystals are more volatile than the pure enantiomers (Tab. 17).

Tab. 17: Change of the L-ee of neat valine at 200 °C.

Initial L-ee (%)	Duration of heating (h)	Initial amount (mg)	Residue left (mg)	L-ee (%) in the residue	L-ee (%) in the sublimate (hotter to colder region)
93.1	3	200.5	147.0	99.7	96.5, 85.9, 81.2
92.9	24	200.3	25.0	99.9	89.2, 90.3, 90.5
100.0	24	200.8	20.4	99.9	99.4, 99.8, 99.9
Racemic	24	200.1	*	–	0.3, 0.1, 0.1, 0.1

* too less for analysis

Homochirality on Earth could have been triggered by the exogenous delivery of non-racemic organics (Mason, 1997; Bailey et al., 1998). The surface of a meteorite is heated during atmospheric entry. This creates a temperature gradient which can cause the partial sublimation of amino acids. Similarly, partial sublimation of amino acids could have occurred in the early history of meteorite parent bodies (asteroids). The experiments described above demonstrate the principle possibility that the L-ee of amino acids can increase in different parts of a meteorite or asteroid by sublimation. Subsequently, different fragments of this meteorite or asteroid can deliver amino acids with different L-ee to Earth.

3 Summary

The onset of life on Earth was preceded by an abiotic chemistry in which complex molecules were formed from simpler ones. In the presence of energy sources such as UV radiation, lightning and geothermal energy, a wide range of organic compounds probably formed on the young Earth. Stanley Miller was the first to study this scenario experimentally. He showed that amino acids were synthesized under simulated conditions of the primitive Earth's atmosphere. Initially, it was believed that the Earth's early atmosphere contained high concentrations of CH₄, NH₃, CO, and H₂ and was thus strongly reducing. However, later it was assumed that the early atmosphere was redox neutral and was composed of N₂, CO₂, and H₂O as main constituents. Isotopic data from zircons indicate that liquid water might have been present already around 4.2 billion years ago. So called banded iron formations confirm the presence of liquid water at least 3.8 billion years ago. The early geological histories of Earth and Mars were probably very similar. About 4 billion years ago, both planets had liquid water, volcanoes, and a dense atmosphere without free oxygen, and they experienced intense meteoritic and cometary impacts. Therefore, the simulation experiments described in the present thesis may also be relevant to the early Mars. Among the possible prebiotic molecules, amino acids are generally considered especially important for the origin of life. The main reason for this is that they serve as building blocks of proteins which are the pillars of metabolism in all organisms. There is practically no doubt that amino acids were present on the young Earth. They originated from endogenous and exogenous (i.e. extraterrestrial) sources. Glycine is the most abundant amino acid in carbonaceous meteorites and Miller-type experiments.

In the present work, the deep black residue was studied that forms when glycine is heated at 200 °C. Similar residues have been named "thermo-melanoid" by others. The experiments were performed under a pure nitrogen atmosphere in order to simulate the oxygen-free early atmosphere of the Earth. It was found that the formation of the thermo-melanoid from neat glycine started at 160 °C and was relatively fast and complete at 200 °C. However, the residues that formed at high temperatures (250–350 °C) were different from the thermo-melanoid. The thermo-melanoid was also present in the residues obtained by heating the glycine homopeptides 2,5-diketopiperazine (DKP), diglycine, triglycine, and tetraglycine at 200 °C. In contrast, penta- and hexaglycine remained almost unreacted at this temperature. Deuterolysis experiments revealed that C=C bonds are a characteristic structural feature of the thermo-melanoid. These bonds form by an unusual condensation reaction between C=O

and CH₂ groups. Glycine, DKP, and diglycine were released during hydrolysis of the thermo-melanoid in water at 100 °C. In these experiments, the thermo-melanoid slowly dissolved. After 10 days, for example, a mass loss of ~75 % was observed. Therefore, the thermo-melanoid can be regarded as a kind of storage form of glycine and glycine oligopeptides. The lower solubility of the thermo-melanoid as compared to glycine and its homopeptides may have influenced the distribution of glycine units on the early Earth. Moreover, additional experiments have shown that the thermo-melanoid mixed with soil continuously produced a higher amount of CO₂ during a six-months period than samples without the thermo-melanoid. Obviously, the thermo-melanoid was decomposed in the soil. The decomposition was probably caused by microorganisms. Therefore, one can hypothesize that the thermo-melanoid could have served as nutrient for early heterotrophic (pre-)organisms.

The salt concentration of the late Hadean/early Archean ocean was at least twice as high as the concentration in the present-day oceans. There are good reasons to assume that the ions were Na⁺, K⁺, Ca²⁺, Mg²⁺, and Cl⁻. SO₄²⁻ and PO₄³⁻ were possibly not present in significant concentrations as the early atmosphere of the Earth was anoxic. In relation to this, the thermal behavior of glycine was investigated in the presence of various salts. It was found that glycine changed from the initial α- to the γ-modification when it crystallized together with NaCl and NaCl–KCl mixtures. At 200 °C, the glycine that was embedded in the NaCl or NaCl–KCl salt crusts transformed into the thermo-melanoid and a small amount of DKP. Only ~5 % of unreacted glycine was left after seven days in the presence of NaCl. The results showed that the presence of these salts and the change in the modification were nearly ineffective in protecting glycine from transformation into the thermo-melanoid. In contrast to NaCl and KCl, CaCl₂ formed a coordination compound with glycine, namely CaCl₂(Hgly) · H₂O, when solutions of CaCl₂ · 2H₂O and glycine were evaporated. It was found that more than 90 % of the glycine were still present in CaCl₂(Hgly) · H₂O after heating at 200 °C for seven days. The coordination of glycine to Ca²⁺ prevented the transformation of glycine into the thermo-melanoid up to 250 °C. Yusenko et al. reported that at 350 °C, small volatile N-heterocycles such as pyrroles formed from CaCl₂(Hgly) · H₂O. Pyrroles are the building blocks of porphyrin-type biomolecules such as cytochromes and chlorophylls. CaCl₂(Hgly) · H₂O was also identified in mixtures of glycine with artificial sea salt (AS) prepared from NaCl (705 mmol), KCl (15 mmol), MgCl₂ · 6H₂O (80 mmol), CaCl₂ · 2H₂O (15 mmol), and glycine (10 mmol). About 84 % of the initial glycine had survived after heating an AS–Hgly mixture for seven days at 200 °C. In contrast, neither

complex formation nor change in the modification of glycine was observed in gypsum–Hgly and MgCO₃–Hgly mixtures.

Clay minerals are mainly produced by the weathering of volcanic rock. They are not only found on Earth, but also on Mars. A possible role of clay minerals in chemical evolution was first suggested by Bernal more than half a century ago. In the present work, the thermal behavior of glycine embedded in smectites (Ca-montmorillonite, Na-montmorillonite, and nontronite) and kaolinite was investigated. The glycine-loaded clay minerals were heated at 200 and 250 °C for two days. HPLC and MALDI–TOF/TOF MS analyses of glycine-loaded Ca-montmorillonite that had been heated at 200 °C showed the presence of unreacted glycine, DKP, and linear peptides up to decaglycine. The comparison between the smectite clay minerals revealed that glycine was best protected by Ca-montmorillonite. ~63 % of the amino acid survived in its free form at 200 °C. This was followed by Na-montmorillonite (~53 %) and nontronite (~39 %) under similar experimental conditions. These results demonstrated that smectite clay minerals protect glycine from complete decomposition and sublimation, partly by promoting its polymerization. In contrast to smectites, kaolinite has no interlayer spaces available for intercalation. Therefore, glycine is only attached to the surface of the kaolinite particles. Sublimation of glycine and newly formed DKP was observed when kaolinite mixed with glycine was heated at 200 and 250 °C. All investigated clay minerals prevented the transformation of glycine into the thermo-melanoid during thermal treatments.

Various heating experiments were conducted with mixtures of glycine and volcanic rock (basaltic sand from the island of La Réunion, Indian Ocean) or Martian soil simulants (JSC Mars-1A, P-MRS, and S-MRS). Glycine and DKP were identified in the residues and sublimates after heating basaltic sand–Hgly and JSC Mars-1A–Hgly at 200 °C for two days. Additionally, the thermo-melanoid was found in the residue of basaltic sand–Hgly. JSC Mars-1A contains mainly volcanic glass. Forsterite (Mg₂SiO₄) was identified as the major crystalline mineral in the basaltic sand. Glycine cannot be intercalated in JSC Mars-1A and basaltic sand as they have no clay minerals. As a result, glycine in these two matrices undergoes thermal alterations similar to neat glycine. In contrast, glycine, DKP, and linear peptides from di- to hexaglycine were detected after heating a P-MRS–glycine mixture. This observation can be easily explained by the fact that P-MRS contains 70 % of clay minerals that protect the amino acid from complete decomposition and thus allow the formation of larger peptides. The S-MRS–glycine residue contained only DKP, glycine, and diglycine, obviously because the mineral matrix consisted only of rock, anhydrous iron oxides, and

gypsum, but not clay minerals. These experiments again demonstrated the influence of clay minerals on the behavior of glycine when exposed to higher temperatures.

Another focus of the work was on the thermal behavior of chiral amino acids intercalated in Ca-montmorillonite. The heating experiments were conducted with different L-enantiomeric excesses (ee) of alanine [L-ee = 0 (i.e. racemic), 4, 20, 50, and 100 %] under a pure nitrogen atmosphere. The residues were analyzed by GC-MS/FID after derivatization. It was found that the racemization process was fast during the first 2–3 days and thereafter slowed down considerably. After eight weeks at 200 °C, the residues still contained 17.5–25.0 % of the respective starting L-ee. Complete racemization of L-alanine was not observed even after 24 weeks of heating. It was also found that, as expected, Ca-montmorillonite did not have any specific preference for the formation of either the D- or L-enantiomer. Interestingly, it could be observed that L-isovaline influenced the racemization of alanine. The presence of L-isovaline increased the rate of formation of D-alanine. In addition, higher temperatures greatly accelerated the racemization. For instance, after eight weeks at 220 °C, 85 % of the initial L-ee of alanine had been lost by racemization, whereas at 120 °C only 25 % racemization was observed. These experiments made use of the fact that Ca-montmorillonite largely protects amino acids from sublimation. In contrast, neat amino acids such as alanine undergo considerable sublimation in a few hours or less, depending on the temperature. Using a racemization kinetics model, it was estimated that L-alanine can survive in Ca-montmorillonite at elevated temperatures for years.

In the literature, there are several reports on enantiomeric excesses of certain amino acids in meteorites. In relation to this, experiments were performed to demonstrate the enantiomeric enrichment of amino acids by partial sublimation. After 3 and 24 hours at 200 °C, the L-ee of alanine and valine increased in the sublimation residue, whereas the L-ee of the sublimates was lower than the initial one. Thus, it seems that racemic alanine and racemic valine crystals are more volatile than enantiomerically pure crystals. It may be assumed that similar processes take place during the atmospheric entry of meteorites and in the aqueous alteration phase of asteroids.

The experimental results described in the present thesis suggest that various modes of interaction of amino acids with inorganic matrices such as salt mixtures and clay minerals existed on the young Earth. These results may help to better understand some of the processes of the prebiotic chemical evolution.

Zusammenfassung

Dem Beginn des Lebens auf der Erde ging eine abiotische Chemie voraus, in der komplexe Moleküle aus einfacheren gebildet wurden. In Gegenwart von Energiequellen wie UV-Strahlung, Blitzen und geothermaler Energie bildete sich wahrscheinlich eine breite Palette organischer Verbindungen auf der jungen Erde. Stanley Miller war der erste, der dieses Szenario experimentell erforschte. Er hat gezeigt, dass sich unter Bedingungen, die die frühe Erdatmosphäre simulierten, Aminosäuren bildeten. Anfänglich wurde angenommen, dass die frühe Atmosphäre der Erde hohe Konzentrationen an CH_4 , NH_3 , CO und H_2 enthielt und daher stark reduzierend war. Später ging man jedoch davon aus, dass die frühe Atmosphäre redoxneutral und aus den Hauptbestandteilen N_2 , CO_2 und H_2O zusammengesetzt war. Isotopenmesswerte aus Zirkonen zeigen, dass flüssiges Wasser schon vor etwa 4,2 Milliarden Jahren vorhanden gewesen sein könnte. So genannte "Banded Iron Formations" bestätigen die Anwesenheit von flüssigem Wasser seit mindestens 3,8 Milliarden Jahren. Die frühe geologische Entwicklung der Erde und des Mars verlief wahrscheinlich sehr ähnlich. Vor ungefähr 4 Milliarden Jahren besaßen beide Planeten flüssiges Wasser, Vulkane und eine dichte Atmosphäre ohne freien Sauerstoff und erlebten zahlreiche Einschläge von Meteoriten und Kometen. Daher dürften die Simulationsexperimente, die in der vorliegenden Arbeit beschrieben werden, auch für den frühen Mars relevant sein. Unter den möglichen präbiotischen Molekülen werden Aminosäuren allgemein als besonders wichtig für den Ursprung des Lebens angesehen. Dies wird hauptsächlich deshalb angenommen, weil sie als Bausteine für Proteine dienen, welche in allen Organismen die Grundlage des Stoffwechsels darstellen. Es gibt praktisch keinen Zweifel daran, dass Aminosäuren auf der jungen Erde vorhanden waren. Sie stammten aus endogenen und exogenen (d. h. außerirdischen) Quellen. Glycin ist die häufigste Aminosäure in kohligen Meteoriten und in Experimenten des Miller-Typs.

In der vorliegenden Arbeit wurde der tiefschwarze Rückstand untersucht, der sich bildet, wenn Glycin auf 200 °C erhitzt wird. Ähnliche Rückstände sind von anderen als „Thermomelanoid“ bezeichnet worden. Die Versuche wurden unter reiner Stickstoffatmosphäre durchgeführt, um die sauerstofffreie frühe Atmosphäre der Erde zu simulieren. Es wurde festgestellt, dass die Bildung des Thermomelanoids aus reinem Glycin bei 160 °C beginnt und bei 200 °C verhältnismäßig schnell und vollständig ist. Die Rückstände, die sich bei hohen Temperaturen ($250\text{--}350\text{ °C}$) bildeten, unterschieden sich jedoch vom Thermomelanoid. Das Thermomelanoid war auch in den Rückständen vorhanden, die durch Erhitzen

der Glycin-Homopeptide 2,5-Diketopiperazin (DKP), Diglycin, Triglycin und Tetraglycin bei 200 °C erhalten wurden. Im Gegensatz dazu zeigten Penta- und Hexaglycin bei dieser Temperatur fast keine Reaktion. Deuterolyseversuche haben gezeigt, dass C=C-Doppelbindungen ein charakteristisches strukturelles Merkmal des Thermomelanoids sind. Diese Bindungen bilden sich durch eine ungewöhnliche Kondensationsreaktion zwischen C=O- und CH₂-Gruppen. Während der Hydrolyse des Thermomelanoids bei 100 °C in Wasser wurden Glycin, DKP und Diglycin freigesetzt. In diesen Versuchen löste sich das Thermomelanoid allmählich auf. Nach 10 Tagen wurde beispielsweise ein Masseverlust von etwa 75 % beobachtet. Daher kann das Thermomelanoid als eine Art Speicherform von Glycin und Glycin-Oligopeptiden betrachtet werden. Die geringere Löslichkeit des Thermomelanoids im Vergleich zum Glycin und seinen Homopeptiden könnte die Verteilung von Glycin-Einheiten auf der frühen Erde beeinflusst haben. Außerdem haben weitere Versuche gezeigt, dass das Thermomelanoid mit Boden vermischt in einem Zeitraum von sechs Monaten kontinuierlich eine größere Menge CO₂ freisetzte als Vergleichsproben ohne das Thermomelanoid. Offensichtlich wurde das Thermomelanoid in der Erde zersetzt. Die Zersetzung wurde wahrscheinlich von Mikroorganismen verursacht. Daher kann man vermuten, dass das Thermomelanoid frühen heterotrophen (Vor-)Organismen als Nährstoff gedient haben könnte.

Die Salzkonzentration des Ozeans im späten Hadaikum/frühen Archaikum war mindestens doppelt so hoch wie die Konzentration in den heutigen Ozeanen. Es gibt gute Gründe anzunehmen, dass es sich bei den Ionen um Na⁺, K⁺, Ca²⁺, Mg²⁺ und Cl⁻ handelte. SO₄²⁻ und PO₄³⁻ waren möglicherweise nicht in wesentlichen Konzentrationen vorhanden, da die frühe Atmosphäre der Erde nichtoxidierend war. In Zusammenhang damit wurde das thermische Verhalten von Glycin in Anwesenheit verschiedener Salze untersucht. Es konnte festgestellt werden, dass sich Glycin von der ursprünglichen α-Modifikation in die γ-Modifikation umwandelte, wenn es gemeinsam mit NaCl oder NaCl-KCl-Mischungen auskristallisierte. Bei 200 °C wandelte sich das Glycin, das in den NaCl- oder den NaCl-KCl-Salzkrusten eingebettet war, in das Thermomelanoid und wenig DKP um. In Anwesenheit von NaCl verblieben nach sieben Tagen nur etwa 5 % unreaktiertes Glycin. Die Ergebnisse haben gezeigt, dass die Anwesenheit dieser Salze und die Modifikationsänderung so gut wie nicht dazu in der Lage waren, Glycin vor der Umwandlung in das Thermomelanoid zu schützen. Im Gegensatz zu NaCl und KCl bildete CaCl₂ eine Koordinationsverbindung mit Glycin, nämlich CaCl₂(Hgly) · H₂O, wenn man Lösungen von CaCl₂ · 2H₂O und Glycin eintrocknen ließ. Es wurde festgestellt, dass mehr als 90 % des

Glycins im $\text{CaCl}_2(\text{Hgly}) \cdot \text{H}_2\text{O}$ noch vorhanden waren, nachdem man es für sieben Tage bei $200\text{ }^\circ\text{C}$ erhitzt hatte. Die Koordination des Glycins an Ca^{2+} verhinderte die Umwandlung der Aminosäure in das Thermomelanoid bis hinauf zu $250\text{ }^\circ\text{C}$. Yusenko et al. berichteten, dass sich aus $\text{CaCl}_2(\text{Hgly}) \cdot \text{H}_2\text{O}$ bei $350\text{ }^\circ\text{C}$ kleine flüchtige N-Heterozyklen wie zum Beispiel Pyrrole bilden. Pyrrole sind die Bausteine von Biomolekülen des Porphyrin-Typs, wie zum Beispiel Cytochrome und Chlorophylle. $\text{CaCl}_2(\text{Hgly}) \cdot \text{H}_2\text{O}$ wurde auch in Mischungen von Glycin mit künstlichem Meersalz (AS) nachgewiesen, die aus NaCl (705 mmol), KCl (15 mmol), $\text{MgCl}_2 \cdot 6\text{H}_2\text{O}$ (80 mmol), $\text{CaCl}_2 \cdot 2\text{H}_2\text{O}$ (15 mmol) und Glycin (10 mmol) hergestellt wurden. Ungefähr 84 % des anfänglichen Glycins war noch vorhanden, nachdem eine AS–Hgly-Mischung für sieben Tage bei $200\text{ }^\circ\text{C}$ erhitzt worden war. Im Gegensatz dazu konnten in Gips–Hgly- und MgCO_3 –Hgly-Mischungen weder Komplexbildung noch eine Modifikationsänderung des Glycins beobachtet werden.

Tonminerale entstehen hauptsächlich beim Verwittern vulkanischen Gesteins. Man findet sie nicht nur auf der Erde, sondern auch auf dem Mars. Vor mehr als einem halben Jahrhundert wies erstmals Bernal auf eine mögliche Rolle der Tonminerale in der chemischen Evolution hin. In der vorliegenden Arbeit wurde das thermische Verhalten von Glycin nach der Einbettung in Smektit (Ca-Montmorillonit, Na-Montmorillonit und Nontronit) und Kaolinit untersucht. Die glycinbeladenen Tonminerale wurden für zwei Tage bei 200 und $250\text{ }^\circ\text{C}$ erhitzt. HPLC- und MALDI-TOF/TOF-MS-Analysen von glycinbeladenem Ca-Montmorillonit, das bei $200\text{ }^\circ\text{C}$ erhitzt worden war, zeigten das Vorhandensein von nicht reagiertem Glycin, DKP und linearen Peptiden bis zum Decaglycin. Der Vergleich zwischen den Smektit-Tonmineralen ließ erkennen, dass Glycin am besten durch Ca-Montmorillonit geschützt wurde. Bei $200\text{ }^\circ\text{C}$ waren 63 % der Aminosäure in unveränderter Form erhalten geblieben. Dem folgten Na-Montmorillonit (~53 %) und Nontronit (~39 %) unter ähnlichen experimentellen Bedingungen. Diese Ergebnisse haben gezeigt, dass Smektit-Tonminerale das Glycin vor vollständiger Zersetzung und Sublimation schützen, teilweise indem sie seine Polymerisation begünstigen. Im Gegensatz zu den Smektiten hat Kaolinit keine Zwischenschichtträume, in denen Intercalation stattfinden kann. Daher wird Glycin nur an die Oberfläche der Kaolinitpartikel angelagert. Als Kaolinit, das mit Glycin vermischt worden war, auf 200 und $250\text{ }^\circ\text{C}$ erhitzt wurde, wurde die Sublimation von Glycin und neu gebildetem DKP beobachtet. Alle untersuchten Tonminerale verhinderten, dass sich das Glycin während der thermischen Behandlungen in das Thermomelanoid unwandelte.

In verschiedenen Experimenten wurden Mischungen aus Glycin und Vulkangestein (Basaltsand von der Insel La Réunion, Indischer Ozean) oder simuliertem Marsboden (JSC

Mars-1A, P-MRS und S-MRS) erhitzt. In den Rückständen und Sublimaten wurden Glycin und DKP identifiziert, nachdem Basaltsand–Hgly und JSC Mars-1A–Hgly für zwei Tage bei 200 °C erhitzt worden waren. Zusätzlich wurde das Thermomelanoid im Rückstand des Basaltsandes mit Hgly gefunden. JSC Mars-1A enthält hauptsächlich vulkanisches Glas. Forsterit (Mg_2SiO_4) wurde als das hauptsächliche kristalline Mineral im Basaltsand identifiziert. Glycin kann in JSC Mars-1A und im Basaltsand nicht intercaliert werden, da sie keine Tonminerale enthalten. Demzufolge erfährt Glycin in diesen zwei Matrices ähnliche thermische Veränderungen wie das reine Glycin. Im Gegensatz dazu wurden nach dem Erhitzen einer P-MRS–Glycin-Mischung Glycin, DKP und lineare Peptide vom Di- bis zum Hexaglycin gefunden. Diese Beobachtung kann leicht damit erklärt werden, dass P-MRS 70 % Tonminerale enthält, die die Aminosäure vor vollständiger Zersetzung schützen und folglich die Bildung der größerer Peptide erlauben. Der S-MRS–Glycin-Rückstand enthielt nur DKP, Glycin und Diglycin, offensichtlich weil die mineralische Matrix nur aus Gesteinen, wasserfreien Eisenoxiden und Gips bestand, aber nicht aus Tonmineralen. Diese Versuche demonstrierten erneut den Einfluss von Tonmineralen auf das Verhalten von Glycin, wenn es höheren Temperaturen ausgesetzt ist.

Einen weiteren Schwerpunkt der Arbeit bildete das thermische Verhalten chiraler Aminosäuren, die in Ca-Montmorillonit intercaliert waren. Die Experimente wurden mit verschiedenen L-Enantiomerenüberschüssen (ee) von Alanin [L-ee = 0 (d. h. racemisch), 4, 20, 50 und 100 %] in einer reinen Stickstoffatmosphäre durchgeführt. Nach Derivatisierung wurden die Rückstände mittels GC-MS/FID analysiert. Es wurde festgestellt, dass der Racemisierungsvorgang während der ersten 2–3 Tage schnell verlief und danach beträchtlich langsamer wurde. Nach acht Wochen bei 200 °C enthielten die Rückstände noch 17.5–25.0 % des jeweiligen Start-L-ee. Eine vollständige Racemisierung des L-Alanins konnte selbst nach 24 Wochen Erhitzen nicht beobachtet werden. Es wurde außerdem festgestellt, dass Ca-Montmorillonit, wie erwartet, weder für die Bildung des D- noch des L-Enantiomers eine spezifische Präferenz aufwies. Interessanterweise konnte beobachtet werden, dass L-Isovalin die Racemisierung des Alanins beeinflusste. Die Anwesenheit von L-Isovalin erhöhte die Bildungsgeschwindigkeit von D-Alanin. Des Weiteren beschleunigten höhere Temperaturen die Racemisierung sehr stark. Zum Beispiel waren nach acht Wochen bei 220 °C 85 % des ursprünglichen L-ee durch Racemisierung verloren gegangen, während bei 120 °C nur 25 % Racemisierung beobachtet wurde. Diese Versuche nutzten die Tatsache, dass Ca-Montmorillonit Aminosäuren weitgehend vor Sublimation schützt. Im Gegensatz dazu erfahren reine Aminosäuren wie zum Beispiel Alanin beträchtliche, temperaturabhängige

Sublimation innerhalb einiger Stunden oder weniger. Mithilfe eines Modells für die Kinetik der Racemisierung ließ sich abschätzen, dass L-Alanin in Ca-Montmorillonit bei erhöhten Temperaturen jahrelang überdauern kann.

In der Literatur gibt es zahlreiche Berichte über Enantiomerenüberschüsse bestimmter Aminosäuren in Meteoriten. In Zusammenhang damit wurden Versuche durchgeführt, um die Enantiomerenanreicherung von Aminosäuren durch partielle Sublimation zu zeigen. Nach 3 und 24 Stunden bei 200 °C hatte sich der L-ee von Alanin und Valin im Sublimationsrückstand erhöht, während der L-ee im Sublimat geringer war als der anfängliche. Folglich scheint es, dass Kristalle des racemischen Alanins und racemischen Valins flüchtiger sind als enantiomerenreine Kristalle. Man kann annehmen, dass ähnliche Prozesse während des Eintritts von Meteoriten in die Atmosphäre und in der „Aqueous Alteration“-Phase von Asteroiden stattfinden.

Die experimentellen Ergebnisse, die in der vorliegenden Arbeit beschrieben werden, legen nahe, dass auf der jungen Erde vielfältige Möglichkeiten der Wechselwirkung von Aminosäuren mit anorganischen Matrices, wie zum Beispiel Salzmischungen und Tonmineralen, existierten. Diese Ergebnisse dürften dazu beitragen, einige der Vorgänge der präbiotischen chemischen Evolution besser zu verstehen.

4 Materials and Methods

4.1 Analytical methods

4.1.1 High performance liquid chromatography (HPLC)

The measurements were performed with an HPLC instrument from Sykam (Fürstfeldbruck, Germany). The column was ODS (Octadecyl silane) Hypersil GOLD with 200 mm length, 2.1 mm internal diameter, and 5 μm particle size from Thermo Fisher Scientific (Dreieich, Germany). The oven temperature was set to 35 $^{\circ}\text{C}$, and the flow rate was 1 mL min^{-1} . The detection was realized with a deuterium lamp at a wavelength of 201 nm in a DAD mode (Sykam S3210 UV/Vis detector). An injection volume of 50 μL was used for quantification. Glycine, DKP, and glycine homopeptides were identified using a 10 mM solution of sodium hexanesulfonate ($\text{C}_6\text{H}_{13}\text{SO}_3\text{Na}$) as a mobile phase, whereas for alanine and its peptides the mobile phase was a solution of $\text{C}_6\text{H}_{13}\text{SO}_3\text{Na}$ (5 mM) and KH_2PO_4 (3.5 mM). Both mobile phases were prepared in water and were acidified to pH 2.5 with H_3PO_4 .

The major components of the HPLC system were:

Reagent organizer: Sykam S7121, solvent delivery system: Sykam S1122, low pressure gradient mixer: Sykam S811, injector valve bracket: Sykam S5111.

4.1.2 Infrared spectroscopy

The measurements were performed with a Nicolet 5700 FT-IR instrument (Thermo Fisher Scientific; Dreieich, Germany). All spectra were recorded in ATR-mode with use of an ATR-Smart Orbit.

Measurement range: 4000–400 cm^{-1} , number of scans for each measurement: 64, resolution: 4 cm^{-1} .

4.1.3 Gas chromatography with mass spectrometric and flame ionization detection (GC-MS and GC-FID)

The GS-MS measurements were performed with a selective detector gas chromatograph 6890 N Network GC System and mass selective detector 5973 Network from Agilent Technologies (Waldbronn, Germany). A capillary column DB5-MS was used for the MS detection (Agilent Technologies, length: 30 m, inner diameter: 0.25 mm, film thickness: 0.25 μm). Helium was used as a carrier gas with a stream velocity of 0.4 mL min^{-1} . Ionization energy: 70 eV, inlet temperature: 280 $^{\circ}\text{C}$, injection volume: 0.2 μL , solvent delay: 1.95 min, mass range:

15–350 amu (full scan mode with 2.36 scans s⁻¹). For the separation of amino acid enantiomers, a chiral capillary column ChiraSil-L-valine was used (Varian BV, Middelburg, The Netherlands; length: 25 m, inner diameter: 0.25 mm, film thickness: 0.12 μm).

Temperature program for the identification of products with the DB5-MS column and MSD: 50 °C (3 min) → 5 °C min⁻¹ → 200 °C (2 min) → 15 °C min⁻¹ → 300 °C (1 min)

Temperature program for the separation of amino acid enantiomers using the ChiraSil-L-valine column and MSD:

90 °C (5 min) → 20 °C min⁻¹ → 180 °C (4.5 min) → 20 °C min⁻¹ → 200 °C

Temperature program for the separation of amino acid enantiomers using the ChiraSil-L-valine column and flame ionization detection:

120 °C (5 min) → 20 °C min⁻¹ → 180 °C (3 min) → 20 °C min⁻¹ → 200 °C

Derivatization of amino acids

Derivatization of amino acids was performed prior to GC analysis. It is a necessary step to transform the amino acids into volatile derivatives. Moreover, the introduction of functional groups increases the recognition of amino acids by hydrogen bonding on the stationary phase (Schurig, 1984). First, 200 μL of aqueous amino acid-containing extract were air-dried into small watch glasses (for the extraction process see 4.5.4). Afterwards, these dried samples were derivatized. The method used for the derivatization of amino acids was modified from the literature (Erbe and Brückner, 1999). A mixture of an alcohol and acetyl chloride (AcCl) in a 7:3 ratio (i.e. 350 μL:150 μL) was prepared in a reaction vial, which was already kept in an ice bath. This mixture was used for the esterification of the carboxyl group of the amino acid. 500 μL of this mixture was added to the dried samples in watch glasses. Samples were then transferred into teflon-lined screw-cap vials (Wheaton reaction vessel) and heated at 100 °C for one hour. Afterwards, the solvents were completely removed with a stream of nitrogen, and the samples were re-dissolved in 200 μL of dichloromethane. For alanine and valine samples, 50 μL of trifluoroacetic anhydride (TFAA) or pentafluoropropionic anhydride (PFPA) were added, whereas acetic anhydride (Ac₂O) was used for isovaline samples to obtain better separation of enantiomers. The samples were again heated at 100 °C for 15–20 minutes, followed by the careful removal of solvents with a nitrogen stream as the amino acid derivatives are volatile in nature. The derivatives were finally dissolved in 200 μL of dichloromethane and introduced into the gas chromatograph.

The esterification step was performed using 2-propanol (2-PrOH) or methanol (MeOH). The acylation step was achieved by using TFAA or PFPA. The scheme for derivatization of alanine with methanol and trifluoroacetic anhydride is shown in Figure 39. Various combinations of alcohol and acid anhydride were used: (i) 2-PrOH and TFAA, (ii) 2-PrOH and PFPA, (iii) MeOH and TFAA, (iv) MeOH and PFPA, and (v) 2-PrOH and Ac₂O (for isovaline). These combinations reduce the possibility that any other substance may interfere with the signal to be analyzed.

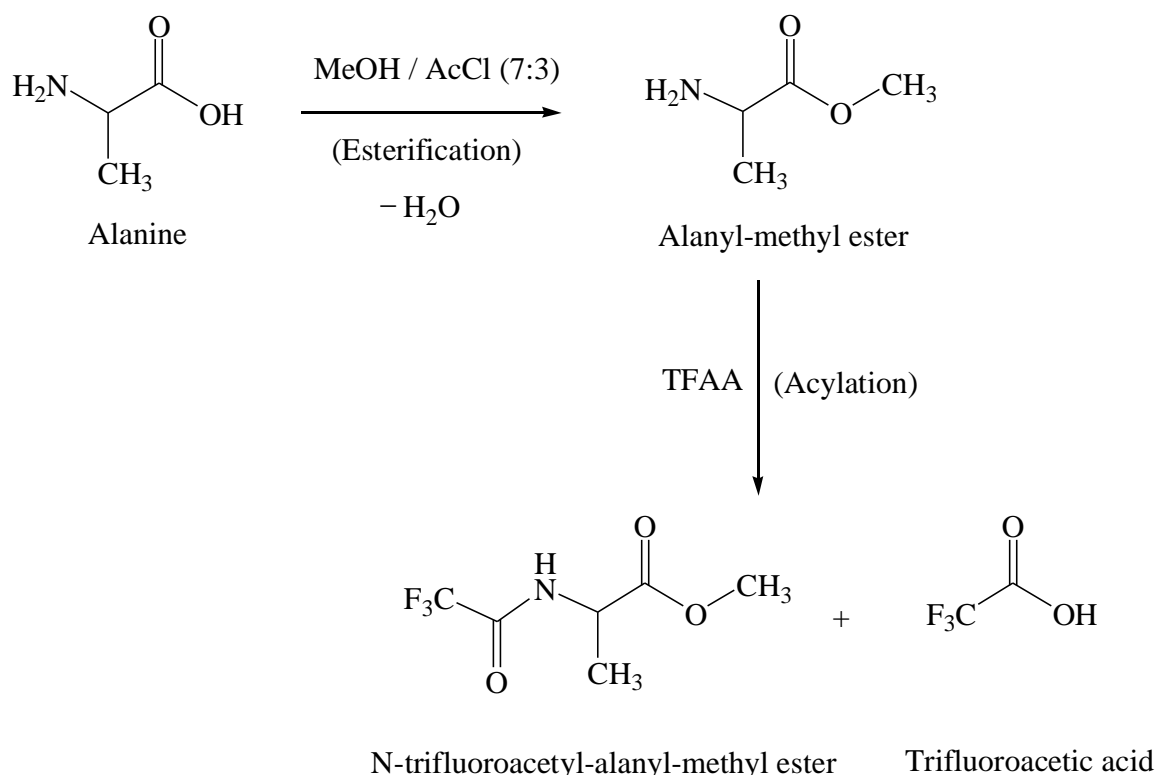


Fig. 39: Derivatization of alanine for GC analysis.

4.1.4 Matrix-assisted laser desorption ionization–time of flight / time of flight mass spectrometry (MALDI–TOF/TOF mass spectrometry)

MALDI–TOF/TOF mass spectrometric analyses were performed with an Autoflex III instrument from Bruker Daltonics (Bremen, Germany). α -Cyano-4-hydroxycinnamic acid was used as the matrix. The matrix solution was prepared by dissolving 5 mg of the matrix compound in 0.5 mL water, 0.499 mL acetonitrile, and 0.001 mL trifluoroacetic acid. Analyte and matrix solutions were mixed, and small droplets of the mixtures were transferred onto the target plate.

4.1.5 Thermogravimetric analysis (TGA)

The thermogravimetric curves were recorded on a thermal balance L81-11 from Linseis Messgeräte (Selb, Deutschland). All measurements were conducted under a nitrogen atmosphere (99.999 % N₂ with gas flow of 4 L h⁻¹) starting from room temperature to 900 °C with a heating rate of 2 K min⁻¹. In general, 10 mg were used for analysis.

4.1.6 Powder X-ray diffractometry (Powder XRD)

Powder X-ray diffractograms were measured with a Focus D8 instrument from Bruker-AXS (Karlsruhe, Germany). Data were collected with the use of Cu-K α radiation ($\lambda = 1.5418 \text{ \AA}$) in the 2θ range 5–60°. For forsterite identification, the 2θ range was 5–80°. The X-ray tube (KFL CU 2K, Siemens) was operated at 30 kV and 30 mA. The Sol-X energy dispersive detector was used. Some samples (e.g. clay minerals) were covered with a polyimide foil during the measurement.

4.1.7 Elemental analysis

The C, H, N, Ca, and Na contents in the clay minerals were obtained from Mikroanalytisches Labor Pascher (Remagen-Bandorf, Germany). In addition, the Ca²⁺ content was determined by complexometric titration with 0.1 mol L⁻¹ ethylenediaminetetraacetic acid (EDTA). The Cl⁻ content was determined by Mohr's titration using 0.1 mol L⁻¹ silver nitrate solution.

4.2 List of Chemicals

Tab. 18: Chemicals that were obtained from commercial sources and used without further purification.

Substance	Purity	Commercial Source
Glycine (Hgly)	>99 %	Acros Organics
2,5-Diketopiperazine (DKP)	98 %	Fluka Analytical
Diglycine (Gly ₂)	99 %	Fluka Analytical
Triglycine (Gly ₃)	p.a.	Sigma-Aldrich
Tetraglycine (Gly ₄)	p.a.	Sigma-Aldrich
Pentaglycine (Gly ₅)	p.a.	Sigma-Aldrich
Hexaglycine (Gly ₆)	99 %	Sigma-Aldrich
Heptaglycine (Gly ₇)	90.5 %	Genecust, Luxemburg
Octaglycine (Gly ₈)	76.3 %	Genecust, Luxemburg

Nonaglycine (Gly ₉)	70.7 %	Genecust, Luxemburg
Decaglycine (Gly ₁₀)	88.6 %	Genecust, Luxemburg
DL-alanine	99 %	Acros Organics
L-alanine	≥99.5 %	Fluka Analytical
DL-alanine anhydride	99 %	Acros Organics
L-alanyl-L-alanine	p.a.	Sigma-Aldrich
L-alanyl-L-alanyl-L-alanine	p.a.	Sigma-Aldrich
DL-valine	≥99 %	Sigma-Aldrich
L-valine	≥99.5 %	Sigma-Aldrich
L-isovaline monohydrate	>99 %	Acros Organics
Sodium hexanesulfonate	98 %	Acros Organics
Acetic anhydride	p.a.	Acros Organics
Potassium dihydrogen orthophosphate	p.a.	Fischer Scientific
Trifloroacetic anhydride	≥99 %	Fluka Analytical
Hydrochloric acid	p.a., ≥37 % wt	Fluka Analytical
Acetyl chloride	≥99 %	Fluka Analytical
Dichloromethane	99.9 %	Fluka Analytical
Ethyl acetate	≥99 %	Fluka Analytical
α-Cyano-4-hydroxycinnamic acid	≥99.9 %	Fluka Analytical
Dimethylformamide	≥99.8 %	Fluka Analytical
Phosphoric acid	p.a., ≥85 % wt	Fluka Analytical
Pentafluoropropionic anhydride (PFPA)	99 %	ABCR
Acetamide	99 %	Sigma-Aldrich
Deuterium chloride (DCl)	99 atom-% D	Sigma-Aldrich
Deuterated dichloromethane (CD ₂ Cl ₂)	99.9 atom-% D	Sigma-Aldrich
Deuterium oxide (D ₂ O)	99.9 atom-% D	Sigma-Aldrich
CD ₃ OD	100 %, 99.96 atom-% D	Sigma-Aldrich
CD ₃ COCl	99 atom-% D	Sigma-Aldrich
2-Propanol, anhydrous	99.5 %	Sigma-Aldrich
Ammonium oxalate monohydrate	≥99.5 %	Sigma-Aldrich
Dimethyl sulfoxide	99 %	Sigma-Aldrich
Toluene	99.8 %	Sigma-Aldrich

Pyridine	99.9 %	Sigma-Aldrich
Hexane	p.a.	Sigma-Aldrich
Acetone	p.a.	Sigma-Aldrich
Succinimide	p.a.	Sigma-Aldrich
Magnesium chloride hexahydrate	p.a.	Merck
Calcium chloride dihydrate	p.a.	Merck
Calcium sulfate dihydrate	>99 %	Merck
Sodium chloride	p.a.	Merck
Sodium hydroxide	p.a.	Merck
Sodium bicarbonate	p.a.	Merck
Potassium sulfate	>99 %	Merck
Nitric acid	p.a., 69 % wt	Merck
Methanol	p.a.	Merck
Ethanol	p.a.	Merck
Magnesium carbonate	p.a.	Magnesia GmbH
Potassium chloride	p.a.	Neolab Migge
Silver nitrate	≥99.9 %	Carl Roth
Acetonitrile	99.99 %	Fischer Scientific
Chloroform	99.8 %	J. T. Baker
Tetrahydrofuran	≥99.9 %	J. T. Baker

Double distilled water

The preparation of salt mixtures, loading of clay minerals with amino acids, titrations, and extraction of amino acids and peptides were conducted with double distilled water. It was obtained by using a special quartz glass distillation apparatus.

4.3 Heating apparatus

The heating experiments were conducted in an apparatus (Fig. 40), which was a simplified version of the thermolysis apparatus developed by Fox and Strasdeit (2013). The central part of the apparatus had a quartz tube (3) (120 cm length, 4.0 cm inner diameter) placed in a Carbolite CTF 12/75/700 tube furnace (5). The quartz tube protruded from both sides of the furnace. On the left side, a closing cap (6) was connected with Teflon sealed plain joints (9) to the quartz tube. This closing cap had a gas inlet (1) and a glass rod guideway. The sample was placed into a quartz sample container (4) that was first kept in the non-heating zone of the quartz tube (10). Different sizes of quartz sample containers were used depending on the quantity of the sample to ensure homogenous heating. The sample was purged with nitrogen gas for two days. Nitrogen was used to simulate the anoxic atmosphere of the early Earth. Moreover, the nitrogen stream transported the sublimates, if formed, to the right side of the quartz tube. The flow rate of the nitrogen gas was adjusted to 7.7 L h^{-1} . The furnace was preheated to a desired temperature. With use of the glass rod (2), the quartz sample container was pushed to the center of the heating zone (11). On the right side, a closing end cap (7) with a gas outlet (8) was also mounted with Teflon sealed plain joints (9). Depending on the experiment different temperatures and heating times were used.

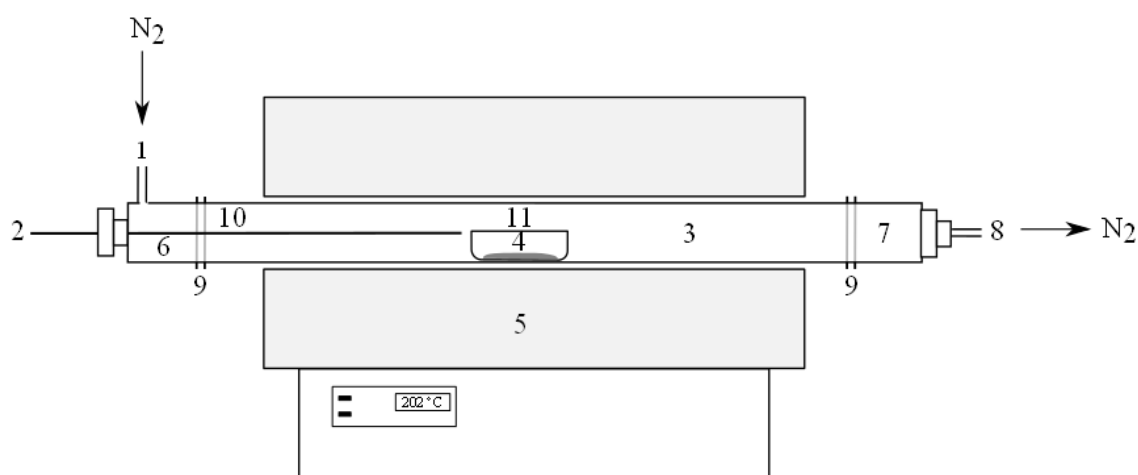


Fig. 40: The heating apparatus.

1: gas inlet, 2: glass rod, 3: quartz tube, 4: quartz sample container, 5: tube furnace, 6: left side closing end cap, 7: right side closing end cap, 8: gas outlet, 9: teflon sealed plain joints, 10: non-heating zone, and 11: heating zone.

4.4 Analysis of the thermo-melanoid

The thermo-melanoid is the black residue formed after heating glycine at 200 °C for two days. Prior to analyses, the thermo-melanoid was washed with double distilled water and dried at 50 °C.

4.4.1 Hydrolysis of the thermo-melanoid

300 mg of the washed thermo-melanoid were hydrolyzed in 300 mL of water at 100 °C. After 10 days, the water extract was analyzed glycine and glycine homopeptides by HPLC. In addition, the thermo-melanoid (5 mg) was also acid-hydrolyzed with 500 μL of 6 mol L^{-1} HCl or DCl/D₂O at 110 °C for 1–6 hours. The hydrolyzed samples were then derivatized and analyzed by GC (see 4.1.3).

4.4.2 Biodegradability of the thermo-melanoid in soil

The experiment was performed in special glass chambers called “microcosmoses” (Fig. 41). Naturally wet soil from an agricultural field was sieved to <2 mm particle size. For the sample preparation, 100 g of this soil and 500 mg of the washed thermo-melanoid were used. In total, 14 microcosmoses were prepared: five microcosmoses contained soil mixed with the thermo-melanoid, five microcosmoses contained only soil, and four microcosmoses were empty.

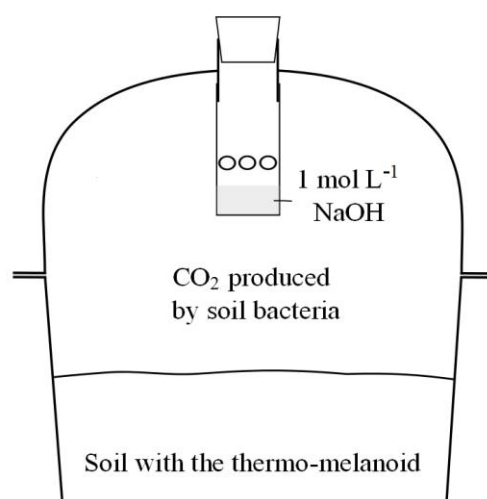


Fig. 41: The microcosmos apparatus.

2 mL of 1 mol L^{-1} NaOH solution were filled into the small container in the microcosmos, which was then closed properly with a stopper. The sample-containing microcosmos apparatuses were then incubated in a climate chamber at 20 °C for 3–4 days. The released

CO₂ dissolved in the NaOH solution as Na₂CO₃. After incubation, 0.5 mL of the NaOH solution was titrated with 0.1 mol L⁻¹ HCl with phenolphthalein as indicator. The empty NaOH containers in the microcosmoses were refilled with 2 mL of fresh NaOH solution for the next incubation period. The process was repeated for the time period of six months.

4.5 Preparative methods

4.5.1 Salts and salt mixtures with embedded glycine: Syntheses and thermal treatment

NaCl–Hgly

An equimolar mixture of NaCl (30 mmol) and glycine (30 mmol) was dissolved in 225 mL of double distilled water. The solution was evaporated in a Petri dish and then finally dried to constant weight in vacuo. The dried sample was analyzed by infrared spectroscopy and powder X-ray diffractometry (see 2.3.1). 400 mg samples of NaCl–Hgly were separately heated at 200 °C for two days and seven days.

NaCl–KCl–Hgly

A solution containing NaCl (705 mmol), KCl (15 mmol), and glycine (10 mmol) was prepared by dissolving the components in 225 mL of double distilled water. This solution was completely evaporated and then vacuum-dried to constant weight. The dried sample was analyzed by infrared spectroscopy and powder X-ray diffractometry (see 2.3.1). 12 g of the dried mixture were heated at 200 °C for seven days.

CaCl₂(Hgly) · H₂O

CaCl₂ · 2H₂O (100 mmol) and glycine (100 mmol) were dissolved in 60 mL of double distilled water. The water was evaporated at the rotary evaporator with the water bath at 50 °C. The remaining product was finally dried to constant weight in vacuo. The infrared band positions of this product (see 2.3.1) and of the product mentioned in a previous work (Yusenko et al., 2008) were identical. The heating experiments were performed for seven days with 1.5 g of CaCl₂(Hgly) · H₂O at 200 °C and with 10 g at 230, 250, and 350 °C.

AS–Hgly

AS–glycine was prepared from NaCl (705 mmol), KCl (15 mmol), MgCl₂ · 6H₂O (80 mmol), CaCl₂ · 2H₂O (15 mmol), and glycine (10 mmol). The components were completely dissolved in 225 mL of double distilled water. The solution was first evaporated and then

dried in vacuo. Infrared spectroscopy and powder X-ray diffractometry were employed for the characterization of the dried AS–glycine mixture (see 2.3.1). 3.5 g of AS–glycine were heated at 200 °C for seven days.

Gypsum–Hgly

Gypsum ($\text{CaSO}_4 \cdot 2\text{H}_2\text{O}$) dissolves slowly in water. Therefore, $\text{CaSO}_4 \cdot 2\text{H}_2\text{O}$ (2 mmol) was first added to 200 mL of double distilled water, and the cloudy solution was shaken overnight. After complete dissolution of $\text{CaSO}_4 \cdot 2\text{H}_2\text{O}$, glycine (0.4 mmol) was added. The solution was divided into two large Petri dishes to fasten the process of air drying. The solid crust formed after complete evaporation was carefully scratched out. The mixture was analyzed by infrared spectroscopy and powder X-ray diffractometry. 200 mg of the gypsum–Hgly mixture were filled into a small quartz container and heated at 200 °C for seven days.

MgCO₃–Hgly

This mixture was prepared by dry mixing of MgCO_3 (2 mmol) and glycine (0.4 mmol). Glycine was pulverized to a fine powder with pestle and mortar. It was transferred into a 100 mL round bottom flask with MgCO_3 already inside. The flask was closed with a stopper and shaken properly to ensure homogenous mixing of glycine and MgCO_3 . Dry mixing had to be used because MgCO_3 is practically insoluble in water. The mixture was analyzed by infrared spectroscopy. 200 mg of MgCO_3 –Hgly mixture were filled into a small quartz container and heated at 200 °C for seven days.

All the heating experiments were performed in the heating apparatus described in section 4.3. The residues obtained after heating were analyzed by infrared spectroscopy, powder X-ray diffractometry, and HPLC.

4.5.2 Clay minerals with embedded amino acids: Loading procedure and thermal treatment

Sedimentation of clay minerals

Ca-montmorillonites (SAz-1 and STx-1), Na-montmorillonite, nontronite (NAu-1), and kaolinite (KGa-1) were used for the experiments. These clay minerals, except Na-montmorillonite, were purchased from the Clay Minerals Society. The minerals were crushed to fine particles in a planetary ball mill (PM 100, Retsch, Germany). For this, 60 g of the clay mineral were mixed with 60 mL of double distilled water in an agate grinding jar

with agate crushing balls. The ball mill apparatus was operated at 100 rpm for five days. The homogenized sample was then diluted with water and poured into Atterberg cylinders. These cylinders were left undisturbed for a particular settling time. The bigger particles sank down at a faster rate. The settling time was calculated using a small computer program (“Atterberg”) after the input of particle density, desired maximum particle diameter, and height of fall. The suspended clay particles in a specified height were then decanted through a siphon at the Atterberg cylinder. Material with a particle size of $\leq 2 \mu\text{m}$ was obtained after the sedimentation process and used in all subsequent experiments. The initial suspension was centrifuged for 10 minutes at 15,000 rpm. The supernatant was discarded, and the sedimented clay mineral was dried and pulverized. These samples were then stored in a desiccator for at least two days over a saturated solution of $\text{Ca}(\text{NO}_3)_2$ to maintain 51 % relative humidity.

Preparation of Na-montmorillonite from Ca-montmorillonite by ion exchange

Na-montmorillonite was prepared from the Ca-montmorillonite SAz-1. To 15 g of wet SAz-1 with a particle size of $\leq 2 \mu\text{m}$, 200 mL of a 2 mol L^{-1} NaCl solution were added. The mixture was shaken for two hours and then centrifuged for 10 minutes at 15,000 rpm. The presence of calcium in the supernatant was tested by adding 3–4 drops of concentrated ammonia and ammonium oxalate solution. The process of shaking with NaCl solution was repeated until no precipitation of calcium oxalate was observed. Afterwards, the sample was washed with double distilled water and tested for the presence of chloride by adding a few drops of nitric acid and silver nitrate solution. The sample was washed repeatedly until no precipitation of silver chloride occurred. As a result, Na-montmorillonite had been produced from natural Ca-montmorillonite by Ca–Na exchange. The elemental analysis for C, H, N, Ca, and Na in Ca- and Na-montmorillonite was obtained from Mikroanalytisches Labor Pascher (Remagen, Germany).

Loading of various clay minerals with glycine

The loading process was performed by suspending 9 g of clay mineral (stored at 51 % relative humidity) in 0.5 mol L^{-1} glycine solution (2.82 g of glycine in 75 mL double distilled H_2O). The suspension was kept on a shaker overnight. Afterwards, it was centrifuged for 10 minutes at 15,000 rpm. The supernatant was discarded. The resulting glycine-containing mineral was pressed between two Whatman filter papers (185 mm diameter, Häberle Labortechnik). This was a necessary step to remove residual glycine solution from the surface of the mineral particles. The glycine-loaded clay minerals were then dried and pulverized.

This method of loading was named the “distribution method” because it was based on the distribution of the amino acid between the solid and the liquid phase. Kaolinite has no interlayer spaces where glycine could be intercalated. Therefore, mixtures of kaolinite and glycine mixture were prepared directly in small quartz containers (“direct loading method”). For this, 10 mg of glycine were dissolved in a minimum amount of double distilled water. The solution was added to 200 mg of the kaolinite (stored at 51 % relative humidity). The mixture was air-dried to a muddy consistency. Afterwards, water was again added onto the walls of the container to wash glycine into the kaolinite. Finally, the kaolinite–glycine mixture was completely air-dried.

Glycine-loaded clay minerals were again kept in a desiccator over a saturated $\text{Ca}(\text{NO}_3)_2$ solution for two days to maintain 51 % relative humidity. This step ensured that no variation of the water content of the minerals occurred, which otherwise could have affected the quantitative results.

Thermal treatment of clay minerals loaded with glycine

Glycine-loaded clay minerals (stored at 51 % relative humidity) were heated in the apparatus described in section 4.3 (Tab. 19). The residues obtained after heating were extracted with double distilled water and analyzed by HPLC (see 4.5.4).

Tab. 19: Experimental parameters of the thermal treatment of various glycine-loaded clay minerals.

Mineral loaded with glycine	Initial amount of loaded clay (mg)	Temperature (°C)	Duration of thermal treatment (days)
Ca-montmorillonite SAz-1	500	200	Two
	500	250	Two
	200	200	Seven
Ca-montmorillonite STx-1	200	200	Seven
	200	200	Two
Na-montmorillonite	200	200	Two
	200	250	Two
Nontronite N Au-1	500	200	Two
	500	250	Two
Kaolinite KGa-1	210	200	Two
	210	250	Two

Ca-montmorillonite (SAz-1) loaded with different L-ee of chiral amino acids

For loading, 9 g of Ca-montmorillonite (stored at 51 % relative humidity) were suspended in 0.5 mol L⁻¹ of amino acid solution (3.34 g of alanine or 4.39 g of valine in 75 mL double distilled water). The suspension was shaken overnight and then centrifuged for 10 minutes at 15,000 rpm. The supernatant was discarded, and the sedimented amino acid-containing Ca-montmorillonite was pressed between two Whatman filter papers, air-dried, and pulverized. This method was mentioned above as the “distribution method”. Afterwards, the sample was stored in a desiccator over a saturated solution of Ca(NO₃)₂ to maintain 51 % relative humidity. 4.5 g of Ca-montmorillonite loaded with amino acid (various L-ee) were heated at 200 °C for eight weeks under a pure nitrogen atmosphere. One experiment with Ca-montmorillonite loaded with enantiopure L-alanine was also conducted for 24 weeks. Additionally, Ca-montmorillonite loaded with L-alanine was heated at 120, 150, 180, and 220 °C for eight weeks. The L-enantiomeric excess (ee) of an amino acid can be calculated from the formula:

$$\% \text{ L-ee} = 100 (\text{L}-\text{D})/(\text{L}+\text{D})$$

The following samples were prepared:

100 % L-ee alanine: from 3.34 g of L-alanine

50 % L-ee alanine: from 1.67 g of DL-alanine and 1.67 g of L-alanine

20 % L-ee alanine: from 2.67 g of DL-alanine and 0.67 g of L-alanine

4 % L-ee alanine: from 3.21 g of DL-alanine and 0.13 g of L-alanine

0 % L-ee (racemic) alanine: from 3.34 g of DL-alanine

100 % L-ee valine: from 4.39 g of L-valine

During the thermal treatment, ~200 mg samples were taken out at certain intervals. In the first two days, two samples per day (in the morning and evening) and in the next five days one sample per day were collected. After the first week, only one sample per week was taken out. These samples were kept in a desiccator over a saturated solution of Ca(NO₃)₂ for 2–3 days and finally stored at -4 °C. For analysis, the samples were brought to room temperature, then extracted with double distilled water (see 4.5.4), derivatized, and analyzed by gas chromatography (see 4.1.3).

Direct loading of Ca-montmorillonite (SAz-1) with chiral amino acids

The “direct loading” method was applied to compare the results with those obtained with the distribution method. For the direct loading method, 4.2 g of Ca-montmorillonite (stored at 51 % relative humidity) and 315 mg of L-alanine were suspended/dissolved in a minimum quantity of water. These amounts corresponded to a loading rate of 7.5 % of amino acid in Ca-montmorillonite (for discussion see 2.4.1). The suspension was air-dried to a muddy consistency. Afterwards, 3–4 mL of water were again added onto the walls of the container to wash dried amino acid back into the Ca-montmorillonite. This process of adding water was repeated two times. After complete air drying, the loaded mineral was pulverized. The sample was then stored over a saturated solution of $\text{Ca}(\text{NO}_3)_2$ to maintain 51 % relative humidity. All samples prepared by direct mixing were separately heated at 200 °C.

Similarly, Ca-montmorillonite was also loaded with 7.5 % of L-isovaline. For this, 1.37 g of Ca-montmorillonite was suspended in a minimum amount of water that contained 129.9 mg of L-isovaline monohydrate. Additionally, Ca-montmorillonite with 3.75 % of (L- or DL-) alanine and 3.75 % of L-isovaline was prepared by mixing 4.14 g of Ca-montmorillonite with 168.8 mg of (L- or DL-) alanine and 194.7 mg of L-isovaline monohydrate. ~200 mg samples were taken out during the heating experiment. In the first two days, two samples per day (in the morning and evening) and in the next five days one sample per day were collected. Afterwards, only one sample per week was taken out. For Ca-montmorillonite loaded with L-isovaline only, the heated samples were collected after the 1st, 2nd, 4th, 6th, and 8th week. All samples were kept in a desiccator over saturated $\text{Ca}(\text{NO}_3)_2$ solution for 2–3 days and finally stored at –4 °C. For analysis, samples were brought to room temperature, extracted with double distilled water (4.5.4), derivatized, and analyzed by GC (see 4.1.3).

4.5.3 Preparation and thermal treatment of glycine-loaded terrestrial volcanic rock and Martian soil simulants

Terrestrial volcanic rock with glycine

The basaltic sand used was a product of the 2007 eruption of the Piton de la Fournaise volcano on the island of La Réunion, Indian Ocean. A few days after being collected in 2011, the basaltic sand was dried at 80 °C for 2 hours and then sterilized at 150 °C for 24 hours in our laboratory. Prior to use, the sterilized material was crushed to powder with a pestle and

mortar. Mineral constituents of the basalt sand were identified using powder X-ray diffractometry and infrared spectroscopy.

Mixtures of Mars regolith simulants with glycine

Two of the three Martian soil simulants used were “Phyllosilicatic Mars Regolith Simulant” (P-MRS) and “Sulfatic Mars Regolith Simulant” (S-MRS). They were provided by the Museum für Naturkunde, Berlin, and ordered from the geo-material merchant Dr. F. Krantz, Rheinisches Mineralien-Kontor, Bonn. The soil simulants were produced by mixing terrestrial igneous rocks, phyllosilicates, carbonates, sulfates, and iron oxides. These minerals and rocks were similar to those detected by Mars orbiter and rover missions (Poulet et al., 2005; Bibring et al., 2005; Chevrier and Mathé, 2007; Morris et al., 2010). These two Martian soil simulants represented the environmental changes during the early geological history of Mars. The third Martian soil simulant, JSC Mars-1A, was purchased from the Orbital Technologies Corporation (ORBITEC), Madison, Wisconsin. It is a reproduction of JSC Mars-1 (1997) Martian soil simulant. “JSC” refers to “NASA Johnson Space Center”. These Mars regolith simulants are weathering products of volcanic ash from Pu’u Nene, a cinder cone on the island of Hawaii.

For heating experiments, 465 mg of terrestrial volcanic rock or Martian soil simulant (stored at 51 % relative humidity) were mixed with 35 mg of glycine dissolved in a minimum quantity of water. The suspensions were completely air-dried, before they were heated at 200 °C for two days under a pure nitrogen atmosphere. The residues were analyzed by infrared spectroscopy. Additionally, the residues were extracted with double distilled water and analyzed by HPLC (see 4.5.4 and 4.1.1).

4.5.4 Extraction of amino acids and peptides from clay minerals

Clay minerals containing amino acids and peptides were extracted 10 times with double distilled water. For 100 mg of the sample, three extraction turns were performed with 650 µL of double distilled water and the next seven turns with 450 µL each. The suspensions were shaken for one hour. After every turn of shaking, the samples were centrifuged for three minutes at 15,000 rpm. The supernatants were collected every time and the final volume was 5 mL. Prior to analysis, the combined extracts were again centrifuged to remove any solid particles present. This procedure ensured a practically complete extraction of amino acids and peptides. The combined extracts were then analyzed by HPLC and GC. For GC analysis, 200 µL were air-dried and derivatized (see 4.1.3).

Determination of the amino acid content of clay minerals

The percentage of amino acid in Ca-montmorillonite was determined by conductometric titration and HPLC. For titration, 400 mg of amino acid-containing clay mineral (stored at 51 % relative humidity) were suspended in 200 mL of double distilled water. The suspension was stirred for one hour. By this, the amino acid was released from the mineral. The suspension was titrated with 0.1 mol L⁻¹ NaOH solution. The factor of the NaOH solution was determined by titration with 200 mg of potassium hydrogen phthalate dissolved in 100 mL of water. The total mass of amino acid was calculated from the following formula:

$$m_{(\text{amino acid})} = c_{(\text{NaOH})} * V_{(\text{NaOH})} * M_{(\text{amino acid})} * F_{(\text{NaOH})}$$

where $m_{(\text{amino acid})}$ = unknown mass of amino acid

$M_{(\text{amino acid})}$ = molar mass of amino acid

$c_{(\text{NaOH})}$ = 0.1 mol L⁻¹

$V_{(\text{NaOH})}$ = volume (L) of NaOH solution required for the neutralization

$F_{(\text{NaOH})}$ = factor of NaOH solution

Additionally, the concentrations of glycine, DKP, diglycine, and triglycine in Ca-montmorillonite were determined by HPLC with the help of calibration curves. For calibration, a series of standard solutions with known concentrations was prepared. The absolute amount in the injected volume of standard solution was plotted against the area under the peak. It was found that the calibration curves for glycine, diglycine, and triglycine were linear, meaning that the Lambert-Beer law was followed. However, DKP did not follow this law. This may have caused additional errors in the quantification of DKP. Glycine contents determined by titration and HPLC were in good agreement with each other (see Tab. 9). The value that was used to calculate the yield after the thermal treatment was the mean of the titration and HPLC value.

5 Literature

Abelson, P. H. (1966) Chemical events on the primitive Earth. *Proc Natl Acad Sci USA* **55**: 1365–1372.

Acuña, M. H., Connerney, J. E. P., Wasilewski, P., Lin, R. P., Anderson, K. A., Carlson, C. W., McFadden, J., Curtis, D. W., Mitchell, D., Reme, H., Mazelle, C., Sauvaud, J. A., d’Uston, C., Cros, A., Medale, J. L., Bauer, S. J., Cloutier, P., Mayhew, M., Winterhalter, D., and Ness, N. F. (1998) Magnetic field and plasma observations at Mars: Initial results of the Mars Global Surveyor mission. *Science* **279**: 1676–1680.

Alargov, D. K., Deguchi, S., Tsujii, K., and Horikoshi, K. (2002) Reaction behaviors of glycine under super- and subcritical water conditions. *Orig Life Evol Biosph* **32**: 1–12.

Alexander, C. M. O’D., Bowden, R., Fogel, M. L., Howard, K. T., Herd, C. D. K., and Nittler, L. R. (2012) The provenances of asteroids, and their contributions to the volatile inventories of the terrestrial planets. *Science* **337**: 721–723.

Allen, C. C., Jager, K. M., Morris, R. V., Lindstrom, D. J., Lindstrom, M. M., and Lockwood, J. P. (1997) JSC Mars-1: A Martian soil simulant. Presented at the 28th Lunar and Planetary Science Conference, Houston, Texas USA, p 1797.

Ambujam, K., Selvakumar, S., Anand, D. P., Mohamed, G., and Sagayaraj, P. (2006) Crystal growth, optical, mechanical and electrical properties of organic NLO material γ -glycine. *Cryst Res Technol* **41**: 671–677.

Anderson, D. M. and Banin, A. (1975) Soil and water and its relationship to the origin of life. *Orig Life Evol Biosph* **6**: 23–36.

Bada, J. L. (1995) Origin of homochirality. *Nature* **374**: 594–595.

Bada, J. L. (2004) How life began on Earth: A status report. *Earth Planet Sci Lett* **226**: 1–15.

Bada, J. L., Wang, X. S., Poinar, H. N., Pääbo, S., and Poinar, G. O. (1994) Amino acid racemization in amber-entombed insects: Implications for DNA preservation. *Geochim Cosmochim Acta* **58**: 3131–3135.

Bailey, J., Chrysostomou, A., Hough, J. H., Gledhill, T. M., McCall, A., Clark, S., Ménard, F., and Tamura, M. (1998) Circular polarization in star-formation regions: Implications for biomolecular homochirality. *Science* **281**: 672–674.

- Balakrishnan, T., Ramesh Babu, R., and Ramamurthi, K. (2008) Growth, structural, optical and thermal properties of γ -glycine crystal. *Spectrochim Acta A* **69**: 1114–1118.
- Balasubramanian, R. (1983) Possible mechanism for origin of chiral specificity during origins of life. *Orig Life Evol Biosph* **13**: 109–112.
- Balasubramanian, R. (1985) Conformational studies on nucleotide–amino acid interactions leading to origin of life. *J Biosciences* **8**: 823–835.
- Bandfield, J. L., Glotch, T. D., and Christensen, P. R. (2003) Spectroscopic identification of carbonate minerals in the Martian dust. *Science* **301**: 1085–1087.
- Bar-Nun, A., Bar-Nun, N., Bauer, S. H., and Sagan, C. (1970) Shock synthesis of amino acids in simulated primitive environments. *Science* **168**: 470–473.
- Basiuk, V. A. and Navarro-Gonzalez, R. (1998) Pyrolytic behavior of amino acids and nucleic acid bases: Implications for their survival during extraterrestrial delivery. *Icarus* **134**: 269–278.
- Bellec, A. and Guillemin, J.-C. (2010) A simple explanation of the enhancement or depletion of the enantiomeric excess in the partial sublimation of enantiomerically enriched amino acids. *Chem Commun* **46**: 1482–1484.
- Benincasa, E., Brigatti, M. F., Lugli, C., Medici, L., and Poppi, L. (2000) Interaction between glycine and Na-, Ca- and Cu-rich smectites. *Clay Miner* **35**: 635–641.
- Bernal, J. D. (1949) The physical basis of life. *Proc Natl Acad Sci USA* **62**: 597–618.
- Bernstein, M. P., Dworkin, J. P., Sandford, S. A., Cooper, G. W., and Allamandola, L. J. (2002) Racemic amino acids from the ultraviolet photolysis of interstellar ice analogues. *Nature* **416**: 401–403.
- Bhat, M. N. and Dharmaprasanth, S. M. (2002a) Effect of solvents on the growth morphology and physical characteristics of nonlinear optical γ -glycine crystals. *J Cryst Growth* **242**: 245–252.
- Bhat, M. N. and Dharmaprasanth, S. M. (2002b) Growth of nonlinear optical γ -glycine crystals. *J Cryst Growth* **236**: 376–380.
- Bibring, J.-P., Langevin, Y., Gendrin, A., Gondet, B., Poulet, F., Berthé, M., Soufflot, A., Arvidson, R., Mangold, N., Mustard, J., Drossart, P., and the OMEGA team (2005) Mars

surface diversity as revealed by the OMEGA/Mars Express observations. *Science* **307**: 1576–1581.

Bibring, J.-P., Langevin, Y., Mustard, J. F., Poulet, F., Arvidson, R., Gendrin, A., Gondet, B., Mangold, N., Pinet, P., Forget, F., and the OMEGA team (2006) Global mineralogical and aqueous Mars history derived from OMEGA/Mars Express data. *Science* **312**: 400–404.

Bischoff, J. L. (1972). Ferroan nontronite from red sea geothermal system. *Clay Clay Miner* **20**: 217–223.

Bishop, J. L., Dobrea, E. Z. N., McKeown, N. K., Parente, M., Ehlmann, B. L., Michalski, J. R., Milliken, R. E., Poulet, F., Swayze, G. D., Mustard, J. F., Murchie, S. L., and Bibring, J.-P. (2008) Phyllosilicate diversity and past aqueous activity revealed at Mawrth Vallis, Mars. *Science* **321**: 830–833.

Blackmond, D. G. (2007) “Chiral Amnesia” as a driving force for solid-phase homochirality. *Chem Eur J* **13**: 3290–3295.

Blackmond, D. G. and Klussmann, M. (2007) Spoilt for choice: Assessing phase behavior models for the evolution of homochirality. *Chem Commun* **39**: 3990–3996.

Bondy, S. C. and Harrington M. E. (1979) L-amino acids and D-glucose bind stereospecifically to a colloidal clay. *Science* **203**: 1243–1245.

Bonner, W. A. (1991a) The origin and amplification of biomolecular chirality. *Orig Life Evol Biosph* **21**: 59–111.

Bonner, W. A. (1991b) Terrestrial and extraterrestrial sources of molecular homochirality. *Orig Life Evol Biosph* **21**: 407–420.

Bonner, W. A. (1995) Chirality and life. *Orig Life Evol Biosph* **25**: 175–190.

Bonner, W. A. and Kavasmaneck, P. R. (1976) Asymmetric adsorption of DL-alanine hydrochloride by quartz. *J Org Chem* **41**: 2225–2226.

Bonner, W. A. and Rubenstein, E. (1987) Supernovae neutron stars and biomolecular chirality. *Biosystems* **20**: 99–111.

Bonner, W. A., Blair, N. E., Lemmon, Flores, J. J., and Pollock, G. E. (1979). The radoracemization of isovaline. Cosmochemical implications. *Geochim Cosmochim Acta* **43**: 1841–1846.

- Bonner, W. A., Kavasmaneck, P. R., Martin, F. S., and Flores, J. J. (1974) Asymmetric adsorption of alanine by quartz. *Science* **186**: 143–144.
- Bonner, W. A., Kavasmaneck, P. R., Martin, F. S., and Flores, J. J. (1975) Asymmetric adsorption by quartz: A model for the prebiotic origin of optical activity. *Orig Life Evol Biosph* **6**: 367–376.
- Botta, O., Glavin, D. P., Kminek, G., and Bada, J. L. (2002) Relative amino acid concentrations as a signature for parent body processes of carbonaceous chondrites. *Orig Life Evol Biosph* **32**: 143–163.
- Böttger, U., de Vera, J.-P., Fritz, J., Weber, I., Hübers, H.-W., and Schulze-Makuch, D. (2012) Optimizing the detection of carotene in cyanobacteria in a martian regolith analogue with a Raman spectrometer for the ExoMars mission. *Planet Space Sci* **60**: 356–362.
- Brack, A. (2002) Water, the Spring of Life. In: G. Horneck and C. Baumstark-Khan (eds.), *Astrobiology: The quest for the conditions of life*. Physics and astronomy online library. Springer, Berlin, pp 79–88.
- Brack, A. (2007) From interstellar amino acids to prebiotic catalytic peptides: A review. *Chem Biodivers* **4**: 665–679.
- Brandenburg, A., Andersen, A. C., and Multamäki, T. (2005) Homochirality – The problem of left handed amino acids. *Orig Life Evol Biosph* **35**: 22–31.
- Breslow, R. (1959) On the mechanism of the formose reaction. *Tetrahedron Lett* **1**: 22–26.
- Breslow, R. and Cheng, Z.-L. (2009) On the origin of terrestrial homochirality for nucleosides and amino acids. *Proc Natl Acad Sci USA* **106**: 9144–9146.
- Bridges, J. C. and Grady, M. M. (2000) Evaporite mineral assemblages in the nakhlite (Martian) meteorites. *Earth Planet Sci Lett* **176**: 267–279.
- Bridges, J. C., Catling, D. C., Saxton, J. M., Swindle, T. D., Lyon, I. C., and Grady, M. M. (2001) Alteration assemblages in Martian meteorites: Implications for near-surface processes. *Space Sci Rev* **96**: 365–392.
- Brigatti, M. F., Galan, E., and Theng, B. K. G. (2006) Structures and mineralogy of clay minerals. In: F. Bergaya, B. K. G. Theng, and G. Lagaly (eds.), *Handbook of clay science*. Elsevier, Amsterdam, pp 19–86.

- Brinton, K. L. F., Engrand, C., Glavin, D. P., Bada, J. L., and Maurette, M. (1998) Search for extraterrestrial amino acids in carbonaceous antarctic micrometeorites. *Orig Life Evol Biosph* **28**: 413–424.
- Bullock, M. A. and Moore, J. M. (2007) Atmospheric conditions on early Mars and the missing layered carbonates. *Geophys Res Lett* **34**: 1–6.
- Bywater, R. P. and Conde-Frieboes, K. (2005) Did life begin on the beach? *Astrobiology* **5**: 568–574.
- Cairns-Smith, A. G. (1986) Introducing clay. In: A. G. Cairns-Smith and H. Hartman (eds.), *Clay minerals and the origin of life*. Cambridge University Press, Cambridge, pp 13–22.
- Cairns-Smith, A. G. (2008) Chemistry and the missing era of evolution. *Chem Eur J* **14**: 3830–3839.
- Carr, M. H. and Head III, J. W. (2010) Geologic history of Mars. *Earth Planet Sci Lett* **294**: 185–203.
- Çelik, M., Karakaya, N., and Temel, A. (1999) Clay minerals in hydrothermally altered volcanic rocks, eastern Pontides, Turkey. *Clay Clay Miner* **47**: 708–717.
- Chassefière, E. and Leblanc, F. (2004) Mars atmospheric escape and evolution, interaction with the solar wind. *Planet Space Sci* **52**: 1039–1058.
- Chevrier, V. and Mathé, P. E. (2007) Mineralogy and evolution of the surface of Mars: A review. *Planet Space Sci* **55**: 289–314.
- Clark, B. C. and Van Hart, D. C. (1981) The salts of Mars. *Icarus* **45**: 370–378.
- Clayton, R. N. and Mayeda, T. K. (1988) Isotopic composition of carbonate in EETA 79001 and its relation to parent body volatiles. *Geochim Cosmochim Acta* **52**: 925–927.
- Cleaves, H. J. and Miller, S. L. (1998) Oceanic protection of prebiotic organic compounds from UV radiation. *Proc Natl Acad Sci USA* **95**: 7260–7263.
- Cleaves, H. J., Chalmers, J. H., Lazcano, A., Miller, S. L., and Bada, J. L. (2008) A reassessment of prebiotic organic synthesis in neutral planetary atmospheres. *Orig Life Evol Biosph* **38**: 105–115.
- Cloutis, E. A., Grasby, S. E., Last, W. M., Leveille, R., Osinski, G. R., and Sherriff, B. L. (2010) Spectral reflectance properties of carbonates from terrestrial analogue environments: Implications for Mars. *Planet Space Sci* **58**: 522–537.

- Cohen, B. A. and Chyba, C. F. (2000). Racemization of meteoritic amino acids. *Icarus* **145**: 272–281.
- Constantino, E., Rimola, A., Sodupe, M., and Rodríguez-Santiago, L. (2009) Coordination of (Glycyl)_nglycine ($n = 1-3$) to Co^+ and Co^{2+} . *J Phys Chem A* **113**: 8883–8892.
- Cronin, J. R and Pizzarello, S. (1983) Amino acids in meteorites. *Adv Space Res* **3**: 5–18.
- Cronin, J. R. and Pizzarello, S. (1999) Amino acid enantiomer excesses in meteorites: Origin and significance. *Adv Space Res* **23**: 293–299.
- Dartnell, L. R., Desorgher, L., Ward, J. M., and Coates, A. J. (2007) Martian sub-surface ionising radiation: Biosignatures and geology. *Biogeosciences* **4**: 545–558.
- Davies, J. K., Roush, T. L., Cruikshank, D. P., Bartholomew, M. J., Geballe, T. R., Owen, T., and Bergh, C. D. (1997) The detection of water ice in comet hale-Bopp. *Icarus* **127**: 238–245.
- Deamer, D. and Weber, A. L. (2010). Bioenergetics and life's origins. *Cold Spring Harb Perspect Biol*, a004929.
- Deamer, D., Dworkin, J. P., Sandford, S. A., Bernstein, M. P., and Allamandola, L. J. (2002) The first cell membranes. *Astrobiology* **2**: 371–381.
- Degens, E. T., Matheja, J., and Jackson, T. A. (1970) Template catalysis: Asymmetric polymerization of amino-acids on clay minerals. *Nature* **227**: 492–493.
- Derry, L. A. and Jacobsen, S. B. (1988) The Nd and Sr isotopic evolution of Proterozoic seawater. *Geophys Res Lett* **15**: 397–400.
- DeWitt, H. L., Hasenkopf, C. A., Trainer, M. G., Farmer, D. K., Jimenez, J. L., McKay, C. P., Toon, O. B., and Tolbert, M. A. (2010) The formation of sulfate and elemental sulfur aerosols under varying laboratory conditions: Implications for early Earth. *Astrobiology* **10**: 773–781.
- DIAMOND – Crystal and Molecular Structure Visualization, Version 3.1, Crystal Impact, Bonn 2005.
- Douda, J. and Basiuk, V. A. (2000) Pyrolysis of amino acids: Recovery of starting materials and yields of condensation products. *J Anal Appl Pyrol* **56**: 113–121.
- Ehlmann, B. L., Mustard, J. F., Murchie, S. L., Poulet, F., Bishop, J. L., Brown, A. J., Calvin, W. M., Clark, R. N., Marais, D. J. D., Milliken, R. E., Roach, L. H., Roush, T. L., Swayze, G.

A., and Wray, J. J. (2008) Orbital identification of carbonate-bearing rocks on Mars. *Science* **322**: 1828–1832.

Elbeyli, İ. Y., Derun, E. M., Gülen, J., and Piskin, S. (2003) Thermal analysis of borogypsum and its effects on the physical properties of Portland cement. *Cement Concrete Res* **33**: 1729–1735.

Elsila, J. E., Dworkin, J. P., Bernstein, M. P., Martin, M. P., and Sandford, S. A. (2007) Mechanisms of amino acid formation in interstellar ice analogs. *Astrophys J* **660**: 911–918.

Elsila, J. E., Glavin, D. P., and Dworkin, J. P. (2009) Cometary glycine detected in samples returned by Stardust. *Meteorit Planet Sci* **44**: 1323–1330.

Engrand, C., DeEloule, E., Robert, F., Maurette, M., and Kurat, G. (1999) Extraterrestrial water in micrometeorites and cosmic spherules from Antarctica: An ion microprobe study. *Meteorit Planet Sci* **34**: 113–186.

Erbe, T. and Brückner, H. (1999) Microwave treatment of dietary gelatin does not generate cis-4-hydroxy-L-proline, an inhibitor of collagen biosynthesis. *Z Lebensm Unters Forsch* **208**: 424–428.

Fairén, A. G., Fernández-Remolar, D., Dohm, J. M., Baker, V. R., and Amils, R. (2004) Inhibition of carbonate synthesis in acidic oceans on early Mars. *Nature* **431**: 423–426.

Fan, C., Schulze-Makuch, D., and Xie, H. (2006) Sulfate formation and its relevance to environmental conditions on early Mars. Presented at the 37th Lunar and Planetary Science Conference, League City, Texas, USA, p 7033.

Ferris, J. P. (2006) Montmorillonite-catalysed formation of RNA oligomers: The possible role of catalysis in the origins of life. *Philos Trans R Soc Lond B Biol Sci* **361**: 1777–1786.

Fishbaugh, K. E., Poulet, F., Chevrier, V., Langevin, Y., and Bibring, J.-P. (2007) On the origin of gypsum in the Mars north polar region. *J Geophys Res* **112**: 1–17.

Fletcher, S. P., Jagt, R. B. C, and Feringa, B. L. (2007) An astrophysically-relevant mechanism for amino acid enantiomer enrichment. *Chem Commun* **25**: 2578–2580.

Flores, J. J. and Bonner, W. A. (1974) On the asymmetric polymerization of aspartic acid enantiomers by kaolin. *J Mol Evol* **3**: 49–56.

Folsome, C. E., Brittain, A., Smith A., and Chang, S. (1981) Hydrazines and carbohydrazides produced from oxidized carbon in Earth's primitive environment. *Nature* **294**: 64–65.

- Foster, M. D. (1954). The relation between composition and swelling in clays. *Clay Clay Miner* **3**: 205–220.
- Fox, S. and Strasdeit, H. (2013) Possible prebiotic origin on volcanic islands of oligopyrrole-type photopigments and electron transfer cofactors. *Astrobiology* **13**: 578–595.
- Fox, S. W. and Harada, K. (1961) Synthesis of uracil under conditions of a thermal model of prebiological chemistry. *Science* **133**: 1923–1924.
- Frank, F. C. (1953) On spontaneous asymmetric synthesis. *Biochem Bioph Acta* **11**: 459–463.
- Friedman, M. (1999) Chemistry, nutrition, and microbiology of D-amino acids. *J Agr Food Chem* **47**: 3457–3479.
- Fripiat, J. J. and Cruz-Cumplido, M. I. (1974) Clays as catalysts for natural processes. *Annu Rev Earth Planet Sci* **2**: 239–256.
- Gendrin, A., Mangold, N., Bibring, J.-P., Langevin, Y., Gondet, B., Poulet, F., Bonello, G., Quantin, C., Mustard, J., Arvidson, R., and LeMouélic, S. (2005) Sulfates in Martian layered terrains: The OMEGA/Mars Express view. *Science* **307**: 1587–1591.
- Gilat, G. (1985) Chiral interactions in biomolecules. *Chem Phys Lett* **121**: 9–12.
- Gilbert, W. (1986) The RNA world. *Nature* **319**: 618.
- Glavin, D. P. and Bada, J. L. (2001) Survival of amino acids in micrometeorites during atmospheric entry. *Astrobiology* **1**: 259–269.
- Glavin, D. P. and Dworkin, J. P. (2009) Enrichment of the amino acid L-isovaline by aqueous alteration on CI and CM meteorite parent bodies. *Proc Natl Acad Sci USA* **14**: 5487–5492.
- Glavin, D. P., Dworkin, J. P., and Sandford, S. A. (2008) Detection of cometary amines in samples returned by stardust. *Meteorit Planet Sci* **43**: 399–413.
- Glavin, D. P., Matrajt, G., and Bada, J. L. (2004) Re-examination of amino acids in antarctic micrometeorites. *Adv Space Res* **33**: 106–113.
- Glotch, T. D., Bandfield, J. L., Tornabene, L. L., Jensen, H. B., and Seelos, F. P. (2010) Distribution and formation of chlorides and phyllosilicates in Terra Sirenum, Mars. *Geophys Res Lett* **37**: 1–5.
- Goldanskii, V. I., Avetisov, V. A., and Kuz'min, V. V. (1986) Chiral purity of nucleotides as a necessary condition of complementarity. *FEBS Lett* **207**: 181–183.

- Goodfriend, G. A. (1991) Patterns of racemization and epimerization of amino acids in land snail shells over the course of the Holocene. *Geochim Cosmochim Acta* **55**: 293–302.
- Goodfriend, G. A. and Meyer, V. R. (1991) A comparative study of the kinetics of amino acid racemization/epimerization in fossil and modern mollusk shells. *Geochim Cosmochim Acta* **55**: 3355–3367.
- Gooding, J. L. (1978) Chemical weathering on Mars: Thermodynamic stabilities of primary minerals (and their alteration products) from mafic igneous rocks. *Icarus* **33**: 483–513.
- Gooding, J. L. (1988) Calcium carbonate and sulfate of possible extraterrestrial origin in the EETA 79001 meteorite. *Geochim Cosmochim Acta* **52**: 909–915.
- Gooding, J. L., Wentworth, S. J., and Zolensky, M. E. (1991) Aqueous alteration of the Nakhla meteorite. *Meteoritics* **26**: 135–143.
- Greeley, R. and Spudis, P. D. (1981) Volcanism on Mars. *Rev Geophys* **19**: 13–41.
- Gross, D. and Grodsky, G. (1954) On the sublimation of amino acids and peptides. *J Am Chem Soc* **77**: 1678–1680.
- Halevy, I., Zuber, M. T., and Schrag, D. P. (2007) A sulfur dioxide climate feedback on early Mars. *Science* **318**: 1903–1907.
- Harada, K. and Fox, S. W. (1964) Thermal copolymerization of amino acids to a product resembling protein. *Science* **128**: 1214.
- Harrison, T. M., Blichert-Toft, J., Müller, W., Albarede, F., Holden, P., and Mojzsis, S. J. (2005) Heterogeneous Hadean hafnium: Evidence of continental crust at 4.4 to 4.5 Ga. *Science* **310**: 1947–1950.
- Harvey, R. P. (2010) Carbonates and Martian climate. *Science* **329**: 400–401.
- Harvey, R. P. and McSween Jr., H. Y. (1996) A possible high-temperature origin for the carbonates in the Martian meteorite ALH84001. *Nature* **382**: 49–51.
- Hazen, R. M., Filley, T. R., and Goodfriend, G. A. (2001) Selective adsorption of L- and D-amino acids on calcite: Implications for biochemical homochirality. *Proc Natl Acad Sci USA* **98**: 5487–5490.
- Hazen, R. M., Papineau, D., Bleeker, W., Downs, R. T., Ferry, J. M., McCoy, T. J., Sverjensky, D. A., and Yang, H. (2008) Mineral evolution. *Am Mineral* **93**: 1693–1720.

- Hennet, R. J.-C., Holm, N. G., and Engel, M. H. (1992) Abiotic synthesis of amino acids under hydrothermal conditions and the origin of life: A perpetual phenomenon. *Naturwissenschaften* **79**: 361–365.
- Heyns, K. and Pavel, K. (1957a) Thermal transformation products of amino acids. I. *Z Naturforsch* **12**: 97–109.
- Heyns, K. and Pavel, K. (1957b) Thermal transformation products of amino acids. II. Thermo-glycine-melanoid. *Z Naturforsch* **12**: 109–115.
- Hillier, S. (1995) Origin of clays by rock weathering and soil formation. In: B. Velde (ed.), *Origin and mineralogy of clays*. Springer, Berlin, pp 162–219.
- Holm, N. G. and Andersson, E. M. (2005) Hydrothermal simulation experiments as a tool for studies of the origin of life on Earth and other terrestrial planets: A review. *Astrobiology* **5**: 444–460.
- Hoskin, P. W. O. (2005) Trace-element composition of hydrothermal zircon and the alteration of Hadean zircon from the Jack Hills, Australia. *Geochim Cosmochim Acta* **69**: 637–648.
- Imai, E-i., Honda, H., Hatori, K., Brack, A., and Matsuno, K. (1999) Elongation of oligopeptides in a simulated submarine hydrothermal system. *Science* **283**: 831–833.
- Inoue, A. and Utada, M. (1983) Further investigations of a conversion series of dioctahedral mica/smectites in the Shinzan hydrothermal alteration area, Northeast Japan. *Clay Clay Miner* **31**: 401–411.
- Iitaka, Y. (1961) The crystal structure of γ -glycine. *Acta Crystallogr* **14**: 1–10.
- Jackson, M. L. (1959) Frequency distribution of clay minerals in major soil groups as related to factors of soil formation. *Clay Clay Miner* **6**: 133–143.
- Jackson, T. A. (1971a) Preferential polymerization and adsorption of L-optical isomers of amino acids relative to D-optical isomers on kaolinite templates. *Chem Geol* **7**: 295–306.
- Jackson, T. A. (1971b) Evidence for selective adsorption and polymerization of the L-optical isomers of amino acids relative to the D-optical isomers on the edge faces of kaolinite. *Cell Mol Life Sci* **27**: 242–243.
- Johnson, A. P., Cleaves, H. J., Dworkin, J. P., Glavin, D. P., Lazcano, A., and Bada, J. L. (2008) The Miller volcanic spark discharge experiment. *Science* **322**: 404.

- Joyce, G. F. (2002) The antiquity of RNA-based evolution. *Nature* **418**: 214–221.
- Julg, A. and Ozias, Y. (1988) Asymmetric adsorption of ethyliminium cation on kaolinite and L-homochirality of amino acids in proteins. *J Mol Struct-Theochem* **179**: 17–25.
- Kahn, R. (1985) The evolution of CO₂ on Mars. *Icarus* **62**: 175–190.
- Kalenskii, S. V., Promislov, V. G., Alakoz, A. V., Winnberg, A., and Johansson, L. E. B. (2000) Probing the properties of methyl cyanide sources. *Astron Astrophys* **354**: 1036–1040.
- Kasting, J. F. (1991) CO₂ condensation and the climate of early Mars. *Icarus* **94**: 1–13.
- Kasting, J. F. (1993) Earth's early atmosphere. *Science* **259**: 920–926.
- Kasting, J. F. and Catling, D. (2003) Evolution of a habitable planet. *Annu Rev Astron Astrophys* **41**: 429–463.
- Kasting, J. F. and Howard, M. T. (2006) Atmospheric composition and climate on the early Earth. *Philos Trans R Soc Lond B Biol Sci* **361**: 1733–1742.
- Kasting, J. F., Zahnle, K. J., Pinto, J. P., and Young, A. T. (1989) Sulfur, ultraviolet radiation, and the early evolution of life. *Orig Life Evol Biosph* **19**: 95–108.
- Kauffman, S. (2007) Question 1: Origin of life and the living state. *Orig Life Evol Biosph* **37**: 315–322.
- Kavasmaneck, P. R. and Bonner, W. A. (1977) Adsorption of amino acid derivatives by d- and l-quartz. *J Am Chem Soc* **99**: 44–50.
- Kawamura, K., Nishi, T., and Sakiyama, T. (2005) Consecutive elongation of alanine oligopeptides at the second time range under hydrothermal conditions using a microflow reactor system. *J Am Chem Soc* **127**: 522–523.
- Keeling, J. L., Raven, M. D., and Gates, W. P. (2000) Geology and characterization of two hydrothermal nontronites from weathered metamorphic rocks at the Uley graphite mine, South Australia. *Clay Clay Miner* **48**: 537–548.
- Khan, A. H., Nurnabi, M., and Bala, P. (2009) Studies on thermal transformation of Na–montmorillonite–glycine intercalation compounds. *J Therm Anal Calorim* **96**: 929–935.
- Kitadai, N., Yokoyama, T., and Nakashima, S. (2011) Hydration–dehydration interactions between glycine and anhydrous salts: Implications for a chemical evolution of life. *Geochim Cosmochim Acta* **75**: 6285–6299.

- Klabunovskii, E. I. (2001) Can enantiomorphic crystals like quartz play a role in the origin of homochirality on Earth? *Astrobiology* **1**: 127–131.
- Klabunovskii, E. I. and Thiemann, W. (2000) The role of quartz in the origin of optical activity on Earth. *Orig Life Evol Biosph* **30**: 431–434.
- Knauth, L. P. (1998) Salinity history of the Earth's early ocean. *Nature* **395**: 554.
- Kondepudi, D. K., Kaufman, R. J., and Singh, N. (1990) Chiral symmetry breaking in sodium chlorate crystallization. *Science* **250**: 975–976.
- Krause, E., Bienert, M., Schmieder P., and Wenschuh, H. (2000) The helix-destabilizing propensity scale of D-amino acids: The influence of side chain steric effects. *J Am Chem Soc* **122**: 4865–4870.
- Krishna, M. S., Sarma, N. S., Pasha, Sk. G., and Venu, K. G. (2010) Aspartic acid geochronology of sediments from the ocean margin off of India. *Org Geochem* **41**: 363–369.
- Kuwahara, H., Eto, M., Kawamoto, Y., Kurihara, H., Kaneko, T., Obayashi, Y., and Kobayashi, K. (2012) The use of ascorbate as an oxidation inhibitor in prebiotic amino acid synthesis: A cautionary note. *Orig Life Evol Biosph* **42**: 533–541.
- Kuwahara, H., Kurihara, H., Kaneko, T., Obayashi, Y., and Kobayashi, K. (2011) Formation of amino acids in non-reducing gas mixtures. Presented at the 11th European Workshop on Astrobiology, Köln, Germany.
- Kuzmin, R. O., Mironenko, M. V., and Evdokimova, N. A. (2009) Spectral and thermodynamic constraints on the existence of gypsum at the Juventae Chasma on Mars. *Planet Space Sci* **57**: 975–981.
- Lahav, N. and White, D. H. (1980) A possible role of fluctuating clay-water systems in the production of ordered prebiotic oligomers. *J Mol Evol* **16**: 11–21.
- Lam, H., Oh, D.-C., Cava, F. Takacs, C. N., Clardy, J., Pedro, M. A. de, and Waldor, M. K. (2009) D-amino acids govern stationary phase cell wall remodeling in bacteria. *Science* **325**: 1552–1555.
- Lambert, J. F. (2008) Adsorption and polymerization of amino acids on mineral surfaces: A review. *Orig Life Evol Biosph* **38**: 211–242.

- Lammer, H., Kasing, J. F., Chassefière, E., Johnson, R. E., Kulikov Y. N., and Tian, F. (2008). Atmospheric escape and evolution of terrestrial planets and satellites. *Space Sci Rev* **139**: 399–436.
- Langevin, Y., Poulet, F., Bibring, J.-P., Schmitt, B., Douté, S., and Gondet, B. (2005) Summer evolution of the north polar cap of Mars as observed by OMEGA/Mars Express. *Science* **307**: 1581–1584.
- Lécuyer, C., Gillet, P., and Robert, F. (1998) The hydrogen isotope composition of seawater and the global water cycle. *Chem Geol* **145**: 249–261.
- Lellouch, E., Encrenaz, T., de Graauw, T., Erard, S., Morris, P., Crovisier, J., Feuchtgruber, H., Girard, T., and Burgdorf, M. (2000) The 2.4–45 μm spectrum of Mars observed with the infrared space observatory. *Planet Space Sci* **48**: 1393–1405.
- Lemmon, R. M. (1970) Chemical evolution. *Chem Rev* **70**: 95–109.
- Levine, J. S., Augustsson, T. R., and Natrajan, M. (1982) On the prebiological paleoatmosphere: Stability and composition. *Orig Life Evol Biosph* **12**: 245–259.
- Levine, M., Kenesky, C. S., Mazori, D., and Breslow, R. (2008) Enantioselective synthesis and enantiomeric amplification of amino acids under prebiotic conditions. *Org Lett* **10**: 2433–2436.
- Limtrakul, J. P. and Rode, B. M. (1985) Solvent structures around sodium and chloride ions in water. *Monatsh Chem* **116**: 1377–1384.
- Limtrakul, J. P., Fujiwara, S., and Rode, B. M. (1985) A quantum chemical analysis of the structural entities in aqueous sodium chloride solution and their concentration dependence. *Anal Sci* **1**: 29–32.
- Lizuka, T., Horie, K., Komiya, T., Maruyama, S., Hirata, T., Hidaka, H., and Windley, B. F. (2006) 4.2 Ga zircon xenocryst in an Acasta gneiss from northwestern Canada: Evidence for early continental crust. *Geology* **34**: 245–248.
- Llorca, J. (2004) Organic matter in meteorites. *Int Microbiol* **7**: 239–248.
- Llorca, J. (2005) Organic matter in comets and cometary dust. *Int Microbiol* **8**: 5–12.
- Love, S. G. and Brownlee, D. E. (1993) A direct measurement of the terrestrial mass accretion rate of cosmic dust. *Science* **262**: 550–553.

- Ma, C. and Eggleton, R. A. (1999) Cation exchange capacity of kaolinite. *Clay Clay Miner* **47**: 174–180.
- Mangold, N., Poulet, F., Mustard, J. F., Bibring, J.-P., Gondet, B., Langevin, Y., Ansan, V., Masson, Ph., Fassett, C., Head III, J. W., Hoffmann, H., and Neukum, G. (2007) Mineralogy of the Nili Fossae region with OMEGA/Mars Express data: 2. Aqueous alteration of the crust. *J Geophys Res* **112**: 1–25.
- Manhas, M. S., Hsieh, R. S., and Bose, A. K. (1970) Mass spectral studies. Part VII. Unusual fragmentation of some N-trifluoroacetyl amino-acid methyl esters. *J Chem Soc C* 116–119.
- Marshall, W. L. (1994) Hydrothermal synthesis of amino acids. *Geochim Cosmochim Acta* **58**: 2099–2106.
- Martin, H., Albarède, F., Claeys, P., Gargaud, M., Marty, B., Morbidelli, A., and Pinti, D. L. (2006). Building of a habitable planet. *Earth Moon Planets* **98**: 97–151.
- Mason, S. F. (1997) Extraterrestrial handedness. *Nature* **389**: 804.
- Matrajt, G., Pizzarello, S., Taylor, S., and Brownlee, D. (2004) Concentration and variability of the AIB amino acid in polar micrometeorites: Implications for the exogenous delivery of amino acids to the primitive Earth. *Meteorit Planet Sci* **39**: 1849–1858.
- McCullough, J. J. and Lemmon, R. M. (1974) The question of the possible asymmetric polymerization of aspartic acid on kaolinite. *J Mol Evol* **3**: 57–61.
- Merritt Jr., C. and Robertson, D. H. (1967) The analysis of proteins, peptides and amino acids by pyrolysis-gas chromatography and mass spectrometry. *J Gas Chromogr* **5**: 96–98.
- Meunier, A., Petit, S., Ehlmann, B. L., Dudoignon, P., Westall, F., Mas, A., Albani, A. E., and Ferrage, E. (2012) Magmatic precipitation as a possible origin of Noachian clays on Mars. *Nat Geosci* **5**: 739–743.
- Miller, S. L. (1953) A production of amino acids under possible primitive Earth conditions. *Science* **117**: 528–529.
- Miller, S. L. (1955) Production of some organic compounds under possible primitive Earth conditions. *J Am Chem Soc* **77**: 2351–2361.
- Miller, S. L. (1987) Which organic compounds could have occurred on the prebiotic Earth? *Cold Spring Harb Symp Quant Biol* **52**: 17–27.

- Miller, S. L. and Bada, J. L. (1988) Submarine hot springs and the origin of life. *Nature* **334**: 609–611.
- Miranda-Trevino, J. C. and Coles, C. A. (2003) Kaolinite properties, structure and influence of metal retention on pH. *Appl Clay Sci* **23**: 133–139.
- Mitra, R. P. and Rajagopalan, K. S. (1952) The electrochemical character of the clay mineral illite and its relation to that of muscovite. *J Soil Sci* **3**: 34–40.
- Mitterer, R. M. and Kriausakul, N. (1989) Calculation of amino acid racemization ages based on apparent parabolic kinetics. *Quaternary Sci Rev* **8**: 353–357.
- Mojzsis, S. J., Harrison, T. M., and Pidgeon, R. T. (2001) Oxygen-isotope evidence from ancient zircons for liquid water at the Earth's surface 4,300 Myr ago. *Nature* **409**: 178–181.
- Moorbath, S. (2005) Oldest rocks, earliest life, heaviest impacts, and the Hadean–Archaean transition. *Appl Geochem* **20**: 819–824.
- Morbidelli, A., Chambers, J., Lunine, J. I., Petit, J. M., Rrobert, F., Valsecchi, G. B., and Cyr, K. E. (2000) Source regions and timescales for the delivery of water to the Earth. *Meteorit Planet Sci* **35**: 1309–1320.
- Morris, R. V., Ruff, S. W., Gellert, R., Ming, D. W., Arvidson, R. E., Clark, B. C., Golden, D. C., Siebach, K., Klingelhöfer, G., Schröder, C., Fleischer, I., Yen, A. S., and Squyres, S. W. (2010) Identification of carbonate-rich outcrops on Mars by the Spirit Rover. *Science* **329**: 421–424.
- Morse, J. W. and Mackenzie, F. T. (1998) Hadean ocean carbonate geochemistry. *Aquat Geochem* **4**: 301–331.
- Morse, J. W. and Marion, G. M. (1999) The role of carbonates in the evolution of early Martian oceans. *Am J Sci* **299**: 738–761.
- Mustard, J. F. and Bell III, J. F. (1994) New composite reflectance spectra of Mars from 0.4 to 3.14 μm . *Geophys Res Lett* **21**: 353–356.
- Mustard, J. F., Murchie, S. L., Pelkey, S. M., Ehlmann, B. L., Milliken, R. E., Grant, J. A., Bibring, J.-P., Poulet, F., Bishop, J., Dobreá, E. N., and 26 other co-authors (2008) Hydrated silicate minerals on Mars observed by the Mars Reconnaissance Orbiter CRISM instrument. *Nature* **454**: 305–309.

- Naughton, J. J., Lewis, V. A., Hammond, D., and Nisetimoto, D. (1974) The chemistry of sublimates collected directly from lava fountains at Kilauea Volcano, Hawaii. *Geochim Cosmochim Acta* **38**: 1679–1690.
- Nelson, K. E., Levy, M., and Miller, S. L. (2000) Peptide nucleic acids rather than RNA may have been the first genetic molecule. *Proc Natl Acad Sci USA* **97**: 3868–3871.
- Nemchin, A. A. (2006) Re-evaluation of the origin and evolution of >4.2 Ga zircons from the Jack Hills metasedimentary rocks. *Earth Planet Sci Lett* **244**: 218–233.
- Nielsen, P. E. (1993) Peptide Nucleic Acid (PNA): A model structure for the primordial genetic material? *Orig Life Evol Biosph* **23**: 323–327.
- Nielsen, P. E. and Egholm, M. (1999) An introduction to peptide nucleic acid. *Curr Issues Mol Biol* **1**: 89–104.
- Nimmo, F. and Tanaka, K. (2005) Early crustal evolution of Mars. *Annu Rev Earth Planet Sci* **33**: 133–161.
- Nisbet, E. G. and Sleep, N. H. (2001) The habitat and nature of early life. *Nature* **409**: 1083–1091.
- Nishino, H., Kosaka, A., Hembury, G. A., Shitomi, H., Onuki, H., and Inoue, Y. (2001) Mechanism of pH-dependent photolysis of aliphatic amino acids and enantiomeric enrichment of racemic leucine by circularly polarized light. *Org Lett* **3**: 921–924.
- Noe Dobrea, E. Z., Poulet, F., and Malin, M. C. (2008) Correlations between hematite and sulfates in the chaotic terrain east of Valles Marineris. *Icarus* **193**: 516–534.
- Norden, B. (1977) Was photoresolution of amino acids the origin of optical activity in life? *Nature* **266**: 567–568.
- Ochiai, E. (1978) The evolution of the environment and its influence on the evolution of life. *Orig Life Evol Biosph* **9**: 81–91.
- Odom, I. E. (1984) Smectite clay minerals: Properties and uses. *Philos Trans R Soc Lond B Biol Sci* **311**: 391–409.
- Oró, J. (1960) Synthesis of adenine from ammonium cyanide. *Biochem Biophys Res Commun* **2**: 407–412.
- Oró, J. and Kimball, A. P. (1961) Synthesis of purines under possible primitive Earth conditions. I. Adenine from hydrogen cyanide. *Arch Biochem Biophys* **94**: 217–227.

- Oró, J. and Kimball, A. P. (1962) Synthesis of purines under possible primitive Earth conditions. II. Purine intermediates from hydrogen cyanide. *Arch Biochem Biophys* **96**: 293–313.
- Osterloo, M. M., Hamilton, V. E., Bandfield, J. L., Glotch, T. D., Baldrige, A. M., Christensen, P. R., Tornabene, L. L., and Anderson, F. S. (2008) Chloride-bearing materials in the southern highlands of Mars. *Science* **319**: 1651–1654.
- Ostwald, R., Adams, P. T., and Tolbert, B. M. (1952) Synthesis of several carbon-14 labeled DL-alanines. *J Am Chem Soc* **74**: 2425–2427.
- Owen, T. and Bar-Nun, A. (1995) Comets, impacts and atmospheres. *Icarus* **116**: 215–226.
- Paecht-Horowitz, M., Berger, J., and Katchalsky, A. (1970) Prebiotic synthesis of polypeptides by heterogeneous polycondensation of amino-acid adenylates. *Nature* **228**: 636–639.
- Palomba, E., Zinzi, A., Cloutis, E. A., D'Amore, M., Grassi, D., and Maturilli, A. (2009) Evidence for Mg-rich carbonates on Mars from a 3.9 μm absorption feature. *Icarus* **203**: 58–65.
- Pankonin, V., Churchwell, E., Watson, C., and Bieging, J. H. (2001) A methyl cyanide search for the earliest stages of massive protostars. *Astrophys J* **558**: 194–203.
- Parsons, I., Lee, M. R., and Smith, J. V. (1998) Biochemical evolution II: Origin of life in tubular microstructures on weathered feldspar surfaces. *Proc Natl Acad Sci USA* **95**: 15173–15176.
- Patterson, C. (1956) Age of meteorites and the earth. *Geochim Cosmochim Acta* **10**: 236–237.
- Pavlov, A. A. and Kasting, J. F. (2002) Mass-independent fractionation of sulfur isotopes in Archean sediments: Strong evidence for an anoxic Archean atmosphere. *Astrobiology* **2**: 27–41.
- Peretó, J. (2005) Controversies on the origin of life. *Int Microbiol* **8**: 23–31.
- Peretó, J., Bada, J. L., and Lazcano, A. (2009) Charles Darwin and the origin of life. *Orig Life Evol Biosph* **39**: 395–406.
- Perry, R. H., Wu, C., Nefliu, M., and Cooks, R. G. (2007) Serine sublimates with spontaneous chiral amplification. *Chem Commun* **14**: 1071–1073.

- Peter, M. E. and Ramasamy, P. (2010) Growth of gamma glycine crystal and its characterisation. *Spectrochim Acta A* **75**: 1417–1421.
- Pinti, D. L. (2005) The Origin and Evolution of the Oceans. In: M. Gargaud, B. Barbier, H. Martin, and J. Reisse (eds.), *Lectures in Astrobiology*, Vol. I. Springer, Berlin, pp 83–112.
- Pizzarello, S. and Cronin, J. R. (2000) Non-racemic amino acids in the Murray and Murchison meteorites. *Geochim Cosmochim Acta* **64**: 329–338.
- Pizzarello, S., Huang, Y., and Alexandre, M. R. (2008) Molecular asymmetry in extraterrestrial chemistry: Insights from a pristine meteorite. *Proc Natl Acad Sci USA* **105**: 3700–3704.
- Pizzarello, S. and Shock, E. (2010) The organic composition of carbonaceous meteorites: The evolutionary story ahead of biochemistry. *Cold Spring Harb Perspect Biol*, a002105.
- Pizzarello, S., Schrader, D. L., Monroea, A. A., and Lauretta, D. S. (2012) Large enantiomeric excesses in primitive meteorites and the diverse effects of water in cosmochemical evolution. *Proc Natl Acad Sci USA* **24**: 11949–11954.
- Pizzarello, S., Zolensky, M., and Turk, K. A. (2003) Nonracemic isovaline in the Murchison meteorite: Chiral distribution and mineral association. *Geochim Cosmochim Acta* **67**: 1589–1595.
- Plankensteiner, K. and Rode, B. M. (2005) Stereoselective differentiation in the salt-induced peptide formation reaction and its relevance for the origin of life. *Peptides* **26**: 535–541.
- Plankensteiner, K., Righi, A., Rode, B. M., Gargallo, R., Jaumot, J., and Tauler, R. (2004) Indications towards a stereoselectivity of the salt-induced peptide formation reaction. *Inorg Chim Acta* **357**: 649–656.
- Pollack, J. B., Kasting, J. F., Richardson, S. M., and Poliakov, K. (1987) The case for a wet, warm climate on early Mars. *Icarus* **71**: 203–224.
- Pollock, G. E., Cheng, C-N., Cronin, S. E., and Kvenvolden, K. A. (1975) Stereoisomers of isovaline in the Murchison meteorite. *Geochim Cosmochim Acta* **39**: 1571–1573.
- Ponnamperna, C., Shimoyama, A., and Friebele, E. (1982) Clay and the origin of life. *Orig Life Evol Biosph* **12**: 9–40.
- Pooga, M., Land, T., Bartfai, T., and Langel, Ü. (2001) PNA oligomers as tools for specific modulation of gene expression. *Biomol Eng* **17**: 183–192.

- Poulet, F., Bibring, J.-P., Mustard, J. F., Gendrin, A., Mangold, N., Langevin, Y., Arvidson, R. E., Gondet, B., Gomez, C., and the Omega Team (2005) Phyllosilicates on Mars and implications for early martian climate. *Nature* **438**: 623–627.
- Poulet, F., Mangold, N., Loizeau, D., Bibring, J.-P., Langevin, Y., Michalski, J., and Gondet, B. (2008) Abundance of minerals in the phyllosilicate-rich units on Mars. *Astron Astrophys* **487**: L41–L44.
- Powner, M. W., Gerland, B., and Sutherland, J. D. (2009) Synthesis of activated pyrimidine ribonucleotides in prebiotically plausible conditions. *Nature* **459**: 239–242.
- Ratcliff Jr., M. A., Medley, E. E., and Simmonds, P. G. (1974) Pyrolysis of amino acids. Mechanistic considerations. *J Org Chem* **39**: 1481–1490.
- Raymond, S. N., O'Brien, D. P., Morbidelli, A., and Kaib, N. A. (2009) Building the terrestrial planets: Constrained accretion in the inner solar system. *Icarus* **203**: 644–662.
- Remko, M. and Rode, B. M. (2001) Catalyzed peptide bond formation in the gas phase. *Phys Chem Chem Phys* **3**: 4667–4673.
- Remko, M. and Rode, B. M. (2004) Catalyzed peptide bond formation in the gas phase. Role of bivalent cations and water in formation of 2-aminoacetamide from ammonia and glycine and in dimerization of glycine. *Struct Chem* **15**: 223–232.
- Ricardo, A., Carrigan, M. A., Olcott, A. N., and Benner, S. A. (2004) Borate minerals stabilize ribose. *Science* **303**: 196.
- Rieder, R., Economou, T., Waenke, H., Turkevich, A., Crisp, J., Brueckner, J., Dreibus, G., and McSween Jr., H. Y. (1997) The chemical composition of Martian soil and rocks returned by the mobile alpha proton X-ray spectrometer, preliminary results from the X-ray mode. *Science* **278**: 1771–1774.
- Righi, D. and Meunier, A. (1995) Origin of clays by rock weathering and soil formation. In: B. Velde (ed.), *Origin and mineralogy of clays*. Springer, Berlin, pp 43–161.
- Rode, B. M. (1999) Peptides and the origin of life. *Peptides* **20**: 773–786.
- Rode, B. M. and Schwendinger, M. G. (1990) Copper-catalyzed amino acid condensation in water – A simple possible way of prebiotic peptide formation. *Orig Life Evol Biosph* **20**: 401–410.

- Rubey, W. W. (1951) Geologic history of sea water: An attempt to state the problem. *Bull Geol Soc Am* **62**: 1111–11484.
- Russell, M. J. and Hall, A. J. (1997) The emergence of life from iron monosulphide bubbles at a submarine hydrothermal redox and pH front. *J Geol Soc London* **154**: 377–402.
- Sagan, C. and Khare, B. N. (1971) Long-wavelength ultraviolet photoproduction of amino acids on the primitive Earth. *Science* **173**: 417–420.
- Saladino, R., Crestini, C., Costanzo, G., and Di Mauro, E. (2005) On the prebiotic synthesis of nucleobases, nucleotides, oligonucleotides, Pre-RNA and Pre-DNA molecules. *Top Curr Chem* **259**: 29–68.
- Saladino, R., Neri, V., Crestini, C., Costanzo, G., Graciotti, M., and Di Mauro, E. (2010) The role of the formamide/zirconia system in the synthesis of nucleobases and biogenic carboxylic acid derivatives. *J Mol Evol* **71**: 100–110.
- Saladino, R., Crestini, C., Costanzo, G., Negri, R., and Di Mauro, E. (2001) A possible prebiotic synthesis of purine, adenine, cytosine, and 4(3H)-pyrimidinone from formamide: Implications for the origin of life. *Bioorg Med Chem* **9**: 1249–1253.
- Sandars, P. G. (2003) A toy model for the generation of homochirality during polymerization. *Orig Life Evol Biosph* **33**: 575–87.
- Scappini, F., Casadei, F., Zamboni, R., Franchi, M., Gallori, E., and Monti, S. (2004) Protective effect of clay minerals on adsorbed nucleic acid against UV radiation: Possible role in the origin of life. *Int J Astrobiol* **3**: 17–19.
- Schlesinger, G. and Miller, S. L. (1983) Prebiotic synthesis in atmospheres containing CH₄, CO, and CO₂ I. Amino acids. *J Mol Evol* **19**: 376–382.
- Schmidt, J. G., Nielsen, P. E., and Orgel, L. E. (1997) Enantiomeric cross-inhibition in the synthesis of oligonucleotides on a nonchiral template. *J Am Chem Soc* **119**: 1494–1495.
- Schroeder, R. A. and Bada, J. L. (1976) Review of the geochemical applications of the amino acid racemization reaction. *Earth Sci Rev* **12**: 347–391.
- Schurig, V. (1984) Gas chromatographic separation of enantiomers on optically active metal-complex-free stationary phases. *Angew Chem* **23**: 747–830.
- Schwendinger, M. G. and Rode, B. M. (1989) Possible role of copper and sodium chloride in prebiotic evolution of peptides. *Anal Sci* **5**: 411–414.

- Schwendinger, M. G. and Rode, B. M. (1991) Salt-induced formation of mixed peptides under possible prebiotic conditions. *Inorg Chim Acta* **186**: 247–251.
- Shanker, U., Bhushan B., Bhattacharjee, G., and Kamaluddin (2012) Oligomerization of glycine and alanine catalyzed by iron oxides: Implications for prebiotic chemistry. *Orig Life Evol Biosph* **42**: 31–45.
- Shapiro, R. (2000) A replicator was not involved in the origin of life. *IUBMB Life* **49**: 173–176.
- Shapiro, R. (2006) Small molecule interactions were central to the origin of life. *Q Rev Biol* **81**: 105–126.
- Shapiro, R. (2007) A simple origin of life. *Sci Am* 46–54.
- Shaw, G. H. (2008) Earth's atmosphere – Hadean to early Proterozoic. *Chem Erde–Geochem* **68**: 235–264.
- Segré, D., Ben-Eli, D., and Lancet, D. (2000) Compositional genomes: Prebiotic information transfer in mutually catalytic noncovalent assemblies. *Proc Natl Acad Sci USA* **97**: 4112–4117.
- Shimoyama, A. and Ogasawara, R. (2002) Dipeptides and diketopiperazines in the Yamato-791198 and Murchison carbonaceous chondrites. *Orig Life Evol Biosph* **32**: 165–179.
- Simoneit, B. R. T. (2004) Prebiotic organic synthesis under hydrothermal conditions: An overview. *Adv Space Res* **33**: 88–94.
- Smith, G. G. and Reddy, G. V. (1989) Effects of the side chain on the racemization of amino acids in aqueous solution. *J Org Chem* **54**: 4529–4535.
- Smith, G. G., Williams, K. M., and Wonnacott, D. M. (1978). Factors affecting the rate of racemization of amino acids and their significance to geochronology. *J Org Chem* **43**: 1–5.
- Smith, J. V. (1998a) Atmospheric weathering and silica-coated feldspar: Analogy with zeolite molecular sieves, granite weathering, soil formation, ornamental slabs, and ceramics. *Proc Natl Acad Sci USA* **95**: 3366–3369.
- Smith, J. V. (1998b) Biochemical evolution. I. Polymerization on internal, organophilic silica surfaces of dealuminated zeolites and feldspars. *Proc Natl Acad Sci USA* **95**: 3370–3375.

- Soai, K., Niwa, S., and Hori, H. (1990) Asymmetric self-catalytic reaction. Self-production of chiral 1-(3-Pyridyl)alkanols as chiral self-catalysts in the enantioselective addition of dialkylzinc reagents to pyridine-3-carbaldehyde. *Chem Commun* 982–983.
- Soai, K., Shibata, T., Morioka, H., and Choji, K. (1995) Asymmetric autocatalysis and amplification of enantiomeric excess of a chiral molecule. *Nature* **378**: 767–768.
- Sohn, M. and Ho, C.-T. (1995) Ammonia generation during thermal degradation of amino acids. *J Agr Food Chem* **43**: 3001–3003.
- Stetter, K. O. (1998) Hyperthermophiles and their possible role as ancestors of modern life. In: A. Brack (ed.), *The molecular origins of life. Assembling Pieces of the Puzzle*. Cambridge University Press, Cambridge, pp 315–335.
- Strasdeit, H. (2010) Chemical evolution and early Earth's and Mars' environmental conditions. *Palaeodiversity* **3** (supplement): 107–116.
- Strydom, C. A. and Potgieter J. H. (1999) Dehydration behaviour of a natural gypsum and a phosphogypsum during milling. *Thermochim Acta* **332**: 89–96.
- Swartzen-Allen, S. L. and Matijevic, E. (1974) Surface and colloid chemistry of clays. *Chem Rev* **74**: 385–400.
- Tanaka, K. L. (1986) The stratigraphy of Mars. *J Geophys Res* **91**: 139–158.
- Tranter, G. E. (1985) Parity violation energy differences of chiral minerals and the origin of biomolecular homochirality. *Nature* **318**: 172–173.
- Valley, J. W., Cavosie, A. J., Fu, B., Peck, W. H., and Wilde, S. A. (2006) Comment on “Heterogeneous Hadean hafnium: Evidence of continental crust at 4.4 to 4.5 Ga”. *Science* **312**: 1139.
- Viedma, C., Ortiz, J. E., de Torres, T., and Cintas, P. (2012) Enantioenrichment in sublimed amino acid mixtures. *Chem Commun* **48**: 3623–3625.
- Wächtershäuser, G. (1988) Before enzymes and templates: Theory of surface metabolism. *Microbiol Rev* **52**: 452–484.
- Wächtershäuser, G. (1990) Evolution of the first metabolic cycles. *Proc Natl Acad Sci USA* **87**: 200–204.
- Wächtershäuser, G. (1993) The cradle chemistry of life: On the origin of natural products in a pyrite-pulled chemoautotrophic origin of life. *Pure Appl Chem* **65**: 1343–1348.

- Wang, A., Freeman, J. J., Jolliff, B. L., and Chou, I-M. (2006) Sulfates on Mars: A systematic Raman spectroscopic study of hydration states of magnesium sulfates. *Geochim Cosmochim Acta* **70**: 6118–6135.
- Watson, E. B. and Harrison, T. M. (2005) Zircon thermometer reveals minimum melting conditions on earliest Earth. *Science* **308**: 841–844.
- Wilde, S. A., Valley, J. W., Peck, W. H., and Graham, C. M. (2001) Evidence from detrital zircons for the existence of continental crust and oceans on the Earth 4.4 Gyr ago. *Nature* **409**: 175–178.
- Wolosker, H., Dumin, E., Balan, L., and Foltyn, V. N. (2008) D-amino acids in the brain: D-serine in neurotransmission and neurodegeneration. *FEBS J* **275**: 3514–3526.
- Wray, J. J., Squyres, S. W., Roach, L. H., Bishop, J. L., Mustard, J. F., and Noe Dobrea, E. Z. (2010) Identification of the Ca-sulfate bassanite in Mawrth Vallis, Mars. *Icarus* **209**: 416–421.
- Yamagishi, A. (1987) Optical resolution and asymmetric syntheses by use of adsorption on clay minerals. *J Coord Chem* **16**: 131–211.
- Yoshino, D., Hayatsu, R., and Anders, E. (1971) Origin of organic matter in early solar system-III. Amino acids: Catalytic synthesis. *Geochim Cosmochim Acta* **315**: 927–938.
- Yusenko, K., Fox, S., Guni, P., and Strasdeit, H. (2008) Model studies on the formation and reactions of solid glycine complexes at the coasts of a primordial salty ocean. *Z Anorg Allg Chem* **634**: 2347–2354.
- Zaia, D. A. M., Zaia, C. T. B. V., and Santana, H. De. (2008) Which amino acids should be used in prebiotic chemistry studies? *Orig Life Evol Biosph* **38**: 469–488.
- Zamaraev, K. I., Romannikov, V. N., Salganik, R. I., Wlassoff, W. A., and Khramtsov, V. V. (1997) Modelling of the prebiotic synthesis of oligopeptides: Silicate catalysts help to overcome the critical stage. *Orig Life Evol Biosph* **27**: 325–337.

6 Appendix

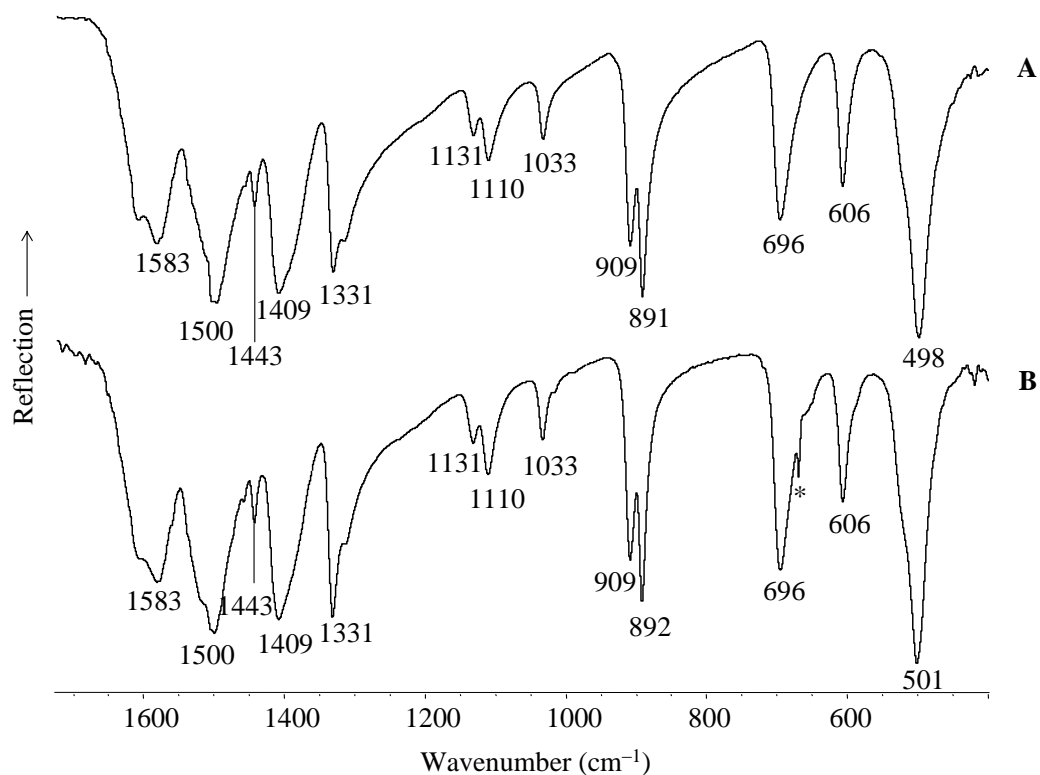


Fig. A-1: Infrared spectra of (A) α-glycine (reference) and (B) residue obtained by heating α-glycine at 160 °C for two days. *Signal due to incomplete background correction.

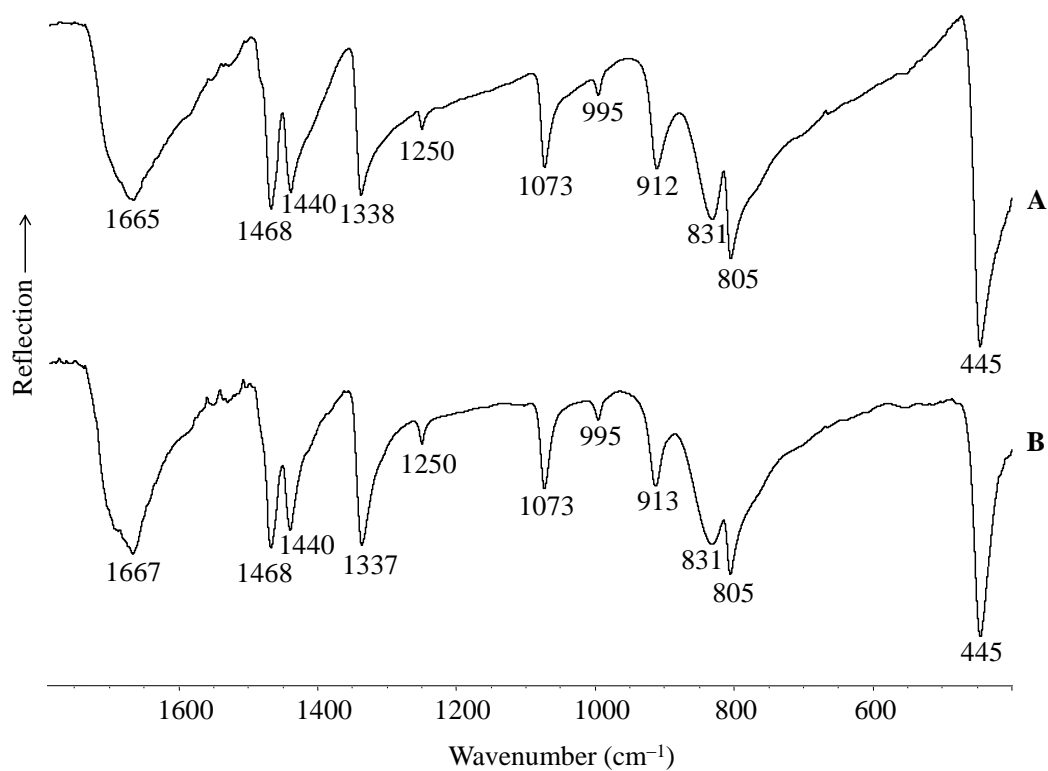


Fig. A-2: Infrared spectra of (A) DKP (reference) and (B) Sublimate obtained after heating α-glycine at 270 °C for two days.

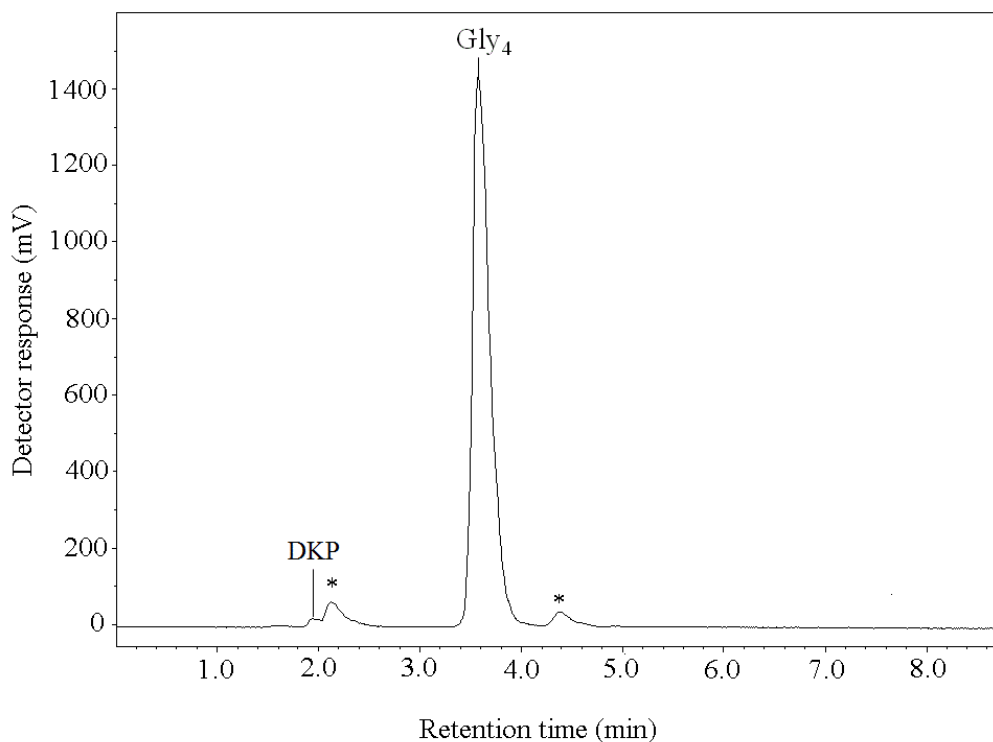


Fig. A-3: HPLC analysis of the water extract of the residue obtained after heating tetraglycine at 200 °C for two days. * Unidentified reaction products.

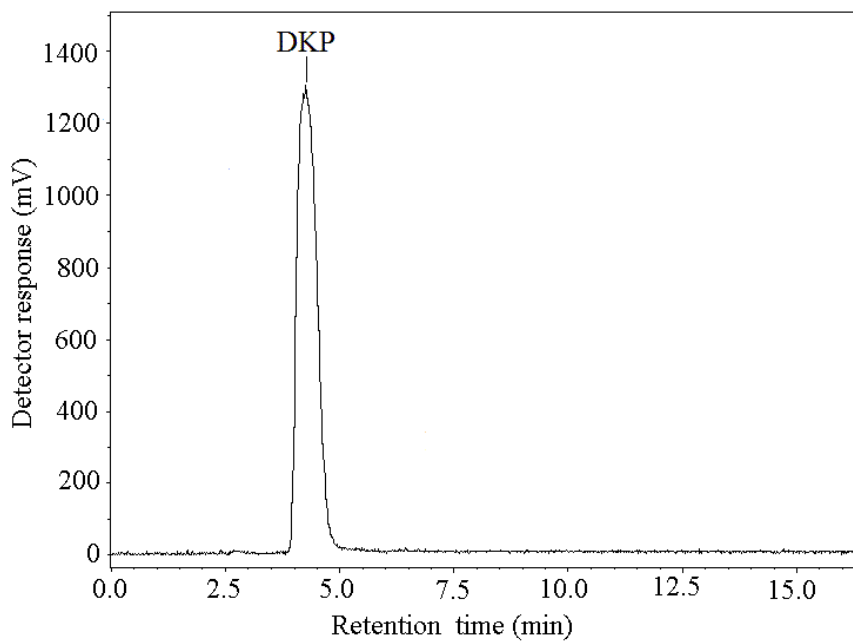


Fig. A-4: HPLC analysis of the water extract of the sublimate obtained after heating linear diglycine at 200 °C for two days.

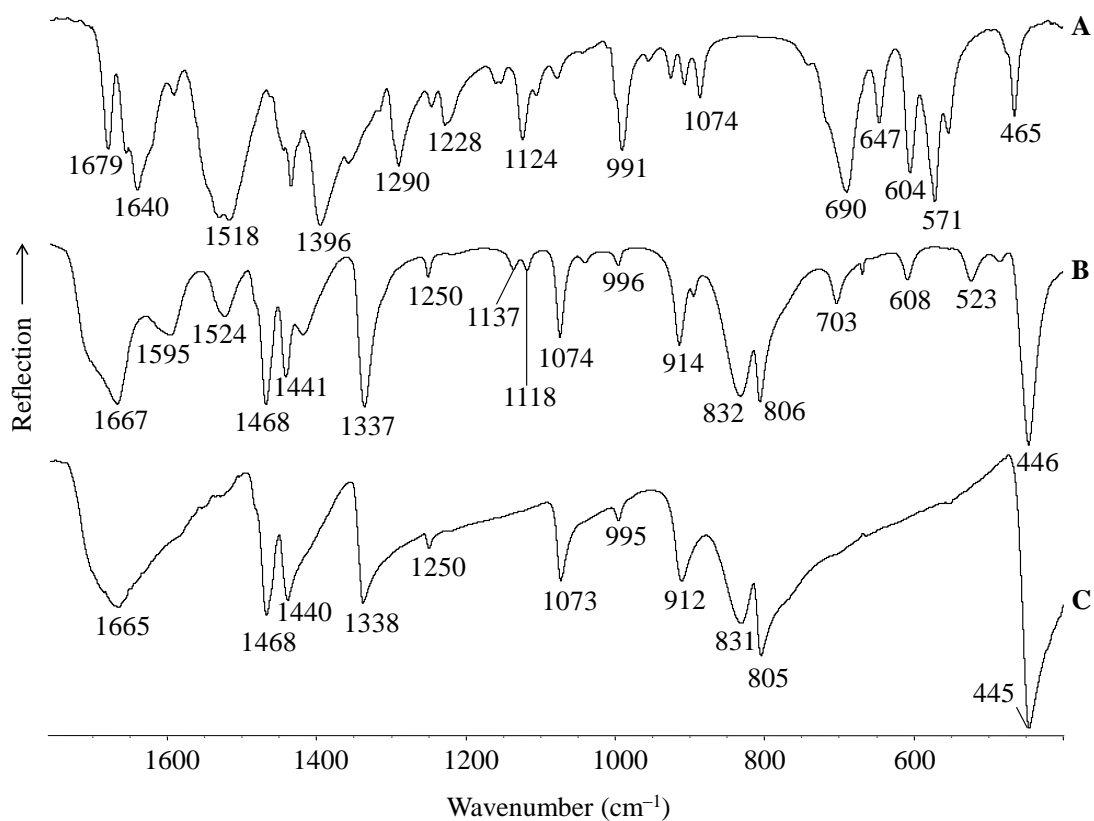


Fig. A-5: Infrared spectra of (A) the sublimate obtained after heating triglycine at 200 °C for two days, (B) triglycine (reference), and (C) DKP (reference).

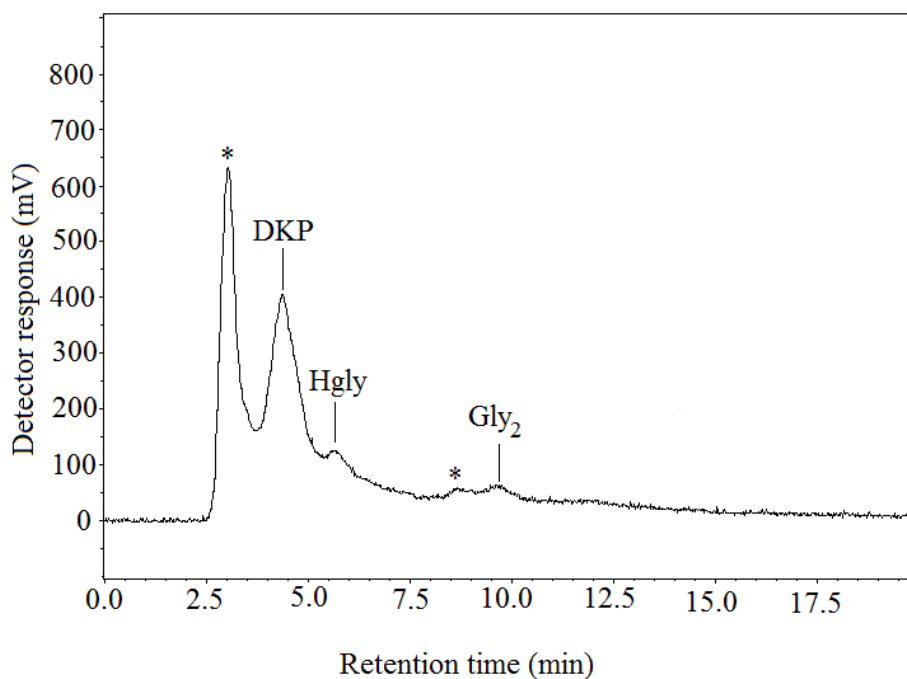


Fig. A-6: HPLC analysis of the water extract obtained after the hydrolysis of the thermomelanoid in water at 100 °C for 10 days. * Unidentified reaction products.

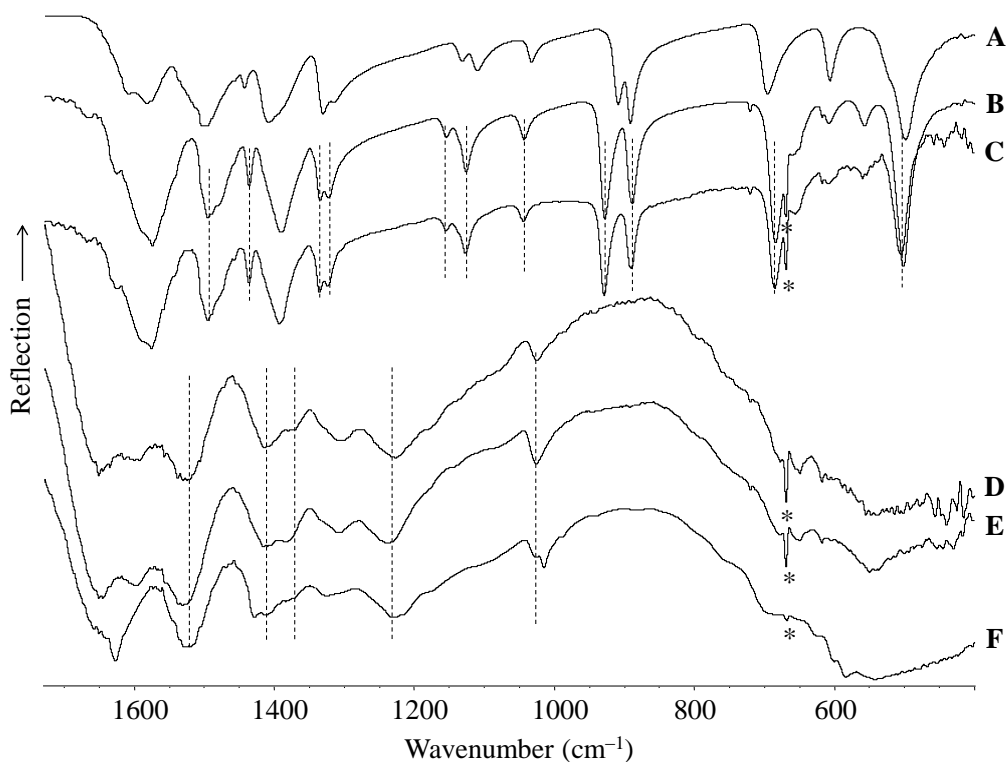


Fig. A-7: Infrared spectra of (A) α -glycine (reference), (B) NaCl-Hgly, (C) NaCl-KCl-Hgly, (D) washed NaCl-Hgly residue obtained after seven days at 200 °C, (E) washed NaCl-KCl-Hgly residue obtained after seven days at 200 °C, and (F) α -glycine residue formed at 200 °C after two days (thermo-melanoid). * Signal due to incomplete background correction. Dashed lines mark identical band positions.

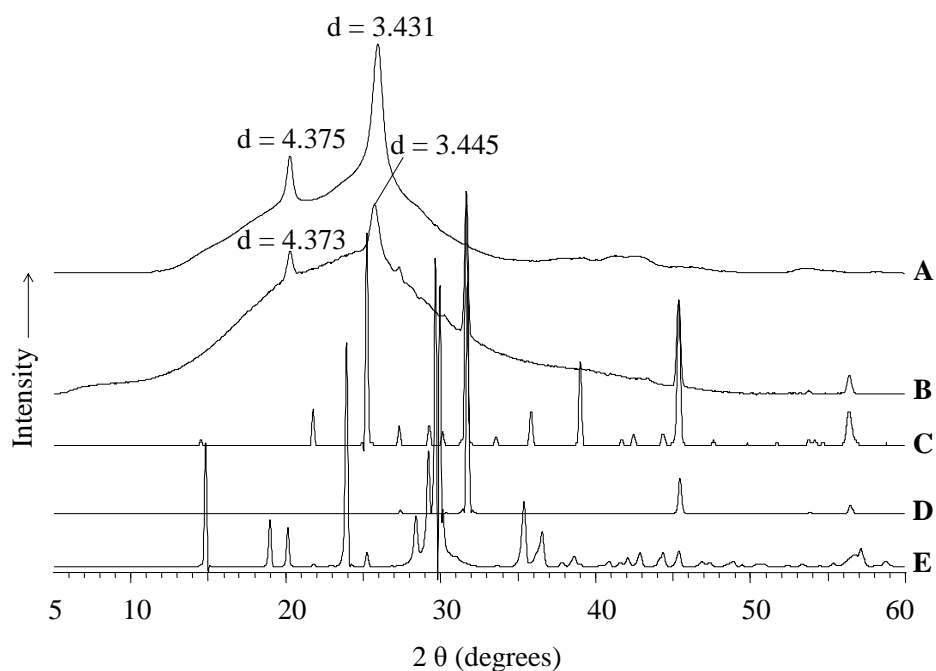


Fig. A-8: Background subtracted powder X-ray diffractogram of (A) α -glycine residue obtained after two days at 200 °C (thermo-melanoid), (B) NaCl-Hgly residue after seven days at 200 °C, (C) NaCl-Hgly, (D) NaCl, and (E) α -glycine (reference). The d values are given in Å.

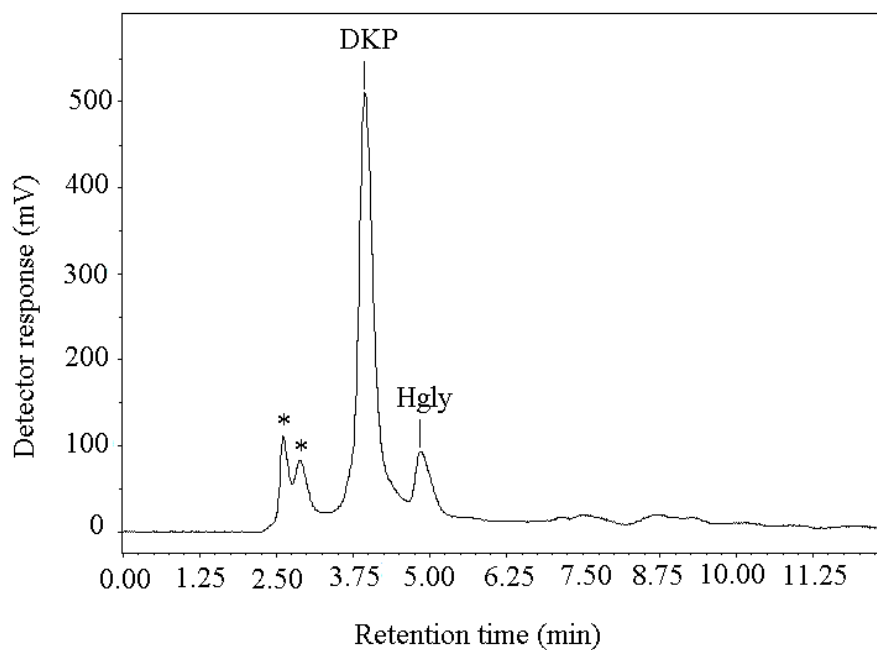


Fig. A-9: HPLC analysis of the water extract of the residue obtained after heating $\text{CaSO}_4 \cdot 2\text{H}_2\text{O}$ -Hgly at 200 °C for seven days. * Unidentified reaction products.

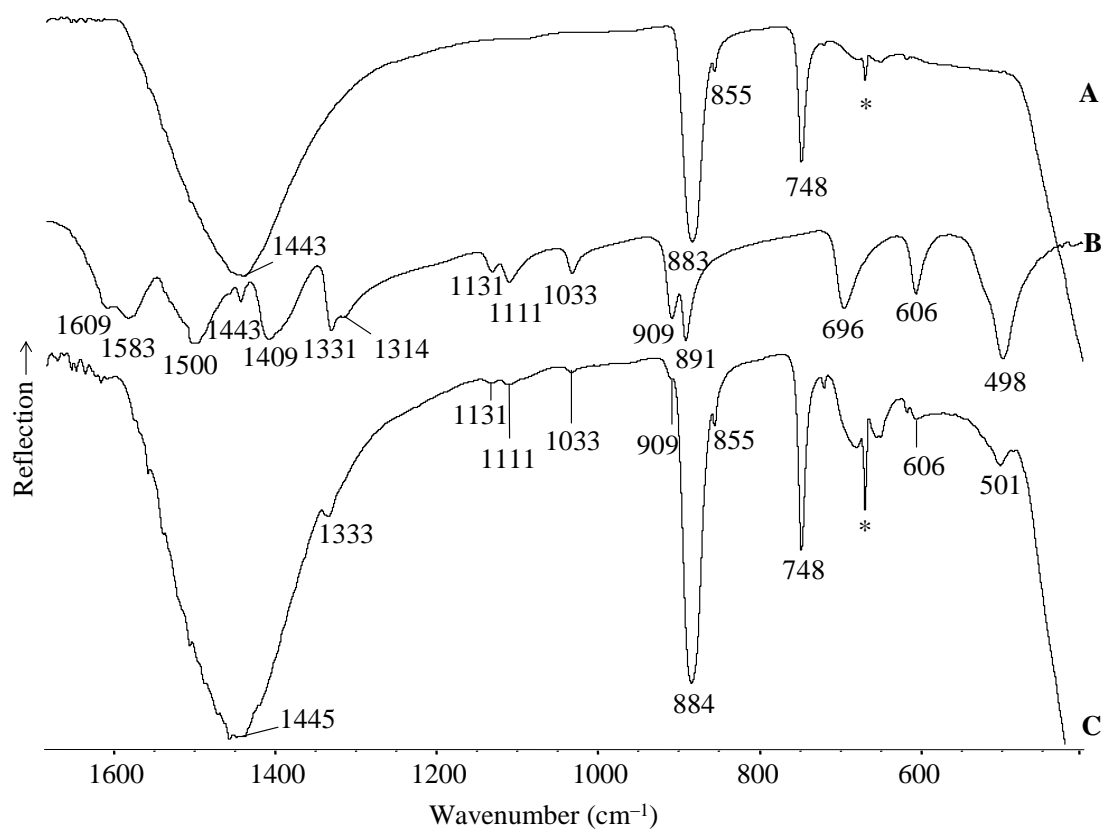


Fig. A-10: Infrared spectra of (A) MgCO_3 , (B) α -glycine (reference), and (C) MgCO_3 -Hgly mixture (for preparation: see 4.5.1). *Signal due to incomplete background correction.

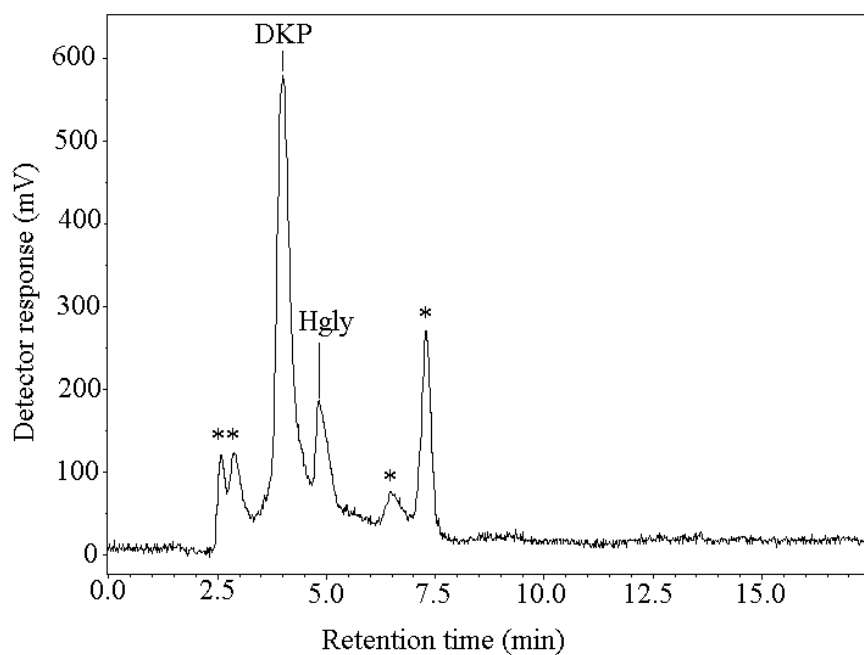


Fig. A-11: HPLC analysis of the water extract of the residue obtained after heating the MgCO_3 -Hgly mixture at 200°C for seven days. * Unidentified reaction products.

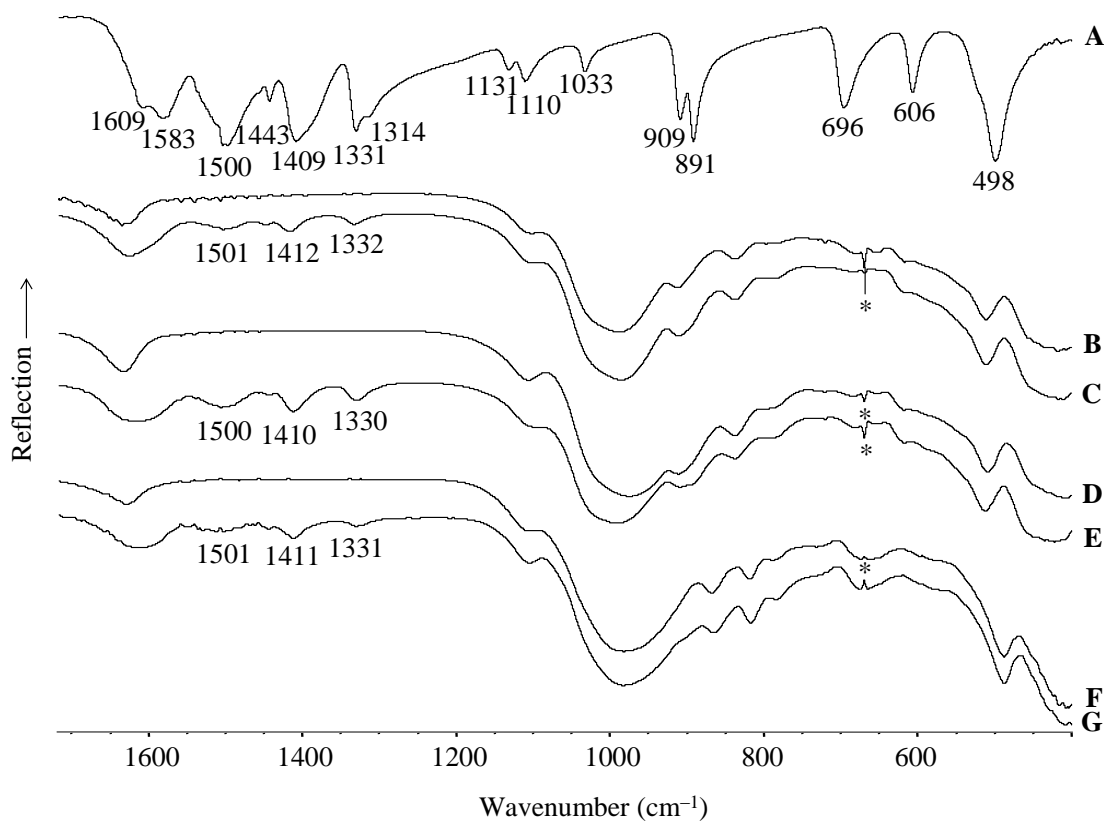


Fig. A-12: Infrared spectra of (A) α -glycine (reference), (B) Ca-montmorillonite, (C) Ca-montmorillonite-Hgly, (D) Na-montmorillonite, (E) Na-montmorillonite-Hgly, (F) Nontronite, and (G) Nontronite-Hgly. *Signal due to incomplete background correction.

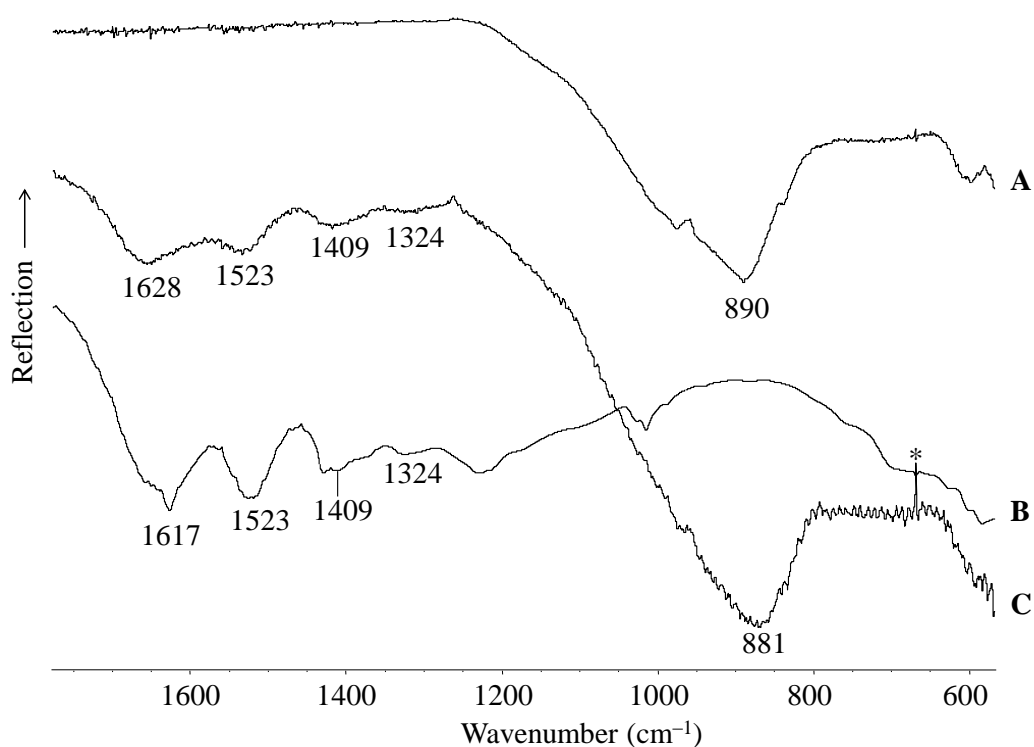


Fig. A-13: Infrared spectra of (A) basaltic sand, (B) α -glycine residue obtained at 200 °C for two days (thermo-melanoid), and (C) basaltic sand-Hgly at 200 °C for two days. *Signal due to incomplete background correction.

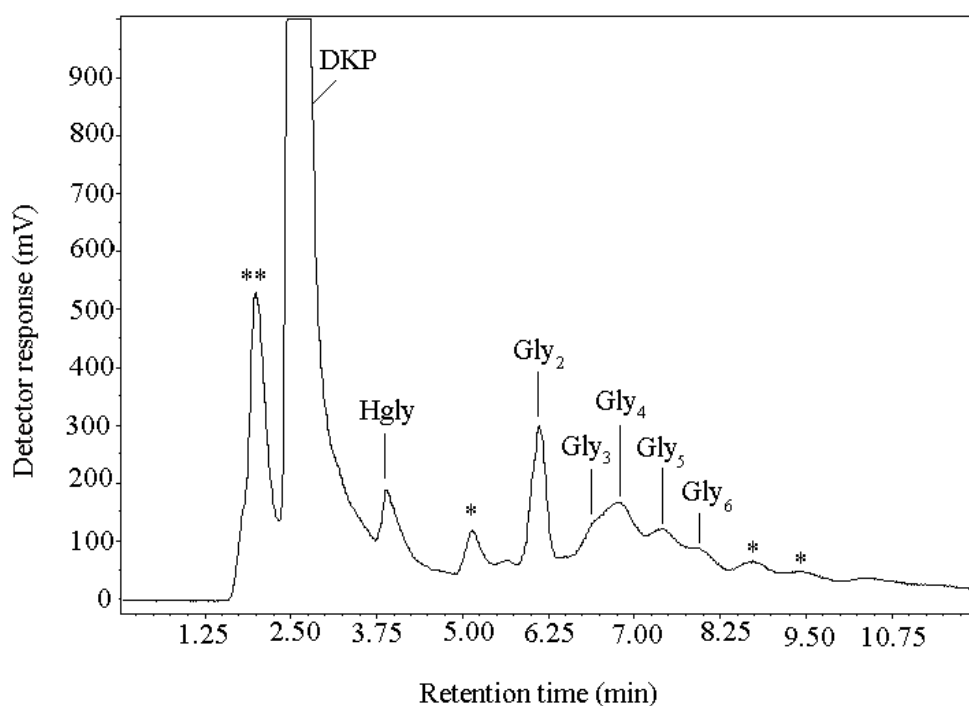


Fig. A-14: HPLC analysis of the water extract of the residue obtained after heating P-MRS-Hgly at 200 °C for two days. *Unidentified decomposition products. ** Solvent peak.

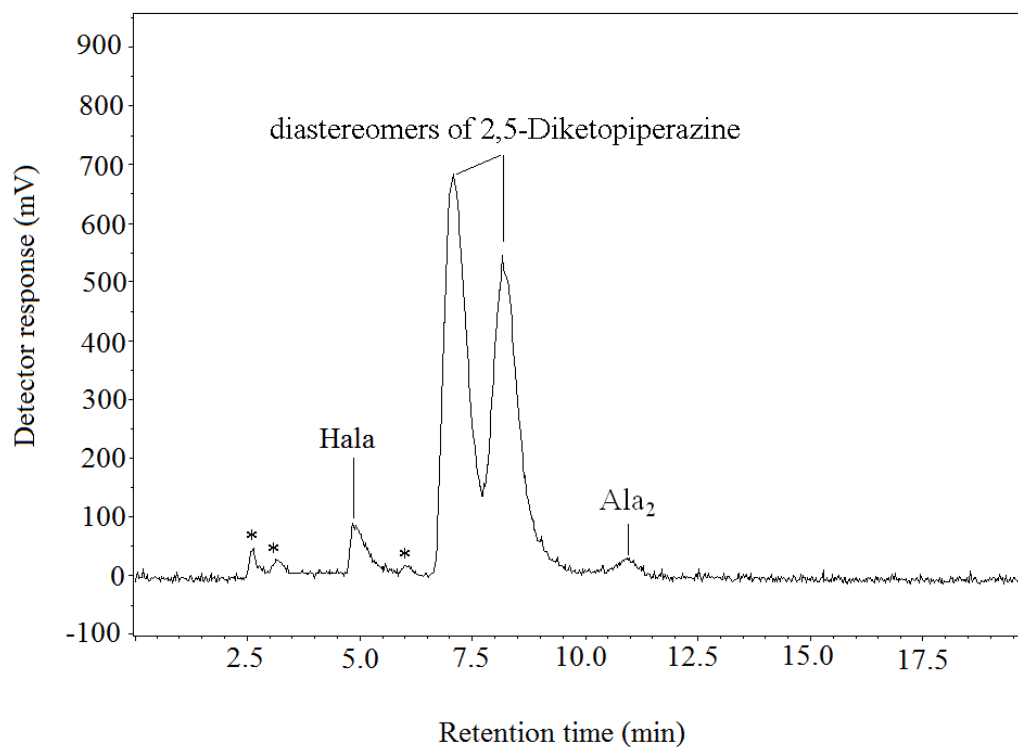


Fig. A-15: HPLC analysis of the water extract of the residue obtained after heating alanine-loaded Ca-montmorillonite at 200 °C for two days. * Unidentified decomposition products.

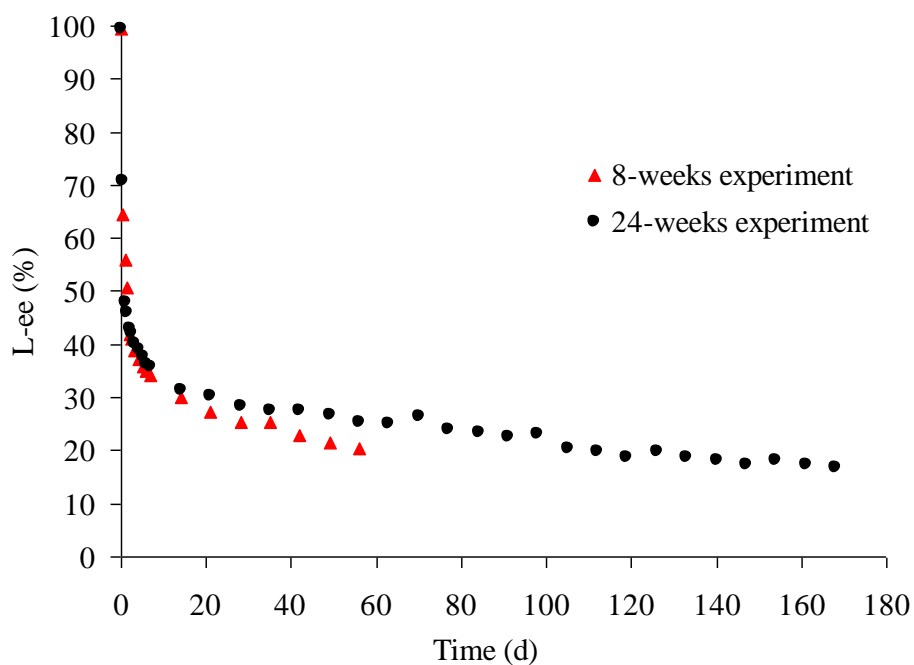


Fig. A-16: Development of the L-ee of alanine intercalated in Ca-montmorillonite during 8 and 24 weeks of heating at 200 °C. The starting L-ee was 100 %.

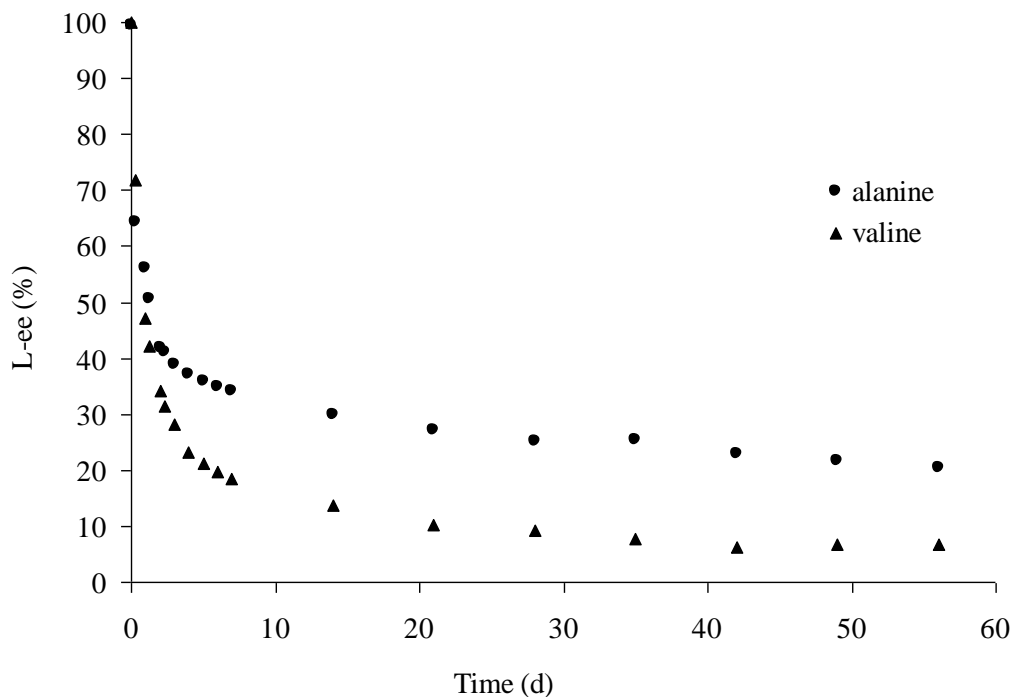


Fig. A-17: Development of the L-ee of alanine and valine separately intercalated in Ca-montmorillonite during eight weeks of heating at 200 °C. The starting L-ee values were 100 %.

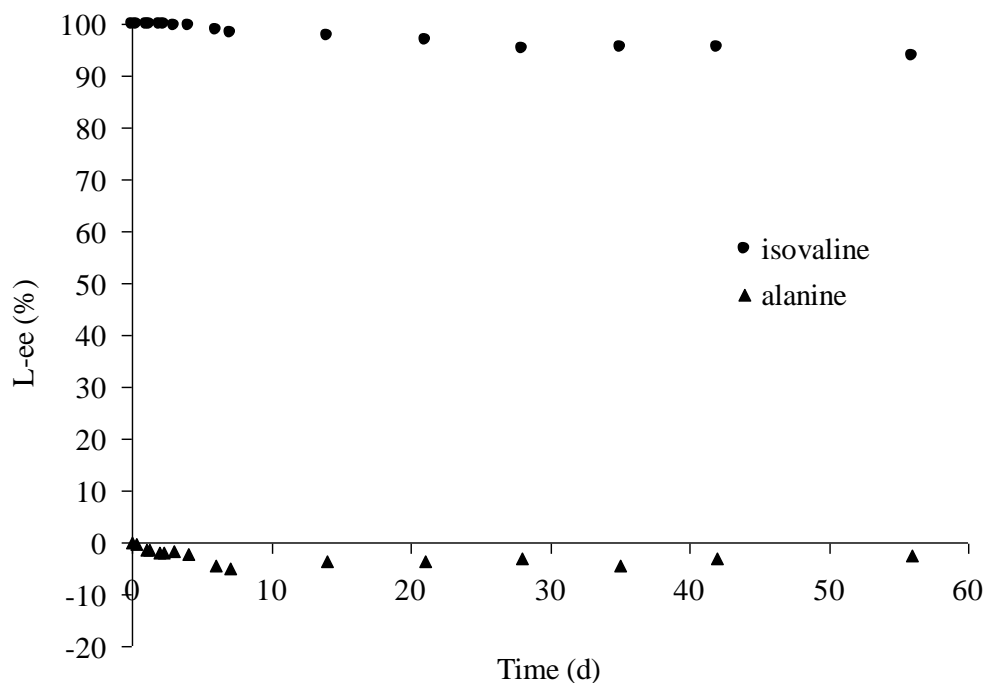


Fig. A-18: Development of the L-ee values of alanine and isovaline jointly intercalated in Ca-montmorillonite during eight weeks of heating at 200 °C. The starting L-ee values were 0 % (racemic) for alanine and 100 % for isovaline.

Tab. A-1: Comparison of the d-spacings of the basaltic sand with those of forsterite and fayalite.

Basaltic sand	Forsterite (literature*)	Fayalite the (literature**)	Difference to forsterite	Difference to fayalite
5.119	5.097	5.235	-0.022	0.116
3.895	3.878	3.969	-0.017	0.074
3.735	3.720	3.778	-0.015	0.043
3.491	3.494	3.541	0.003	0.050
–	3.476	3.063	–	–
2.999	3.005	3.043	0.006	0.044
2.996	2.989	2.826	-0.007	-0.170
2.776	2.764	2.631	-0.012	-0.145
2.521	2.509	2.618	-0.012	0.097
2.467	2.455	2.563	-0.012	0.096
2.359	2.344	2.405	-0.015	0.046
2.322	2.314	2.348	-0.008	0.026
2.275	2.266	2.310	-0.009	0.035
2.258	2.246	2.300	-0.012	0.042
2.164	2.158	2.190	-0.006	0.026
2.037	2.029	2.071	-0.008	0.034
1.949	1.947	2.059	-0.002	0.110
1.944	1.939	1.984	-0.005	0.040
1.883	1.874	1.921	-0.009	0.038
1.795	1.788	1.831	-0.007	0.038
1.750	1.747	1.777	-0.003	0.110
1.736	1.738	1.771	0.002	0.035
1.732	1.729	1.761	-0.003	0.029
1.672	1.669	1.702	-0.003	0.030
1.638	1.634	1.677	-0.004	0.039
1.595	1.600	–	0.005	–
1.591	1.587	–	-0.004	–
1.570	1.565	1.587	-0.005	0.017
1.520	1.514	1.540	-0.006	0.020
1.518	1.513	1.535	-0.005	0.017

1.505	1.502	1.532	-0.003	0.027
1.501	1.498	1.530	-0.003	0.029
1.485	1.494	1.522	0.009	0.037
1.468	1.477	1.514	0.009	0.046
1.464	1.466	1.489	0.002	0.025
1.396	1.396	1.419	-0.000	0.023
1.393	1.392	1.429	-0.001	0.036
1.389	1.387	1.407	-0.002	0.018
1.351	1.350	1.371	-0.001	0.020
1.348	1.345	1.369	-0.003	0.021
1.299	1.310	1.335	0.011	0.036
1.296	1.293	1.323	-0.003	0.027
1.253	1.254	1.282	0.001	0.029
1.249	1.248	-	-0.001	-

* <http://rruff.geo.arizona.edu/AMS/download.php?id=00598.txt&down=dif>

** <http://rruff.geo.arizona.edu/AMS/download.php?id=00618.txt&down=dif>

7 Curriculum Vitae

Punam Dalai

Institute of Chemistry, University of Hohenheim

Garbenstr 30, D-70599 Stuttgart, Germany

Email: pdalai@uni-hohenheim.de

Nationality: Indian

Sex: Female

Date of Birth: 21st May 1982

Marital status: Single

Education

2004–2006 MSc (Chemistry), Indian Institute of Technology (IIT), Roorkee, India

2000–2004 BSc–BEd (Botany, Zoology, Chemistry, and Education), Regional Institute of Education (RIE), Ajmer, India

Teaching experience

2008–present Teaching Assistant in the laboratory of Prof. H. Strasdeit, Institute of Chemistry, University of Hohenheim, Stuttgart, Germany

2004 Taught Chemistry and Biology to intermediate students, Ajmer, India

Research activities

04/2008–present Doctoral work at the University of Hohenheim, Stuttgart, Germany, under the supervision of Prof. H. Strasdeit

Thesis title:

“Thermal behavior of amino acids in inorganic matrices: Relevance for chemical evolution”

06/2007–07/2007 Worked under the supervision of Prof. P. Poddar at National Chemical Laboratory (NCL) Pune, India

12/2005–05/2006 MSc thesis under the supervision of Prof. A. K. Jain at Indian Institute of Technology (IIT), Roorkee, India

Project title:

“Electroanalytical investigation of Ca²⁺ selective sensors based

05/2005–07/2005 on p-isopropylcalix[6]arene”
Summer project under the supervision of Prof. Y. D. Vankar at
Indian Institute of Technology (IIT), Kanpur, India
Project title:
“Synthesis of novel sugar hybrid molecules”

Technical standings

IR, UV/Vis/NIR, GC-MS/FID, powder X-ray diffractometry,
HPLC, TGA
Undergone a MALDI-TOF/TOF-MS training at the Life
Science Centre, University of Hohenheim, Germany (2008)

Awards

Best Poster Award at the 8th Workshop of the European Astrobiology Network Association (EANA), 2008.

Merit-cum-means scholarship granted by Indian Institute of Technology (IIT), Roorkee, for MSc studies (08/2004–05/2006).

Merit-cum-means scholarship granted by NCERT, New Delhi, for BSc–BEEd studies in Regional Institute of Education, Ajmer (08/2000–05/2004).



Anlage 2 zur Promotionsordnung der Universität Hohenheim zum Dr. rer. nat.

Eidesstattliche Versicherung gemäß § 7 Absatz 7 der Promotionsordnung der Universität Hohenheim zum Dr. rer. nat.

1. Bei der eingereichten Dissertation zum Thema

Thermal Behavior of Amino Acids in Inorganic Matrices: Relevance for Chemical Evolution

.....

handelt es sich um meine eigenständig erbrachte Leistung.

2. Ich habe nur die angegebenen Quellen und Hilfsmittel benutzt und mich keiner unzulässigen Hilfe Dritter bedient. Insbesondere habe ich wörtlich oder sinngemäß aus anderen Werken übernommene Inhalte als solche kenntlich gemacht.
3. Ich habe nicht die Hilfe einer kommerziellen Promotionsvermittlung oder -beratung in Anspruch genommen.
4. Die Bedeutung der eidesstattlichen Versicherung und der strafrechtlichen Folgen einer unrichtigen oder unvollständigen eidesstattlichen Versicherung sind mir bekannt.

Die Richtigkeit der vorstehenden Erklärung bestätige ich: Ich versichere an Eides Statt, dass ich nach bestem Wissen die reine Wahrheit erkläre und nichts verschwiegen habe.

Stuttgart

Ort und Datum

Unterschrift